arXiv:hep-ph/9709270v1 6 Sep 1997

EVENT GENERATORS FOR WW PHYSICS

Conveners: D. Bardin and R. Kleiss

Working group: E. Accomando, H. Anlauf, A. Ballestrero, F.A. Berends, E. Boos, F. Caravaglios, D. van Dierendonck, M. Dubinin, V. Edneral, F.C. Erné, J. Fujimoto, V. Ilyin, T. Ishikawa, S. Jadach, T. Kaneko, K. Kato, S. Kawabata, Y. Kurihara, D. Lehner, A. Leike, R. Miquel, G. Montagna, M. Moretti, T. Munehisa, O. Nicrosini, T. Ohl, A. Olchevski, G.J. van Oldenborgh, C.G. Papadopoulos, G. Passarino, D. Perret-Gallix, F. Piccinini, R. Pittau, W. Płaczek, A. Pukhov, V. Savrin, M. Schmitt, S. Shichanin, Y. Shimizu, T. Sjöstrand, M. Skrzypek, H. Tanaka, Z. Wąs

Contents

1 Introduction: the need for Monte Carlo **4**

1.1 Semianalytics versus event generators 4

1.2 The Ultimate Monte Carlo 6

1.3 Comparison generalities 7

1.4 A classification of 4-fermion processes 9

2 Descriptions of 4-fermion codes **11**

2.1 ALPHA 11

2.2 CompHEP 3.0 14

2.3 ERATO 18

2.4 EXCALIBUR 21

2.5 GENTLE/4fan 24

2.6 grc4f 1.0 28

2.7 KORALW 1.03 31

2.8 LEPWW 34

2.9 LPWW02 35

2.10 PYTHIA 5.719 / JETSET 7.4 . . . 39
2.11 WOPPER 1.4 . . . 40
2.12 WPHACT . . . 43
2.13 WTO . . . 46
2.14 WWF 2.2 . . . 49
2.15 WWGENPV/HIGGSPV . . . 52
2.16 Summary . . . 55

3 Comparisons of CC Processes **57**
3.1 *CC10* processes . . . 57
3.1.1 Observables . . . 58
3.1.2 Tuned Comparisons . . . 60
3.1.3 Input parameters . . . 60
3.1.4 Presentation . . . 61
3.1.5 Experimental Errors . . . 62
3.1.6 Canonical Cuts . . . 64
3.1.7 "Unleashed" Comparisons . . . 66
3.1.8 Theoretical uncertainties . . . 69
3.1.9 Total Cross Sections . . . 71
3.1.10 W Production Angle . . . 72
3.1.11 Invariant Masses . . . 74
3.1.12 γ Energy . . . 76
3.1.13 Leptonic Observables . . . 79
3.1.14 Visible γ Energy . . . 79
3.1.15 Final State Radiation . . . 82
3.1.16 Conclusions . . . 86
3.2 *CC11* processes . . . 88

4 Comparisons of NC processes **90**

5 All four-fermion processes **92**

5.1 AYC, Canonical Cuts 92

5.2 AYC, Simple Cuts 94

5.3 Conclusions 94

References **96**

1 Introduction: the need for Monte Carlo

In this report we shall deal with the practical implementation of the theoretical results described in the WW study group report. There, many important results and formulae have been given which have to find their way into the analysis of the LEP2 data, in particular those dealing with the measurement of the W mass and couplings. It is our aim to describe the current state of the art of this implementation.

The simplest detectable final states of relevance are those consisting of four fermions (when we disregard the complications arising from photon bremsstrahlung, gluon bremsstrahlung and hadronization effects), and consequently the phase space has seven dimensions (eight, if we also include the overall azimuthal distribution of events around the beam axis – this distribution, however, is trivial as long as no transversely polarized beams are considered). Obviously, the sets of diagrams that contribute to a given final state is also quite complicated. Below, we shall present a classification of the various sets of diagrams that we have found useful in discussing and comparing results. When we also take into account the complicated peaking structures resulting from the many different Feynman diagrams, it becomes clear that the only way in which we can arrive at experimentally meaningful results in which all cuts can be accommodated is that of Monte Carlo simulation of the full event. This feature is even more pronounced than at LEP1, where the important events have a two-fermion final state, with only one relevant angular variable, and little peaking structure at given energy. There are, of course, processes such as $e^+e^- \to W^+W^- \to q\bar{q}\mu\nu_\mu$ where experimental cuts tend to be not very drastic, but even is such cases the estimate of a given experiment's acceptance and efficiency will probably have to rely on Monte Carlo simulation, even if the final fits are performed in some semi-analytic fashion. This is even more the case if in the above process we replace the muon by the electron.

1.1 Semianalytics versus event generators

Notwithstanding all this, it is very desirable to have at our disposal also calculations that do not rely on explicit event generation. As is the case in LEP1 physics, a number of semi-analytical results have been obtained, mainly in the form of the `GENTLE` code, which extends the formalism of [1] to integrate analytically over a number of variables, and performs the few remaining integrations using standard numerical packages (see [2] and references therein). Although in this way neither all diagrams nor all possible experimental cuts can be incorporated, we feel that the existence of such results, with an inherently much smaller numerical error as well as excellent control over the theoretical input, establishes an important benchmark for the Monte Carlo programs. As will be clear from our comparisons of the results of the various programs, `GENTLE` indeed serves, in many cases, as such a benchmark, especially in the 'tuned comparisons' we describe below.

Essentially all Monte Carlo codes presented here consist of two main ingredients, incorporated in (usually) three steps to produce numerical output. The ingredients are:

- a set of routines that, for given values of the fermions' four-momenta, produce the value of the matrix element, squared, and summed/averaged over the appropriate spins and colors. A wide number of techniques are used to obtain the matrix elements. For example, the `ALPHA` code takes as input the effective action of the theory, and numerically computes the saddle point of the path integral for given external momenta, without explicit reference to Feynman diagrams. The `ERATO, EXCALIBUR, WTO, WPHACT`, and `WWGENPV` codes (among many) use different kinds of helicity techniques, where the relevant diagrams are either put in 'by hand' or generated by some semi-automatic procedure. Yet other codes such as the `CompHEP` and `grc4f` programs employ a fully automated diagram-generating-and-evaluating code. The fact that such disparate treatments manage to come up with agreeing numbers can be viewed as important checks on the correctness of the various individual procedures. Some programs (in particular `ALPHA` and `WWFT`) also incorporate explicit photons into the computation of the matrix element, while the `grc4f`, `PYTHIA` and `WOPPER` programs use 'parton shower' techniques to generate photons, the `KORALW` code employs the so-called YFS approach, and WWGENPV uses a p_T-dependent structure-functions-inspired formulation. It should also be stressed that not all programs can compute all contributing Feynman diagrams: this important fact should be kept in mind when we discuss the results.

- a set of routines that transform uniformly distributed pseudo-random numbers into phase space variables, taking as much of the peaking structure as possible into account by a number of mappings and branch choices. Again, different programs employ widely different techniques to this end. In particular for processes with electrons or positrons in the final state the occurrence of t-channel photon exchange calls for a very careful treatment.

Obviously, the distinction between these two ingredients is not always completely straightforward, especially in codes that employ 'showering', where the phase space generation should itself induce the correct matrix elements. Also, not all programs use pseudo-random numbers as a basis for the phase space generation: some codes employ 'black box' integrators such as provided by the NAG library, while the `WTO` uses quasi-random, deterministic number sets (technically known as shifted Korobov sets).

The running of a typical Monte Carlo consists of three steps:

- initialization: here the input parameters are read in, and various preparatory steps are undertaken. For instance, `EXCALIBUR` will, at this stage, determine the contributing Feynman diagrams and print them, and work out which peaking structures contribute.

- generation: here a event-generating routine is called the desired number of times to arrive at a phase space point together with its matrix element. Also the necessary filling of histograms and other bookkeeping is performed in this step.

- evaluation: when the desired number of events has been produced, the total cross section

is computed as the average event weight, where the event weight is defined as the ratio of the matrix element squared over the phase space Jacobian.

For details about the workings of the various different programs we refer to the next subsection, where more information is given for each individual program, together with the necessary references.

1.2 The Ultimate Monte Carlo

The above rough description does, of course, no justice to the effort that has already gone into all the existing codes: but it is only fair to say that, at this moment, none of them can be considered as the definitive program. This 'Ultimate Monte Carlo' (which may remain out of reach) is approached, by different authors, in different ways, and some programs have desirable features (for instance, explicit, finite-p_T photons), that are not shared by other programs, which however have their own attractions (for instance, inclusion of all Feynman diagrams). As we have already indicated, it must be always kept in mind, when comparing programs, that such differences in approach will unavoidably result in differences in results; *but such differences should* **not** *be regarded as any kind of theoretical uncertainty, but rather as an indication of the importance of the different ingredients*. In fact, the real theoretical uncertainty (due, for example, to unknown higher-order corrections) is quite distinct from the differences between programs. It may be instructive to give a list of the features of the Ultimate Monte Carlo, in order for the user to appreciate to what extent a given program satisfies her/his needs in a particular analysis. The Ultimate Monte Carlo should:

- treat all possible four-fermion final states, with all relevant Feynman diagrams (possibly with the option to restrict the set of diagrams).
- produce gauge-invariant results. If one describes off-shell, unstable W pair production using only the three Feynman diagrams in the *CC03* sector, then gauge dependence will result. Fortunately, at LEP2 energies these effects are very small provided a suitable gauge such as the unitary or 't Hooft-Feynman gauge is chosen: but, especially when t-channel photon exchange takes place, the gauge cancellations can be very delicate. Related to this is the requirement that the various coupling constants are chosen in a consistent manner.
- have a correct treatment of the bosonic widths. This is closely related to the previous point: if one just inserts a running width, gauge invariance is lost, with dramatic results for final states with electrons or positrons. This problem, and its various possible resolutions, are described in detail in [3].
- have the fermion masses taken into account. For instance, `EXCALIBUR` treats the fermions as strictly massless, which accelerates the computation of the matrix elements considerably, but imposes the need to avoid phase space singularities by explicit cuts, and makes it impossible to incorporate Higgs production and decay consistently.

- have explicit, p_T-carrying photons. This is of particular importance for a distinction of "initial" and "final" state radiation in an M_W measurement, as well as the search for anomalous couplings.

- have the higher-order photonic radiative corrections taken into account properly. This probably does not mean, given the experimental accuracy to be expected at LEP2, that very high orders or very high precision are required, but it would be very useful to be able to prove that radiative effects are small for a particular quantity. For instance, the Coulomb singularity which modifies the WW intermediate state is an important effect.

- should have good control over the non-QED radiative correction, preferably in the form of the complete $\mathcal{O}(\alpha)$ corrections, and resummed higher-order effects where necessary.

- incorporate QCD effects, both in the W self-energy and in the gluonic corrections to quark final states. Also relevant is the interference between electroweak and QCD channels in the production of four-quark final states. In this place it should be remarked that it is of course trivial to add the 'naive' QCD correction $1 + \alpha_s/\pi$ to the total cross section, but in the presence of cuts this may be less appropriate: the particular strategy adopted must depend on the interface with a hadronization routine.

- have a good interface to hadronization packages. This is especially relevant to the W mass measurement, together with the next point:

- give information, for each generated event, on how much of the matrix element is contributed by each subset of Feynman diagrams, and/or each color configuration. This is important for problems of color reconnection and Bose-Einstein effects.

- have Higgs production and decay implemented.

- have the possibility of anomalous couplings. This allows for the study of the effects of such couplings to good precision using control-variate techniques (that is, switching the anomalous couplings on and off for a given event sample, thereby avoiding statistical fluctuations that might wash out the small anomalous effects).

1.3 Comparison generalities

The rest of this contribution deals with the description and the comparison of the different codes and their results. It must again be stressed, that the field is still in a state of flux, and probably not one of the programs has taken on its final form. We can, therefore, only present results as they are at this particular moment (December 1995), with the remark that most of the discrepancies are well-understood and are expected to decrease significantly in the near future. There are several ways in which we have compared the various codes:

- **by ingredients**
  To this end, we just compare which of the features of the Ultimate Monte Carlo are part of the different codes. Again, we stress that the choice of code depends to a large extent on the user's particular problem. For instance, background studies will require a code that contains all Feynman diagrams, while high-precision studies of inclusive quantities may be better of with a semi-analytical program such as `GENTLE`. In the next section we present what we feel to be the most relevant information on each program.

- **by 'tuned' comparison**
  This means that we have chosen a minimal process described by a minimal set of diagrams (*CC03* and *CC10*), for which we have computed several quantities. The idea of this exercise is that *all programs should agree on these numbers*. Of course, one must make sure that the physical parameters of the theory such as masses and widths in propagators, and the coupling constants in the Lagrangian, are constructed to be identical in all codes. The aim is twofold. In the first place it allows to establish the *technical precision* of the various codes, and we have come (as will be shown) to a satisfactory number of one per mille or better, at least for a large cluster of dedicated codes. In the second place, such a tuned comparison is a good bug hunting ground, as we have found. Many small differences usually can be traced back either to small bugs or small differences in input parameters or cuts.

- **by 'best you can do' comparison**
  The tuned comparison, useful as it is, is not of direct experimental relevance since it relies on switching off all features in which one program is better than another. The real physics results must of course incorporate more than this bare minimum, and therefore we have computed a number of quantities, for one class of processes, in which (apart from agreed-upon input parameters) each code provides us with its own 'best answer'. Again, we want to stress that these results do not agree, nor should they be expected to: differences in these results reflect differences in the physics approach. Comparisons apart, in the end the programs will have to provide the community with explicit predictions, and this 'best you can' should give an idea of the extent to which these predictions depend on the various pieces of physics input. Whereas the results of the tuned comparison are not expected to change appreciably in the near future, the 'best you can' results must, and probably will, converge over time as more physics input is incorporated into more programs.

- **by 'all you can do' comparison**
  finally, we have let the programs pass an 'all you can do' comparison phase, where each program has computed essentially all the processes it is able to treat. Of course, only some out of all the codes can do *all* four-fermion processes: but from such a game should arise a coherent picture of what the current state-of-the-art is. Another goal of the 'all you can do' comparison, which is also 'tuned', is to provide precision benchmarks for *all four-fermion processes*.

1.4 A classification of 4-fermion processes

For the various four-fermion final states produced in e^+e^- annihilation, the numbers of contributing Feynman diagrams are quite different. On top of double-pole (WW or ZZ) diagrams there are, in general, a lot of so-called background diagrams with different intermediate states, which are single-resonant or non-resonant. In this section we present a classification of all four-fermion final states in the Standard Model [1]. This classification was originally proposed in [5]. The tables presented below are borrowed from papers [2] and [6], while their description is updated.

In general all possible final states can be subdivided into two classes. The first class comprises production of (up, anti-down) and (down, anti-up) fermion pairs,

$$(U_i\ \bar{D}_i)\ +\ (D_j\ \bar{U}_j)\ ,$$

where i, j are generation indices. The final states produced via virtual W-pairs belong to this class. Therefore, we will call these *'CC'*-type final states. The second class is the production of two fermion-antifermion pairs,

$$(f_i\ \ \bar{f}_i)\ +\ (f_j\ \ \bar{f}_j)\ ,\ \ f = U,\ D.$$

As it is produced via a pair of two virtual neutral vector bosons we will call this a final state of 'NC'-type. Obviously these two classes overlap for certain final states.

The number of Feynman diagrams in the *CC* classes are shown in table 1.

	$\bar{d}u$	$\bar{s}c$	$\bar{e}\nu_e$	$\bar{\mu}\nu_\mu$	$\bar{\tau}\nu_\tau$
$d\bar{u}$	*43*	**11**	20	**10**	**10**
$e\bar{\nu}_e$	20	20	*56*	18	18
$\mu\bar{\nu}_\mu$	**10**	**10**	18	*19*	**9**

Table 1: *Number of Feynman diagrams for* 'CC' *type final states.*

Three different cases occur in the table 1 [2]:

(i) The *CC11* family.
The two fermion pairs are different, the final state does not contain identical particles nor electrons or electron neutrinos (numbers in table 1 in **boldface**). The corresponding eleven diagrams are shown in figures 1 and 2. There are less diagrams if neutrinos are produced (`CC9, CC10` processes).

(ii) The *CC20* family.
The final state contains one $e^\pm$ together with its neutrino (Roman numbers in table 1); compared to case (i), the additional diagrams have a t channel gauge boson exchange. For a purely leptonic final state, a *CC18* process results.

[1] The classification is done with the help of `CompHEP` [4].

[2] In [7], a slightly different classification has been introduced; the relation of both schemes is discussed in [5].

(iii) The *CC43/mix43* family and *CC56/mix56* process.
Two mutually charge conjugated fermion pairs are produced (*italic* numbers in table 1). Differing from cases (i) and (ii), the diagrams may proceed via both, WW- and ZZ-exchanges. For this reason, we will also call them *mix*-ed class. There are less diagrams in the *mix43* process if neutrinos are produced (*mix19* process). With the two charge conjugated ($\bar{e}\nu_e$) doublets, one has *mix56* process.

Each of these classes contains the *CC03* process, which is described by the usual three 'double W-pole' Feynman diagrams, figure 1. From the *CC11* set of diagrams only 10 contribute

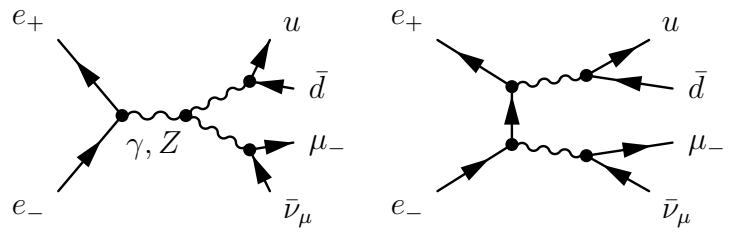


Figure 1: The *CC03* set of Feynman diagrams

to the process $e^+e^- \to \mu^-\bar{\nu}_\mu u\bar{d}$, because the photon doesn't couple to the neutrino (cf. fig. 2).

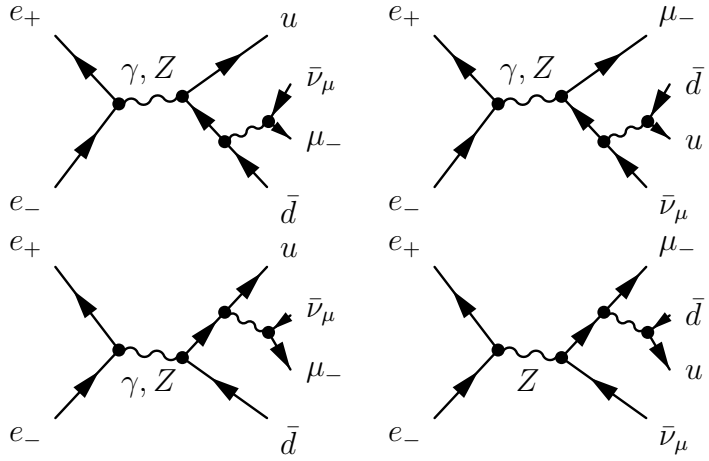


Figure 2: The *CC11* set of Feynman diagrams

For the final states corresponding to the NC class the number of Feynman diagrams is presented in table 2.

(i) The *NC32* family.
The simplest case (numbers in **boldface**) does not contain electrons or identical fermions[3].

[3] We exclude the Higgs boson exchange diagrams from the classification in the tables.

	$\bar{d}d$	$\bar{u}u$	$\bar{e}e$	$\bar{\mu}\mu$	$\bar{\nu}_e\nu_e$	$\bar{\nu}_\mu\nu_\mu$
$\bar{d}d$	4·16	*43*	48	**24**	21	**10**
$\bar{s}s, \bar{b}b$	**32**	*43*	48	**24**	21	**10**
$\bar{u}u$	*43*	4·16	48	**24**	21	**10**
$\bar{e}e$	48	48	4·36	48	*56*	20
$\bar{\mu}\mu$	**24**	**24**	48	4·12	19	*19*
$\bar{\tau}\tau$	**24**	**24**	48	**24**	19	**10**
$\bar{\nu}_e\nu_e$	21	21	*56*	19	4·9	12
$\bar{\nu}_\mu\nu_\mu$	**10**	**10**	20	*19*	12	4·3
$\bar{\nu}_\tau\nu_\tau$	**10**	**10**	20	**10**	12	**6**

Table 2: *Number of Feynman diagrams for 'NC' type final states.*

(ii) The *NC48* and *NC21* families.
The numbers in roman correspond to the final states which include $f = e, \nu_e$ except for cases covered by item (iv). The large number of diagrams here is due to additional t-channel exchange.

(iii) The *NC4·16* family.
With identical fermions f ($f \neq e, \nu_e$), the number of diagrams grows drastically due to the necessity to satisfy the Pauli principle, i.e. to anti-symmetrize the amplitude. For purely leptonic processes this number of diagrams reduces to *4·12* since the gluon exchange doesn't contribute.

(iv) The *NC4·36* and *NC4·9* processes, with the two e^+e^- or $\bar{\nu_e}\nu_e$ pairs in the final state. The corresponding numbers are shown sans serif.

(v) The *mix43* and *mix56* processes.
The numbers in *italic* correspond to final states which are also present in table 1, case (iii).

2 Descriptions of 4-fermion codes

2.1 ALPHA

Authors:

Francesco Caravaglios	caravagl@thphys.ox.ac.uk
Mauro Moretti	moretti@hep1.phys.soton.ac.uk

Description

In ref.[8], we suggested an *iterative* algorithm to compute automatically the scattering matrix elements of any given effective Lagrangian, Γ. By exploiting the relation between Γ and the

connected Green's function generator, Z, we obtained a formula which does not require the use of Feynman graphs, and is suitable to implementation in a numerical routine. The problem of computing the scattering matrix element can be reformulated as the problem of finding the minimum of Z with respect to a *finite* set of variables. Once the stationary conditions for Z are written down, they can be solved iteratively and, truncating the series after a proper number of steps, one obtains the solution. Using this algorithm we have been able to build a Fortran code, `ALPHA`, for the automatic computation of matrix elements. When the initial and final states of the process are specified (type, momenta and spin of the external particles) the program prepares an array b_j for all the possible degrees of freedom (the label j refers to internal and external momenta and to the particles type, color and spin). As shown in [8], the scattering matrix element $\mathcal{A}$ is obtained as

$$\mathcal{A} = a_i b_i + \frac{1}{2} K_{lm} b_l b_m + \frac{1}{6} O_{ijk} b_i b_j b_k. \tag{1}$$

where the b_j are obtained from the equation of motion in presence of a source term a_i.

$$a_i = K_{im} b_m + \frac{1}{2} O_{ijk} b_j b_k, \tag{2}$$

which can be solved iteratively.

The matrix O_{ijk} contains the physical couplings between the degrees of freedom b_j of the fields entering the scattering process and the matrix K_{lm} accounts for the kinetic terms in the Lagrangian. In the Fortran code the matrix elements O_{ijk} and K_{lm} are returned by some subroutines as a function of the finite set of possible momenta P_m.

The `ALPHA` code includes all the electroweak interactions and the whole flavor content of the Standard Model (SM) (presently it does not account for the strong interactions) and it can perform all possible electroweak matrix elements in the SM regardless of the initial or final state type. In addition, due to its simple logic, it allows for modification of the Lagrangian with no excessive effort (by adding the proper subroutines to compute the new O_{ijk} interactions and/or adding the relevant variables for the new particles). Since the algorithm is purely numerical, the output can be immediately used for an integration procedure.

Features of the program

The numerical integration is performed by mean of the package `VEGAS` [9]. The variables have been chosen in such a way that each singularity corresponds to an integration variable allowing `VEGAS` to cope effectively with the pole structure of the physical process. The phase space is factorized as a multiple decay process using the formula

$$d\Phi(P; q_1, q_2, q_3, ..., q_n) = d\Phi(Q = q_1 + q_2; q_1, q_2) d\Phi(P; Q, q_3, ..., q_n)(2\pi)^3 d^2Q \tag{3}$$

where the squared momenta Q^2 corresponds to the physical singularities. For some final states there are multiple channels exhibiting a pole structure. In these cases it is difficult to obtain a good convergence of the integral with a single choice of phase space variables. Therefore we

split the integration domain in different regions, and in each of them we make a different choice of physically motivated variables. One additional real variable is used to map the discrete set of spin configurations. At least for the processes we have considered, the `VEGAS` algorithm has adequately performed a selection of the relevant spin configurations.

In principle, all possible final states can be treated. For most of them the corresponding phase space routines are also implemented: an exception being processes with electrons in the final state. All possible choices of spin configurations can be selected, for instance polarized initial states are immediately available.

The Monte Carlo does not include initial/final-state radiation (ISR/FSR). We have instead used `ALPHA` to compute the rates for the process $e^+e^- \to 4\ fermions\ + \gamma$; all the Standard Model diagrams are evaluated with a finite (constant) width of the electroweak gauge bosons and the physical fermion masses.

Anomalous couplings can be easily added, even with momentum dependent form factors, running widths etc.

Since the method of calculation does not rely on Feynman graphs technique it is not possible, in general, to isolate the contribution of a single graph. Turning on/off each single interactions, the contribution of many subsets of diagrams can be extracted but this might be not practical enough.

Program layout

The program requires as input the center of mass energy and the number of external particles: for each type (*i.e.* top, strange,...Z) we have to enter a number which can be 0 if no particle of that type exists, or 1,2,... as required. A subroutine generates the momenta and the spin configurations according to a phase space preselected among a list of prepared ones. All the couplings of the theory are collected in a single subroutine which is adequately commented and is called only once at the beginning of the run. A subroutine is provided which has as input the external momenta and as output a flag which when set to zero forces the program to ignore the given phase space point, thereby allowing for any kind of cut. Another subroutine is provided to make it possible to produce plots. Each variable to be plotted must be normalized between 0 and 1 and as output a file is produced which registers for each variable N (input number) equispatiated bins containing the (unnormalized) integral and variance. As output the cross section (in picobarn) is also given with its statistical error.

With few modifications, we can therefore provide a code for the computation of *all* processes listed in tables 1 and 2 allowing the user to implement any cuts to change the numerical values of the electroweak couplings and to record all the data required to produce a plot.

Other operations, like allowing the user to compute an arbitrary process or to change the Lagrangian of the model are not completely user-friendly at the moment.

Input parameters and the Lagrangian

We used the common set of Standard Model parameters (as discussed in section 3). All the fermions are massive. The gauge boson propagators include the width, which is constant in order to obtain gauge invariant matrix elements. The inclusion of the proper, physical, running width for the gauge bosons in a gauge invariant way, namely including the relevant corrections to the three and four point Green Functions, is straightforward in our approach and it will be done in a near future. The cuts applied to the four final fermions are the common one used for the comparison tests.

Availability:
The program is available upon e-mail request from the authors.

2.2 CompHEP 3.0

Authors:

E.Boos	boos@theory.npi.msu.su
M.Dubinin	dubinin@theory.npi.msu.su
V.Edneral	edneral@theory.npi.msu.su
V.Ilyin	ilyin@theory.npi.msu.su
A.Pukhov	pukhov@theory.npi.msu.su
V.Savrin	savrin@theory.npi.msu.su
S.Shichanin	shichanin@m9.ihep.su

Description

The main idea in `CompHEP` [10] was to enable on to go directly from the Lagrangian to cross sections and distributions effectively, with a high level of automation.

Version 3.0 has 4 built-in physical models. Two of them are versions of the Standard Model (SU(3)xSU(2)xU(1)) in the unitary and 't Hooft-Feynman gauges with the parameters corresponding to the standard LEP2 input.

The general structure of the `CompHEP` package is represented in Figures 3, 4. It consists of symbolical and numerical modules. The main tasks solved by the symbolical module (written in C) are :

1. to select a process by specifying *in-* and *out-* particles. Any type of five particle final state for decays and five particle final state for collisions can be defined;

2. to generate and display Feynman diagrams. It is possible to delete some diagrams from the further consideration, leaving only limited subsets;

4. to generate and display squared Feynman diagrams (corresponding to squared S-matrix elements);

5. to calculate analytical expressions corresponding to squared diagrams with the help of a fast built-in symbolic calculator. Traces of gamma matrices products are calculated, summing over the final state polarizations. Masses of initial and final particles can be kept nonzero in the squared amplitude calculation and phase space integration;

6. to save symbolic results corresponding to the squared diagrams calculated in the REDUCE and MATHEMATICA codes for further symbolical manipulations;

7. to generate the optimized FORTRAN code for the squared matrix elements for further numerical calculations.

Program layout

The numerical part of the CompHEP package is written in FORTRAN. It uses the CompHEP FORTRAN output, the BASES&SPRING package [11] for adaptive Monte-Carlo integration and unweighted event generation. The main tasks solved by the numerical module are :

1. to choose phase-space kinematical variables. Exact parameterizations of three, four and five particle phase space in the case of massive particles are used [12];

2. to introduce kinematical cuts over any squared momenta transferred and squared masses for any groups of outgoing particles. Any kinematical cuts for noninvariant variables can be introduced using explicit restrictions on the four-momenta;

3. to perform a kinematical regularization (mapping) to remove sharp peaks in the squared matrix elements. The package has a rich choice of optimizing possibilities (various combinations of phase space parameterizations and mappings);

4. to change the BASES parameters for Monte-Carlo integration;

5. to change numerical values of model parameters;

6. to calculate distributions, cross sections or particle widths by the Monte-Carlo method. The output for a cross section value (sequence of MC iterations) and distributions (set of histograms) has the standard BASES form;

7. to perform the same integration taking into account structure function for incoming particles. Initial state radiation (ISR) is implemented in the structure function approach [13]. An interface to the standard PDF library is available. Final state radiation and the Coulomb term are not implemented. Photon radiation from the initial and final states can be introduced by calculation of exact amplitude for $2 \to 5$ process (4 fermions + photon).

8. to generate events and to get histograms simulating the signal and background. SPRING [11] is used for unweighted event generation.

CompHEP is a menu-driven program with a context HELP facility. Each of two variants of the Standard Model (unitary or and 't Hooft-Feynman gauges) is defined by four tables:

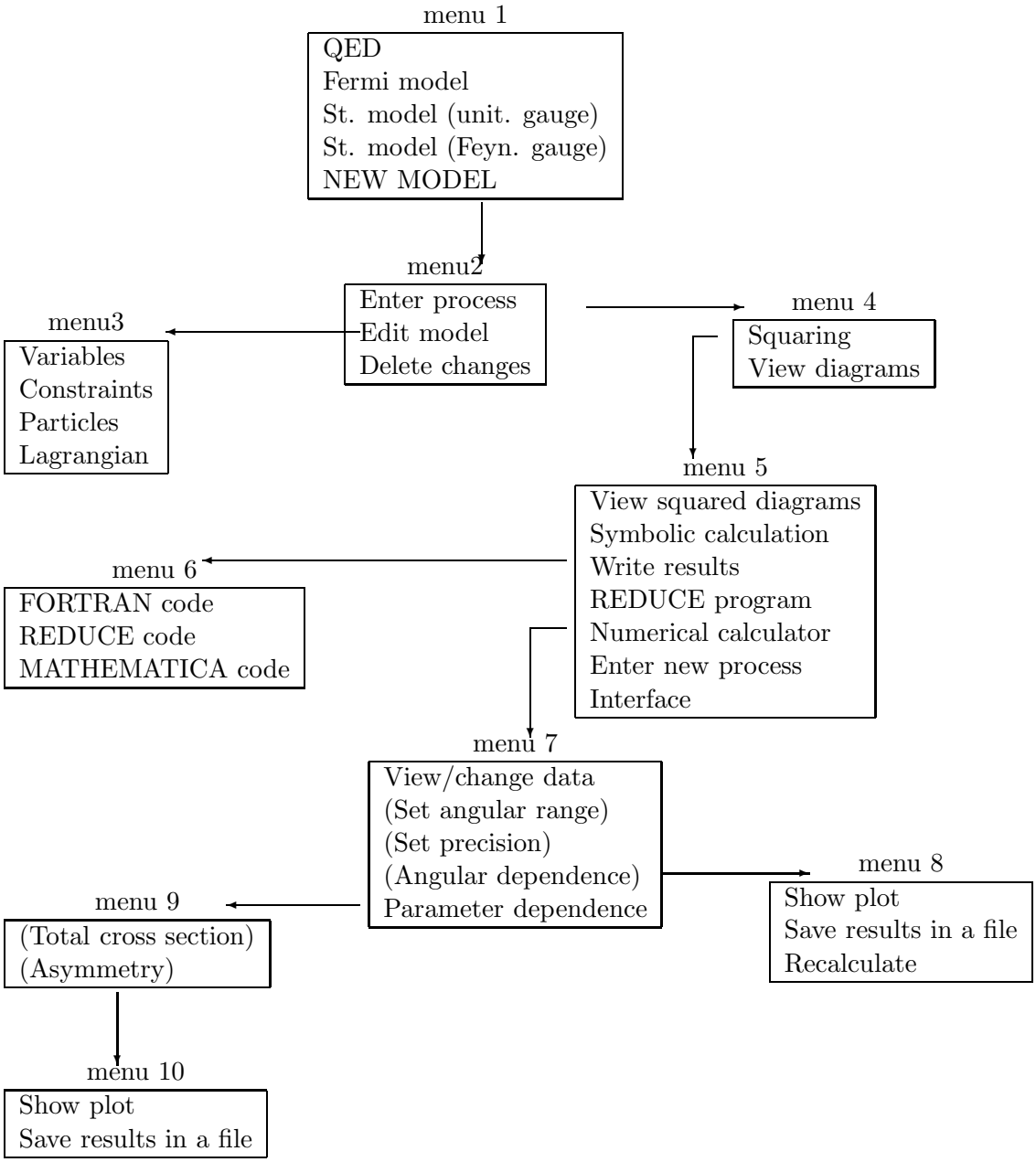


Figure 3: The menu system for the `CompHEP` symbolic part

Main menu

1. Calculation	2. IN state
3. Model parameters	4. Invariant cuts
5. Kinematics	6. MC parameters
7. Regularization	8. Task formation
9. View results	10. User's menu

In state

1. StructF(1) = *OFF*
2. SQRTS = *1000*
3. StructF(2) = *OFF*

Invariant cuts

1. Insert new cut
2. Delete cut
3. Change cut

MC parameters

1. Ncall = *10000*	2. Acc1= *0.1*
3. Itmx1= *5*	4. Acc2= *0.1*
5. Itmx2=*0*	6. Event generator OFF
7. Number of events = *1000*	

Regularization

1. Insert new regularization
2. Delete regularization
3. Change regularization

Task formation

1. Table parameters
2. Set default session
3. Add session to batch

View results

1. session # to view - *3*	2. View result file
3. View protocol file	4. View histogram file

Figure 4: The menu system for the `CompHEP` numerical part

Variables	list of parameters (masses, widths, couplings, mixings)
Constraints	list of functionally dependent parameters
Particles	list of particles and quantum numbers
Lagrangian	list of Feynman rules for vertices

At present, versions for different platforms exist: HP Apollo 9000, IBM RS 6000, DECstation 3000, SPARC station, Silicon Graphics and VAX.

Availability
The package is available from
internet host: theory.npi.msu.su
directory: pub/comphep-3.0
files: 30.tar.Z, install.doc, manual.ps.Z

2.3 ERATO

Author:[4]

Costas G Papadopoulos	papadopo@cernvm.cern.ch
	C.G.Papadopoulos@durham.ac.uk and
	papadopo@alice.nrcps.ariadne-t.gr

Description

`ERATO`[14]-[15] is a four-fermion Monte Carlo[5] . This program is an evolution of an older code where single-W production, $e^-e^+ \to e^-\bar{\nu}_e W$ was calculated including all possible non-standard couplings of the three-boson interactions[14], $WW\gamma$ and WWZ. This code has now been updated in order to include all background graphs for the processes $e^-e^+ \to \ell\bar{\nu}_\ell u\bar{d}$ with $\ell = e, \mu, \tau$. The actual version of the program can now produce results for any four-fermion final state. As far as the matrix element calculation is concerned, the program uses a representation of the basic fermion current $\bar{u}_\lambda(p_1)\gamma^\mu u_\lambda(p_2)$, the 'E-vector',which is given as follows:

$$E^\mu_\lambda(p_1, p_2) \equiv \bar{u}_\lambda(p_1)\gamma^\mu u_\lambda(p_2) \tag{4}$$

where

$$\begin{aligned} E^0_- &= \sqrt{p_1^+ p_2^+} + \frac{(p_{1x} + ip_{1y})(p_{2x} - ip_{2y})}{\sqrt{p_1^+ p_2^+}} \\ E^x_- &= \sqrt{\frac{p_2^+}{p_1^+}}(p_{1x} + ip_{1y}) + \sqrt{\frac{p_1^+}{p_2^+}}(p_{2x} - ip_{2y}) \end{aligned}$$

[4] In several aspects of the program the following people have contributed:
Mark Gibbs, Liverpool `gibbs@afsmail.cern.ch`
Robert Sekulin, DRAL `robert@vax2.rutherford.ac.uk`
Spyros Tzamarias, Liverpool `tzamaria@cernvm.cern.ch`

[5] In ancient Greek mythology EPATΩ was the muse of Music. By accident the name of the program is also part of the gen`ERATO`r group.

$$
\begin{aligned}
E^y_- &= -i\Big(\sqrt{\frac{p_2^+}{p_1^+}}(p_{1x}+ip_{1y}) - \sqrt{\frac{p_1^+}{p_2^+}}(p_{2x}-ip_{2y})\Big) \\
E^z_- &= \sqrt{p_1^+p_2^+} - \frac{(p_{1x}+ip_{1y})(p_{2x}-ip_{2y})}{\sqrt{p_1^+p_2^+}}
\end{aligned}
\tag{5}
$$

with $p^\pm = p^0 \pm p^3$. The above representation is valid only for massless fermions. All matrix elements have been tested against `MadGraph`[16] calculations under the same conditions, and the agreement was at least 13 digits using a `REAL*8` declaration.

In addition to the amplitude calculation, we have implemented a Monte Carlo integration algorithm which is essentially identical to the multichannel approach of references [7, 18]. The problem is that the amplitude we have to integrate over is a very complicated function of the kinematical variables, peaking at different regions of phase space. The idea is to define different kinematical mappings, corresponding to different peaking structures of the amplitude and then use an optimization procedure to adjust the percentage of the generated phase-space points, according to any specific mapping, in such a way that the total error is minimized.

Special care has also been taken in order to include in a gauge-invariant way the width effects. As is well known the introduction of an s-dependent width leads to gauge-violation in the $s-$ and $t-$ channel. This is because the s-dependent width violates the Ward identities at the one loop. The solution is to include consistently all one loop corrections. More precisely, if one restricts oneself to fermionic corrections, one has to include the one-loop fermion 'triangle' to the three-boson vertex function. This way, the gauge-invariance is restored. Bosonic corrections are much more subtle due to the gauge-parameter dependence, but in the case of W and Z line-shape parameters their contribution is suppressed compared to the fermionic one, due to simple kinematical reasons. In `ERATO` the imaginary part at the one-loop level of both two-point and three-point functions of vector bosons is implemented in a very compact analytic form[3].

Leading higher order corrections are also included in `ERATO`, in the form of initial-state radiation (ISR), using the structure function approach with all possible ISR-radiator functions available (β or η option).

An other important feature of `ERATO` is the incorporation of all CP conserving non-standard couplings. In fact the way the program is written enables us to include any non-standard couplings, for instance $ZZ\gamma$ or CP-violating $WW\gamma$ and WWZ parameters.

Features of the program

The main features of the program are the following: it can be used both as an event generator and as an integrator: all final states, and all possible cuts, are in principle allowed. Initial-state radiation is implemented using structure functions; final-state radiation and the Coulomb correction are not implemented. All possible anomalous couplings are implemented, the fermions are assumed to be massless, with a leading-log approximation for the structure functions.

Interface

The output from the `ERATO` generator for the semi-leptonic and four-jet channels contains

colored partons, and consequently it is desirable to include models of QCD effects such as hadronization in the simulation procedure. One way to include these phenomena is to pass the four-momenta generated by ERATO to an existing simulation package. This approach is attractive as there are a number of such packages in existence.

The `ERATO` generator has been interfaced successfully to the `JETSET` [28] and `HERWIG` [17] packages. T he procedure is the same in both cases and can be easily extended to other simulation packages.

Firstly, the event configurations produced by `ERATO` are not of equal probability and have to be selectively used in such a way so as to respect the correct distributions of kinematic variables. This is achieved by unweighting the events; events are used at random with a probability given by the weight of the event divided by the maximum weight. The efficiency of this procedure is typically of order 0.1%.

Secondly, the particle content of the `ERATO` final state has to be selected. At present, this is determined at the start of a simulation run but in principle can be performed on an event- by event- basis.

Thirdly, the `ERATO` program assumes that all the fermions are massless. As a result, the four-momenta of a final state configuration have to be shifted in order to place massive fermions on shell. This is achieved by shifting the three-momenta slightly. As the energies in a typical LEPII event are high compared to the particle masses the change in momenta is a negligible effect. Following these steps, the simulation package is then used for the parton showering and hadronization stages of event generation.

Program layout
The structure of the program will be described in detail in a future publication in CPC.

Input parameters
Any set of input parameters can be implemented. In the most usual version the LEP2 standard input is used. Preferred and comparison values are identical.

Output
In the present form of the program any histogram can be obtained very easily. Cross sections for left and right incoming electrons are given separately. Error estimates are the standard ones.

Availability
From ftp://alice.nrcps.ariadne-t.gr/pub/papadopo/erato/

2.4 EXCALIBUR

Authors:

F.A. Berends	berends@rulgm0.leidenuniv.nl
R. Kleiss	t30@nikhefh.nikhef.nl
R. Pittau	pittau@psw218.psi.ch

Short description:
The program `EXCALIBUR` [7, 18] evaluates cross sections for electron-positron scattering into four final-state fermions. This is done by Monte Carlo simulation, in which events are generated over a phase space determined by a number of a-priori cuts (in many cases, the whole phase space is accessible). Each event carries a weight such that the average event weight gives the total cross section. The distribution of events over the phase space is generated by employing a large number of mappings of random numbers. Given an event, additional cuts can be imposed by hand by setting the weight of unwanted events to zero; and, of course, any number of differential distributions can also be constructed. Since the matrix elements are computed on the level of helicity amplitudes, as sums of distinct diagrams, the contributions of subsets of diagrams and of particular helicity configurations can also be studied.

Program features:

1. **method of integration:**
   the program is a strict Monte-Carlo one, in the sense that no phase space variables are integrated over analytically. This means that *all* phase space variables are amenable to any kind of cut. The generated events come with a non-constant weight: a sample of unweighted events can be selected from the generated sample by the usual rejection techniques. The efficiency of this procedure is in many cases of the order of a few per cent, depending on the final state of choice and the phase space cuts.

2. **possible final states:**
   all possible four-fermion final states are included: the user supplies the choice in the input file. An important restriction is that the fermions are considered to be strictly massless, and therefore Higgs exchange is not included.

3. **possible cuts:**
   since every event is completely specified, in principle any conceivable phase space cut can be implemented. It must be noted that, since all fermion masses are taken to be zero, singularities can occur in photon exchange channels, and these have to be excised by user-supplied a-priori cuts. Therefore, when a final state e^+ or e^- occurs, a cut on its scattering angle and energy is necessary, and when a charged particle-antiparticle pair is produced, a cut on its invariant mass is in order. These cuts are specified in the input file (see discussion below). For calculations based on a restricted set of Feynman graphs without photon exchange (e.g. the *CC03* diagrams) such cuts are of course not necessary.

4. **treatment of ISR:**
   ISR is implemented in the form of two structure functions, *i.e.* two energy fractions x_1 and x_2 are generated, but no bremsstrahlung p_T. The four-fermion event is then generated in the reduced-center-of-mass frame. The actual photon structure functions used are the 'type 2' ones of the W-pair report.

5. **treatment of FSR:**
   No FSR is at the moment included.

6. **treatment of final state decays:**
   since the fermions are considered massless, they are stable and no decay is provided: moreover, the fermions' density matrix is strictly diagonal.

7. **treatment of the Coulomb singularity:**
   the Coulomb term can be easily implemented by multiplying the appropriate WW diagrams by the correct factor, but is not yet included in the standard version.

8. **treatment of anomalous couplings:**
   a version of `EXCALIBUR` is available which includes anomalous triple-gauge-boson couplings. Six CP-conserving anomalous contributions can be put to a nonzero value: these correspond to the quantities x_γ, y_γ, x_Z, δ_Z, y_Z, and z_Z defined in ref. [19]. For zero values of these numbers the minimal Standard Model predictions are recovered.

9. **treatment of fermion masses:**
   as mentioned, these are zero, both in the matrix element and in the phase space momenta.

10. **treatment of hadronization:**
    no interface with hadronization routines are provided in the standard version; but since the momenta are completely specified the necessary `COMMON` can easily be constructed.

11. **subsets of diagrams etc:**
    since in `EXCALIBUR` all diagrams and helicities are explicit, it is simple, for a given final state, to select subsets of diagrams or helicity combinations. There exists the possibility to select, using the input file, only those diagrams that correspond to the WW, ZZ, $We\nu$, Zee or $Z\nu_e\bar{\nu}_e$ final states, or include all tree diagrams.

Program layout

The working of `EXCALIBUR` can be divided into three parts: initialization, generation, and evaluation. The two main parts of the event generation stage are the choosing of a random phase space point, and the computation of the matrix element at that point.

The initialization is performed by the routine `SETPRO`. It reads the data from the input file, and determines from these which are the Feynman tree graphs that will be considered. There are two distinct diagram topologies: 'abelian' graphs, with only fermion-boson couplings, and 'nonabelian' ones with also triple-boson couplings. The program considers all possible permutations of the external momenta over these diagrams, and determines, by quantum numbers

conservation, if they can contribute. Then, also the most significant phase space mappings (so-called *channels*) are determined.

Upon the calling of an event, first the two energies $x_{1,2}$ of the incoming $e^{\pm}$ are generated. Then, in the center of mass frame after this ISR, one particular channel is picked, by which uniform random numbers are mapped into a phase space point. The various channels are constructed from a limited number of explicit mappings, each with its own subroutine: this modular structure ensures transparency of coding, easy debugging, and the possibility of implemented additional channels when necessary. The probability of picking a particular channel is given by its *a-priori weight*: the final cross section is by construction independent of the values of this weights. After this, the event weight is computed, as the ration of the matrix element squared to the generated phase space density. For the computation of the matrix element, we use the fact that every contributing nonabelian graph can, in the minimal standard model, be simply expressed as a combination of two contributing abelian ones. These are computed, for definite helicities, by spinor techniques. The phase space density consists of a sum of the densities appropriate to each contributing channel, weighted with their a-priori weights. At several points during a run of generating events, the a-priori weights are optimized so as to approximate the weight distribution with the minimum possible variance for the available set of channels, as described in [18].

The evaluation stage consists of the estimate of the average weight and its estimated error (and, in fact, the estimated error on the error estimate). Also, the distribution of all nonzero weights is plotted, together with some information on the a-priori weight optimization. More information can be found in [7].

Input parameters

We have used the following sets of input parameters, one for the tuned comparison with the other codes, and one that reflects what (in our view) is the most accurate prediction possible with `EXCALIBUR`. They are given in the table below.

parameter	'comparison'	'best'
Z mass (GeV)	91.1888	91.1546
Z width (GeV)	2.4974	2.49646
W mass (GeV)	80.23	80.02042
W width (GeV)	2.0366	2.03302
$\sin^2\theta_W$	0.231031	0.231031
$1/\alpha$	128.07	128.07
α_s	0	0.103

The following remarks are in order here. The 'best values' for the boson masses and widths are chosen so as to take into account the running of the widths, using the transform described in [20]. The value of α is used for the four-fermion system, but for the ISR the value 1/137 is of course used. The use of α_s is relevant for four-quark and qq-two gluon final states, where the QCD four-jet production diagrams are also included. These values are set internally by the

program. In addition, there are a number of other input parameters, set in the input file:

NPROCESS	the number of processes to be treated
N	The number of events to be generated
ISTEPMAX	the number of times the a-priori weights are to be optimized
OUTPUTNAME	name of the output file
KREL	the set of diagrams to be considered: 0 all diagrams, 1 WW, 2: ZZ, 3: $We\nu$, 4: Zee, 5: $Z\nu_e\bar{\nu}_e$
LQED	0: no ISR, 1: ISR included.
ROOTSMUL	the total energy
SHCUT	minimum invariant mass after ISR
ECUT	minimum energy for the outgoing particles (4 values)
SCUT	minimum invariant mass for outgoing particle pairs (6 values)
CMAX	maximum value of $\cos\theta$ between two particles (14 values)
PAR	labels of the produced fermions (4 character*3 values)

All these values are reproduced in the output file.

Output
The output prints the process considered, with the labeling of the various particle momenta. Also a complete list of all abelian and nonabelian diagrams is given, and a list of all generation channels that will be used. Upon evaluation, information on the weight distribution is given, and the results of the weight optimization procedure.

Availability
The program is available from the authors upon request, as well as from the CPC library.

2.5 GENTLE/4fan

Authors:

D. Bardin[a]	BARDINDY@CERNVM.CERN.CH
M. Bilenky[a]	bilenky@ifh.de
D. Lehner[b]	lehner@ifh.de
A. Leike[a]	LEIKE@CERNVM.CERN.CH
A. Olchevski[a]	OLSHEVSK@VXCERN.CERN.CH
T. Riemann[a]	riemann@ifh.de

[a] FORTRAN code gentle_4fan.f
[b] FORTRAN code gentle_nc_qed.f

Description of the package

The GENTLE/4fan package is designed to compute selected total four-fermion production cross-sections and final-state fermion pair invariant mass distributions for charged current (CC) and neutral current (NC) mediated processes within the Standard Model (SM). For the *CC03* subprocess, the W production angular distribution is also accessible. In the NC case, SM

Higgs Production is included. The phase space integration is carried out by a semi-analytical technique, which is described below. The `GENTLE/4fan` package is written in `Fortran`. It consists of two branches. The basic branch `gentle_4fan.f` contains all features of the package but complete initial-state radiation (ISR) to *NC* processes. The subroutine `fourfan.f` called by `gentle_4fan.f` performs the computation of *NC* cross-sections and is described in [21]. The (as yet) independent branch `gentle_nc_qed.f` includes complete ISR to *NC02* and *NC08* and will soon be merged into `gentle_4fan.f`.

Program features:

1. **Method of integration:**
   The package is a *semi-analytical* one. Without (with) ISR, the phase space is parametrized by five (seven) angular variables and the final state fermion pair invariant masses (plus the reduced center of mass energy squared). All angular variables are integrated analytically. The resulting formulae are input to the package. Invariant masses are subsequently integrated numerically with a self-adaptive Simpson algorithm. Optionally, for the *CC03* subprocess, the W production angle may also be numerically integrated. The method is numerically stable and usually very fast.

2. **Possible final states:**
   The package may treat all four-fermion final states which do not contain identical particles, electrons, or electron neutrinos. This means that the package accesses all final states that are described by *annihilation* and *conversion* type Feynman diagrams (see [5] for a classification):

   (1) *CC03* (with complete ISR) [22]

   (2) *NC02*, *NC08* (with complete ISR) [23]

   (3) *CC9*, *CC10*, *CC11* [2]

   (4) *NC06*, *NC10*, *NC24*, *NC32* [24]

   (5) *NC* + Higgs [6]

   Via flags, cross-sections for subsets of Feynman diagrams may be extracted.

3. **Cuts**
   Cuts may be imposed on invariant masses of fermion pairs and on the invariant mass of the final state four-fermion system. Using the structure function approach in `gentle_4fan.f`, cuts on the electron/positron momentum fraction can be imposed. For the *CC03* subprocess, cuts on the W production angle are enabled.

4. **Initial state radiation**
   ISR is implemented into the package. *Universal* ISR is present for all processes [2]. In addition, the package includes complete, i.e. *universal* and *non-universal* ISR for the *CC03*, *NC02*, and *NC08* processes [22, 23]. *Non-universal* ISR does not contribute to *annihilation* diagrams. It may be argued that *non-universal* ISR is very small, $\mathcal{O}(10^{-3})$,

for *conversion-annihilation* interferences. The speed of the package is slowed down, if *non-universal* ISR is included, due to its complex analytical structure.

5. **Final state radiation**
   Final state radiation is not implemented.

6. **Treatment of final state decays**
   Final state decays are not accounted for.

7. **Treatment of the Coulomb Singularity**
   The Coulomb singularity is included according to reference [25].

8. **Treatment of the Anomalous Couplings**
   Anomalous couplings are not included.

9. **Treatment of masses**
   In general, final-state masses are neglected in the matrix elements. Where needed, however, masses are retained in the phase space. In addition, masses of heavy particles coupling to the Higgs boson are taken into account where appropriate.

10. **Hadronization**
    No interface to hadronization is foreseen.

Input parameters

All input parameters are set inside the `Fortran` code. `gentle_4fan.f` uses the following flags, set in the subroutine `WWINOO`:

`IBCKGR`: *CC03* case (`IBCKGR`=0) or *CC11* case (`IBCKGR`=1)
`IBORNF`: Tree level (`IBORNF`=0) or ISR corrected (`IBORNF`=1) quantities
`ICHNNL`: *CC03* (`ICHNNL`=0), *CC11* with specific final state [$l_1\nu_1 l_2\nu_2$(`ICHNNL` = 1), $l\nu q\bar{q}$ (`ICHNNL` = 2, 3), $q_1\bar{q}_1 q_2\bar{q}_2$ (`ICHNNL` = 4)], and inclusive *CC11* (`ICHNNL`=5)
`ICOLMB`: Inclusion of Coulomb singularity (`ICOLMB`=1,...,5) or not (`ICOLMB`=0)
Recommended value: `ICOLMB`=2
`ICONVL`: Flux function (`ICONVL`=0) or structure function apporach (`ICONVL`=1)
Recommended value: `ICONVL`=0
`IGAMZS`: Constant Z width (`IGAMZS`=0) or s-dependent Z width (`IGAMZS`=1)
`IINPT`: Input for tuned comparison (`IINPT`=0) or preferred Input (`IINPT`=1)
`IIQCD`: Naive inclusive QCD corrections are included (`IIQCD`=1) or not (`IIQCD`=0)
`IMMIM`: Minimal number of a moment requested by `IREGIM`
`IMMAX`: Maximal number of a moment requested by `IREGIM`
`IONSHL`: On-shell (`IONSHL`=0) or off-shell heavy bosons (`IONSHL`=1)
`IPROC` : *CC* case (`IPROC`=1) or *NC* case (`IPROC`=2, call to `fourfan.f` is initialized)
`IQEDHS`: Determination of the *universal* ISR radiator:
$\mathcal{O}(\alpha)$ exponentiated (`IQEDHS`=–1,0);
$\mathcal{O}(\alpha)$ exponentiated plus different $\mathcal{O}(\alpha^2)$ contributions (`IQEDHS`=1,...,4)
Recommended value: `IQEDHS`=3

IREGIM:	Calculation of the total cross-section (IREGIM=0), the moments of the radiative loss of final state four-fermion invariant mass (IREGIM=1), the moments of the radiative energy loss (IREGIM=2), the moments of the W mass shift $\left(\sqrt{s_+}+\sqrt{s_-}-2M_W\right)$ (IREGIM=3), and the first moments of $\cos(n\theta_W)$, $n = 1, ..., 4$ (IREGIM=4)
IRMAX :	Maximum value of IREGIM
IRSTP :	Step in a DO loop over IREGIM
ITVIRT:	*Non-universal* virtual ISR included (ITVIRT=1) or not (ITVIRT=0)
ITBREM:	*Non-universal* bremsstrahlung included (ITBREM=1) or not (ITBREM=0)
IZERO :	See equation (4.5) of [2]. Recommended value: IZERO=1
IZETTA:	See equation (4.21) of [2]. Recommended value: IZETTA=1

In the gentle_nc_qed.f branch, only the flags IBORNF, IONSHL, ITVIRT, ITBREM are used. The additional flag IBOSON in gentle_nc_qed.f distinguishes between the *NC02* and the NC8 process.

The center of mass energy squared is chosen by setting the variable IREG and the parameters ISMAXA or ISMAXB in the main program. The following input may be changed by the user:

GFER	=	G_μ	=	1.16639×10^{-5} GeV^{-2}, the Fermi coupling constant
ALPW	=	$\alpha(2M_W)$	=	$1/128.07$, the running fine structure constant at $2\,M_W$
AME	=	m_e	=	$0.51099906 \times 10^{-3}$ GeV, the electron mass
AMZ	=	M_Z	=	91.1888 GeV, the Z mass,
AMW	=	M_W	=	80.230 GeV, the W mass
GAMZ	=	Γ_Z	=	2.4974 GeV, the Z width
ALPHS	=	$\alpha_s(2M_W)$	=	0.12

Output

The following derived quantities are computed in gentle_4fan.f and printed in the output:

$$
\begin{aligned}
\texttt{GAMW} &= \Gamma_W = \frac{9}{6\sqrt{2}\pi}\,G_\mu M_W^3\left(1+\frac{2\alpha_s(2M_W)}{3\pi}\right)\\
\texttt{SIN2W} &= \sin^2\theta_W = 1 - M_W^2/M_Z^2\\
\texttt{GAE} &= -\frac{e}{4s_W c_W} = -\frac{\sqrt{4\pi\alpha(2M_W)}}{4s_W c_W}\\
\texttt{GVE} &= \texttt{GAE}\cdot(1-4s_W)\\
\texttt{GWF} &= \frac{g}{2\sqrt{2}} = -\texttt{GAE}\cdot\sqrt{2}c_W\\
|\texttt{GWWG}| &= \sqrt{4\pi\alpha(2M_W)}\\
|\texttt{GWWZ}| &= |\texttt{GWWZ}|\cdot\frac{c_W}{s_W}
\end{aligned}
$$

GVE and GAE are the electron vector and axial vector couplings, GWF is the fermion-W coupling, and |GWWG| and |GWWZ| are the trilinear gauge boson couplings for the photon and the Z

respectively. Further the output repeats the flag settings. After the cross-section calculation, the following output is printed:

$$\begin{aligned} \texttt{SQS} &= \sqrt{s} \\ \texttt{XSEC0} &= \sigma_{\rm tot}(s) \quad \text{in nanobarns} \end{aligned} \tag{6}$$

In addition, the calculated `MOMENTS` are printed. In the first column `IREGIM` is printed. The second column is arranged in blocks of three lines each. The first line contains the integer n. The second line contains the n^{th} moment of the physical quantity indicated by `IREGIM`. The third line contains the dimensionless n^{th} moment obtained through division of the n^{th} moment by the proper power of $\sqrt{s}/2$.

Although variable names are slightly different, `gentle_nc_qed.f` uses the same derived quantities as `gentle_4fan.f`. For one run, `gentle_nc_qed.f` outputs the used flag values together with the fermion code numbers `IFERM1/IFERM2`, the color factors `RNCOU1/RNCOU2`, the masses `AM1/AM2`, and the invariant pair mass cuts `CUTM12,CUTM34` for the final state fermion pairs. In addition, the lower cut `CUTXPR` on the ratio of the four-fermion invariant mass squared over the center of mass energy squared, s'/s is output. The main output, however, is an array of center of mass energies and the corresponding total cross-sections.

Availability
The codes are available from the authors upon E-Mail request or via WWW

`gentle_4fan.f`	from	`http://www.ifh.de/~bardin/gentle_4fan.uu`
`gentle_nc_qed.f`	from	`http://www.ifh.de/~lehner/gentle_nc_qed.uu`

2.6 grc4f 1.0

Authors:

J. Fujimoto	junpei@minami.kek.jp
T. Ishikawa	tishika@gal.kek.jp
T. Kaneko	kaneko@minami.kek.jp
K. Kato	kato@sin.cc.kogakuin.ac.jp
S. Kawabata	kawabata@minami.kek.jp
Y. Kurihara	kurihara@minami.kek.jp
D. Perret-Gallix	perretg@cernvm.cern.ch
Y.Shimizu	shimiz@minami.kek.jp
H.Tanaka	tanakah@minami.kek.jp
e-mail:	grc4f@minami.kek.jp

Program features

The program `grc4f` is a Monte Carlo generator for all final 4-fermion states generated by `GRACE`[26].

Several experimental cuts are implemented in default.
QED radiative corrections are implemented with structure functions for the ISR; in several processes QED parton shower (QEDPS) [27] is also an option, also for FSR.
Other final-state decays are implemented using `JETSET`, [28]. Color base information (related to the issue of color reconnection) is available.
The Coulomb term, and anomalous couplings, are both implemented.
Fermion masses can be kept nonzero everywhere.

Program layout

Integration

The numerical integration of the differential cross section over the phase space is carried out by the program `BASES` [29]. The probability information is automatically produced and saved in the file `bases.data`, according to which the event generation is done. An example is as follows:

```
call bsinit                      initialization of BASES/SPRING.
call userin                      initialization of parameters.
call bases( func, estim, sigma, ctime, it1, it2 )  integration
lun = 23
open(lun,file='bases.data',status='unknown',form='unformatted')
call bswrit( lun )               saving the information to a file.
close ( lun )
```

In the arguments of subroutine `bases`, `func` is the name of a function program, `estim` is the cumulative estimate of the integral, `sigma` is the standard deviation of the estimate of the integral, `ctime` is the computing time in seconds and `it1` and `it2` is the number of iterations made in the grid optimization step and integration step.

Event generation

The event generation program `SPRING`[29] samples a hypercube according to `bases.data`, and tests if this point is accepted by comparing the probability at the point to the maximum probability in the hypercube. When `SPRING` accepts a point, the event corresponding to the point is generated with weight one. An example is as follows:

```
implicit real*8 (a-h,o-z)
parameter( nextrn = 6 )
common /sp4vec/ vec(4,nextrn)
....
real*4  p,v
common /lujets/ n,k(4000,5),p(4000,5),v(4000,5)
.....
call bsinit                      initialization of BASES/SPRING.
call userin                      initialization of parameters.
lun = 23
open(lun,file='bases.data',status='old',form='unformatted')
```

```
      call bsread( lun )              reading the probability information.
      close( lun )

      call gr2lnd                     setting parameters for JETSET from GRACE.

*===> Event generation loop
      mxtry  = 50                     number of maximum trials.
      mxevnt = 10000                  number of events.
      do 100 nevnt = 1, mxevnt
         call spring( func, mxtry )
        ( Four-momentum is stored in array vec.)
        ( The event information is converted into common block /lujets/.)
  100 continue
```

Input parameters

In the program `grc4f` the menu modes are supported using the command interpreter **KUIP**[30] developed at CERN and the identical environment to **PAW++**[31] is furnished to users, who select the menu and type parameters in menu windows.

- Selection of 4 fermion process.
- Center of mass energy:$\sqrt{s}$
- Mass and width of all particles.
- Experimental cuts
  - Minimum and maximum angle cuts for each particles (in the laboratory frame) (`coscut`).
  - Minimum and maximum energy cuts for each particles(`engyct`).
  - Minimum and maximum invariant mass cuts(`amasct`). ($Q_1 = (p_3 + p_4)^2$, $Q_2 = (p_5 + p_6)^2$)
  - Resonance mass and width in case of $1/Q_i$-singularity.
- Flag for Coulomb term.
- Flag for anomalous couplings in some processes.
- Selection of the calculation: no-radiation case, structure functions, or QEDPS.
- Parameters for integration step: number of iteration steps and number of sample points.
- Parameters for event generation step: maximum number of trials and number of events.

The general parameters in GRACE can be found in the GRACE manual[26] (spin polarization, graph selection and so on).

Output:

- Total cross section, the standard deviations and the convergence behavior in the integration steps.
- Histograms:
  - $d\sigma/dE_i, i = 3, 4, 5, 6$:Energy distributions of each final particles
  - $d\sigma/d\cos\theta_i, i = 3, 4, 5, 6$
  - Invariant Masses Q_1 and Q_2.
- Scatter plots:
  - $\cos\theta_i$ – E_i
  - Q_1 – Q_2.

The contents of histograms and scatter plots are copied into the HBOOK format file[32].

Availability
By anonymous ftp to ftp location: `/kek/minami/grc4f` at `ftp.kek.jp`

2.7 KORALW 1.03

Authors:

M. Skrzypek	skrzypek@hpjmiady.ifj.edu.pl
S. Jadach	jadach@cernvm.cern.ch
W. Płaczek	placzek@hephp02.phys.utk.edu
Z. Wąs	wasm@cernvm.cern.ch

Description
This program includes not only QED effects in the initial state but also in leptonic decays of W and secondary decays, i.e. in the τ lepton decays. Hadronization of quarks is also performed. The effects of spin are included in combined W-pair production and decay. The τ polarization is also taken into account in its decays. Any experimental cut and apparatus efficiency may be introduced easily by rejecting some of the generated events.

Program changes from version 1.02 to 1.03

Here we describe the main properties of the generator KORALW. We do not present the program, which was published in [33]-[34]. The present version 1.03 features all properties of the previous version 1.02:

- The matrix element for W-pair production and W-pair decay into four fermions (the *CC03* group) with a proper W-spin treatment and finite W width,
- All W decay channels into pairs of leptons or quarks,
- Initial-state multi-photon emission in the full photon phase space (i.e. with finite transverse photon momenta),
- Simulation of the decay of polarized τ leptons (from W decay) in all possible channels, taking into account spin polarization and QED bremsstrahlung [35].
- Photon emission by leptons in W decay, up to double bremsstrahlung [36].
- Arrangement of quarks from W decay into colored strings and fragmentation into hadrons according to the LUND model using `JETSET` [28].
- Massive kinematics with exact four-momentum conservation for the entire W^-W^+ production and decay process.

In version **1.03** the following four major improvements have been introduced:

- Coulomb correction, in a form useful close to the WW threshold.It is taken from ref. [37] and it can be activated in straightforward way, as explained in the program documentation. Starting from the present `KORALW` version `1.03`, the `KeyCul` component of the program input parameter `NPAR(1)` is thus *not* dummy anymore.
- `KORALW` now includes an interface to the external library calculating the correction-weight due to a more complete matrix element (so called background processes). At present, an interface to the `GRACE` library [26] calculating multi-diagram matrix elements is available. On occasion, one may wish to replace the matrix element by a different one, for instance including special combinations of anomalous couplings. Due to the modular structure of `KORALW` and, in particular, due to the full factorizability of the approximate QED matrix element into a Born matrix element and the QED part, it is straightforward to replace the existing Born-level matrix element with any other one, provided that the external library is able to calculate the corresponding matrix elements out of the externally generated four-momenta. To this end an external program, calculating the ratio of the matrix element squared of the particular choice to the basic matrix element squared of the program, has to be provided by the user.

  A pre-defined interface, now included in `KORALW`, will activate those routines with the help of `Key4f` component of `KORALW` input parameter `NPAR(4)= 100*KeyACC +10*Key4f +KeyMix`. For `Key4f=0` no external matrix element is included and for `Key4f=1` it is active. The new position of the weight switch, `KeyWgt=NPAR(3)` is also introduced. For `KeyWgt=2` the program works as for the old and not modified `KeyWgt=0` setting, but the external weights are calculated and transmitted to the common block `wgtall`.

In our distribution directory (see section 4 of program documentation) the additional fortran file is introduced in the directory `interfaces`. On the user side, his own directory has to replace the directory `ampli4f`. The following two routines have to be provided: `AMPINI(XPAR,NPAR)` which should initialize the external matrix element library. Standard `KORALW` input parameter matrices `XPAR` and `NPAR` can be used there for the initialization purposes. The `SUBROUTINE AMP4F(Q1,IFBM1,Q2,IFBM2, P1,IFL1,P2,IFL2,P3,IFL3,P4, IFL4, WTMD4F,WT4F)` should calculate ratio `WTMD4F`, of the new matrix element squared, and the one of the standard `KORALW`. The `Q1,IFBM1,Q2,IFBM2,P1,IFL1,P2,IFL2,P3, IFL3, P4,IFL4` denote respectively four momenta and identifiers (accordingly to the PDG conventions [38]) of initial state effective beams and the final state fermion states before final state bremsstrahlung generation. The additional vector weight `WT4F(I), I=1,9` may optionally be filled by routine `AMP4F`. It is not used in the program but only transmitted to the `KORALW` optional weights common block `wgtall` as `wtset(40+I)`. The `WTMD4F` is set into `wtset(40)`.

An example of the interfaced external matrix-element, based on the `GRACE` code [26], can be obtained upon request from the authors of `KORALW`. In the distribution version we include a dummy `ampli4f` library. It sets the external weight to 1 and prints a warning message.

We found it useful to introduce the `KeyWu` switch which controls the level of sophistication of the W width implementation. Like for the Z (`KeyZet`) case `KeyWu`=0,1,2 denotes respectively $(s/M_W)\Gamma_W$, constant and zero W width. Note that `NPAR(2)= 100000*KeyWu +10000*KeyRed +1000*KeySpn+100*KeyZet +10*KeyMas +KeyBra`.

- Anomalous couplings for the WWV, $V = Z, \gamma$ vertices in the built-in matrix element are parameterized by 2×7 variables $g_1^V, g_4^V, g_5^V, \lambda_V, \kappa_V, \tilde{\lambda}_V, \tilde{\kappa}_V$ as defined in [41]. They can be reached by `KeyACC` component of `KORALW` input parameter `NPAR(4)=100*KeyACC+10*Key4f +KeyMix`. `KeyACC=1` activates their values as set by the user via `KORALW` input parameter vector `xpar` (see routine `KORALW` for more details) and prints them to the output. `KeyACC=0` enforces the Standard Model values.

- The semianalytical part of the program `KORWAN` was enlarged with two functions `s1wan(s1)` and `s1s2wan(s1,s2)` for the one and two dimensional distribution of the single or double W invariant masses. These functions require standard initialization of the `KORWAN` routine with the input parameters as explained in `KORALW` manual. Optionally, if the `KORWAN` input parameter `keymod` is increased by 10000 the calculations in `KORWAN` are not executed and the initialization is performed only.

Still remaining limitations of the program are:

- A simplified matrix element for the QED photon emission,
- Lack of electroweak non-QED corrections[6],

[6]Most probably these corrections are small in comparison with the experimental precision and it is not

- A simplified "color arrangement" for four quark jets.

The above and other shortcomings of the program will be systematically addressed in the forthcoming versions of the program.

Availability
The Version: 1.03 is available from
www: http://hpjmiady.ifj.edu.pl/programs/programs.html

2.8 LEPWW

Author:

F.C. Erné z63@nikhef.nl

Description

The original `LEPWW` event generator[39] contains *CC03* and *NC02* tree-level diagrams for the processes $e^-e^+ \to u\bar{u}u\bar{u}$, $e^-e^+ \to u\bar{u}d\bar{d}$ and $e^-e^+ \to u\bar{u}d\bar{d}$, with massless fermions and W and Z poles. Its present name and version is 'egwwv208.car' in the L3 event generator library. A FORTRAN file is available.

Features of the program

A complete set of final state fermions is available.

Order α initial-state radiation, allowing transverse momentum, is implemented following the procedure in the REMT routines[40].

Final state radiation from electrons, muons and τ's can be switched on optionally, according to the `PHOTOS` package[36].

For τ decay final lepton states of definite helicity are projected out, which allows decay through an adapted version of the `TAUOLA` routines[35].

Non-SM couplings have been implemented with the parameterization of Hagiwara et al[41].

Quark fragmentation proceeds through `JETSET` routines[28].

QCD effects on the boson widths and branching ratios can be taken into account.

No Coulomb term is implemented.

The program aims at a 1 to 2% precision in the description of total and differential processes. The program has been available throughout the LEP2 workshop. The development has been completed.

necessary to include them in the Monte Carlo program – it is enough if they are in the auxiliary semi-analytical program.

Input parameters: data cards

FAW, FAZ	fudge factors for W and Z width
PROC	Generate WW or ZZ
DKW1,DKW2	Decay of W^+, W^- into $q\bar{q}$, $e\nu$, $\mu\nu$, $\tau\nu$
DKZ1,DKZ2	Decay of $Z1, Z2$ into $q\bar{q}$, $\nu\bar{\nu}$, e^+e^-, $\mu^+\mu^-$, $\tau^+\tau^-$
IRAD,FRAD	Flags for initial and final-state radiation
WMAX	Maximum weight
F1G-F7Z	Fourteen variables for the Triple Boson Vertex
LEP2	LEP2 workshop parameters; it overrules the other data cards

Availability
`http://www.fys.ruu.nl/~dieren/LEPWW.html`

2.9 LPWW02

Authors

Ramon Miquel	miquel@alws.cern.ch
Michael Schmitt	schmitt@vxaluw.cern.ch

General description
`LPWW02` is a Monte Carlo program for the simulation of four-fermion final states at LEP2. It contains the Feynman diagrams with two resonating W's and Z's and features, among other things, initial- and final-state radiation, Coulomb singularity effects and effective couplings. It is interfaced to the `JETSET` package to handle gluon radiation, hadronization and decays.

The generator is based on a complete Monte Carlo calculation of the cross section for the process $e^+e^- \to f_1\bar{f}_2 f_3\bar{f}_4$ through a pair of heavy bosons, WW and/or ZZ [42]. Initial- and final- state radiation are incorporated with structure functions. The Monte Carlo algorithm for event generation uses two subgenerators to generate the WW and ZZ topologies. Suitable approximants are used in the generation step to increase its efficiency using the importance sampling technique. At the end, a rejection algorithm ensures that the unweighted events produced are distributed according to the exact matrix element. A complete description of the physics in the program, with results and comparisons with other calculations is available [43].

Features of the program

- `LPWW02` is a Monte Carlo event generator of unweighted events. Any cut can be applied to the generated events.
- The accessible final states are those that can be produced in e^+e^- collisions from intermediate states consisting on two W bosons or two Z bosons: $u\bar{d}\mu^-\bar{\nu}_\mu$, $u\bar{u}\mu^+\mu^-$, $u\bar{u}d\bar{d}$,... In flavor configurations like the last one, the interference between the WW and ZZ diagrams is properly taken into account. In a given run, the user can either specify a fixed final

state or get directly the correct flavor mix for events produced through two W's and/or two Z's.

- Initial state radiation is simulated using the structure-function approach [44, 45]. The Born-like cross section at the reduced center-of-mass energy after initial-state radiation is convoluted with the structure functions of the electron and positron, which take into account their probabilities to radiate. The electron structure function, $D_e(z,s)$, taken from ref. [45], includes soft-photon exponentiation and leading-logarithmic corrections up to $\mathcal{O}(\alpha^2)$. The structure function approach is used in the collinear approximation and, hence, the photon direction is assumed to be that of the incoming beams. Consequently, no real photon four-momenta are generated inside the experimentally accessible regions of phase space. Since the radiation not only changes the effective center-of-mass energy of the event, but also the center-of-mass momentum with respect to the laboratory system, a boost is applied to the generated particles to take this into account.

- We employ the `PHOTOS` package [36] to simulate radiation from final state electrons and muons. Radiation from quarks is taken care of by the `JETSET` package [28] Radiation from taus or their decay products is neglected. The algorithm in `PHOTOS` provides full kinematic information for the splitting $f \to f'\gamma$. It is based on an implementation of $\mathcal{O}$ (α^2) bremsstrahlung calculation in the leading-log approximation. This means that final-state radiation does not influence the total cross section calculation in any way.

- In the first stage, the program produces a final state consisting on four-fermion plus a number of photons. The interface with `JETSET` takes care of hadronization and subsequent decays of hadrons. `JETSET` also takes care of decaying the tau leptons.

- We have implemented the Coulomb correction in the production of two W's following ref. [46]. It is numerically equivalent to the treatment of ref. [25].

- At this time, the possibility of anomalous couplings is not contemplated in the program.

- The fermions are generated with their appropriate masses. However the matrix element is computed in the massless limit.

- `LPWW02` is interfaced with `JETSET`.

- It is straight-forward to get the information on the contributions from different sets of diagrams in view of a possible simulation of the effect of color recombination.

Program layout

The structure of the program can be summarized as follows:

- Initialization. It includes the computation of the maximum weight for the rejection algorithm that will be used later and the initialization of the `PHOTOS` package used for final-state radiation.

- Event Loop. A fixed number of unweighted events are generated. There are a number of steps:
  - The electron and positron effective energies at collision point after radiation are generated.
  - The final state flavor is chosen randomly according to some approximate probabilities that take into account Cabibbo mixing. Alternatively, the final state can be fixed to a particular combination of flavors.
  - One of two subgenerators is chosen randomly to generate the event kinematics. One of them maps the peaks for the WW channel, the other for the ZZ channel.
  - The exact matrix element squared is computed. A weight is assigned to each event according to the ratio of the exact matrix element squared to the approximate weights used in the generation stage, including the ones for choice of flavor composition and initial-state radiation.
  - A rejection algorithm is applied to the final weight to get unweighted events.
  - The four momenta are given their corresponding masses, readjusting the kinematics of the event. The event is boosted to the lab frame according to the incoming electron and positron effective energies.
  - `PHOTOS` is called to provide final-state radiation off electrons and muons only.
  - `JETSET` is invoked to take care of hadronization, decays and final state radiation off quarks or hadrons.
  - Four-vectors are stored in the standard Lund common block.
- Final: The cross section is computed with statistical error. A summary of the run is given.

Input Parameters and Flags

The following is a description of the input parameters and flags together with the values used for the tuned comparisons:

- `XMZ=91.1888`, mass of the Z (GeV).
- `XMW=80.23`, mass of the W (GeV).
- `ALFA0=137.0359895`, $1/\alpha_{QED}(0)$. Used for the photon radiation.
- `ALFA=128.07`, $1/\alpha_{QED}(s)$.
- `GF= 1.16639E-5`, Fermi constant.
- `ALFAS=0.`, $\alpha_s(M_W^2)$. Set to zero for the tuned comparisons.

- WWUSER=2.03367, user value for W width. Ignored if UWFLAG=0.
- ZWUSER=2.4974, user value for Z width. Ignored if UWFLAG=0.
- IRFLAG=1, generate initial-state radiation (1) or not (0).
- CSFLAG=0, include the Coulomb correction (1) or not (0)
- BWFLAG=1, Breit-Wigner with mass-dependent (1) or constant (0) width.
- ASFLAG=0, apply α_s correction for widths (1) or not (0).
- FRFLAG=0, generate final-state radiation (1) or not (0) (PHOTOS).
- IZFLAG=0, include contributions from ZZ diagrams (1) or not (0).
- ILFLAG=0, invoke JETSET for showers, fragmentation, and decay (1) or not (0).
- UWFLAG=1, use total W and Z widths from the user (1) or the SM (0).

The preferred values would differ from the previous ones in the following:

- ALFAS=0.12
- CSFLAG=1
- ASFLAG=1
- FRFLAG=1
- IZFLAG=1
- ILFLAG=1
- UWFLAG=0

Output

The program's output consists on the result of the cross section for the required final state. An estimate of the statistical error is also provided. The four-momenta of the generated particles are available in the event loop through the standard Lund common block.

Availability of the program

LPWW02 is available from the authors.

2.10 PYTHIA 5.719 / JETSET 7.4

Author:

Torbjörn Sjöstrand torbjorn@thep.lu.se

Description

PYTHIA/JETSET is a general-purpose event generator for a multitude of processes in e^+e^-, ep and pp physics [47, 48]. The emphasis is on the detailed modeling of hadronic final states, i.e. QCD parton showers, string fragmentation and secondary decays. The electroweak description is normally restricted to improved Born-level formulae, and so is not competitive for high-precision studies.

Features of the program

- Monte Carlo event generator.
- By default any final state allowed for a process is included in the generation, but it is possible to select a specific combination of final states with large flexibility.
- Several cuts are available, if desired. Examples include the mass ranges for the hard scattering process and for resonances. It is not possible to set cuts directly on the four final fermions, however.
- ISR is implemented in a two-stage process. First structure functions are used to select x_1 and x_2 values for the hard scattering. Currently the structure function is the one recommended for LEP 1 [49], but it would be easy to expand to more alternatives. Thereafter a backwards evolution scheme is used to reconstruct explicit sequences of $e \to e\gamma$ branchings, including $p_\perp$ recoils. The algorithm used is essentially the same as originally developed for QCD applications [50].
- FSR is implemented inside each gauge boson system separately. For a W this means as it would have been obtained in the formal limit $\Gamma_W \to 0$. Again a parton-shower description is used, with explicit matching to the first-order matrix elements, as for final-state QCD radiation [51]. Quarks can radiate both photons and gluons.
- For the hard process $e^+e^- \to W^+W^-$, only x_1, x_2, the two W masses and one relative angle are selected [2], [22]. FS decays are considered in a second step, using the formulae of [52] to calculate the conditional probability for a set of four decay angles (two for each W). The philosophy is the same for other processes.
- Several optional Coulomb formulae are available [53]; the recommended one is the first-order expression in [54].
- No anomalous couplings.
- Finite fermion masses are included in the phase-space factors for partial widths.

- Hadronization comes built-in.
- Since the program does not include interference e.g. between the WW and ZZ processes, each individual event is uniquely assigned to a specific process, and this information is available to the user.

Program layout

At initialization, coefficients are optimized in the analytical expressions subsequently used to select kinematical variables (i.e. phase-space points will be picked more often in those regions where the matrix elements are peaked), and the corresponding maxima of differential cross sections are found. For each event, a process type and a phase-space point is selected by hit-or-miss Monte Carlo. That is, events come with unit weight (but an option with weighted events exists). The maximum found in the initialization is increased if one encounters a larger differential cross-section value. (Formally this introduces an error in the method, but when the increase occurs early in the run and/or is small, this error is negligible.) The cross-section information is improved with increasing statistics. After its selection, the hard scattering is gradually dressed up, by the addition of initial-state radiation, resonance decays, final-state radiation and hadronization.

Note that Γ_Z is not set independently in `PYTHIA`; rather it is given by electroweak relations and is thus too small when one asks for $\alpha_s = 0$.

Each event is listed in full in `COMMON/LUJETS/` (optionally also in `COMMON/HEPEVT/`), so any experimentally definable quantity can be extracted. Also other pieces of event information is available in common blocks. A table of cross sections can be obtained, but this does not include error estimates.

Availability and documentation
The master copies of the programs, documentation and sample main programs are available at web address http://thep.lu.se/tf2/staff/torbjorn/.

The main reference is [47]. A full manual and physics description (over 320 pages) is [48]. An overview, with a table of the most interesting subprocesses, is given in the QCD generators section of this report.

2.11 WOPPER 1.4

Authors:

Harald Anlauf	anlauf@crunch.ikp.physik.th-darmstadt.de
Thorsten Ohl	Thorsten.Ohl@Physik.TH-Darmstadt.de

General description:
`WOPPER` is a fairly standard Monte Carlo event generator for *un*weighted $e^+e^- \to 4f$ events [55]-[57]. Emphasis is put on leading logarithmic radiative corrections to $W^\pm$ pair production

(i.e. doubly resonant four-fermion production at LEP2). An extension to singly resonant four-fermion production is being tested and will be released as `WOPPER` version 1.5. `WOPPER` is interfaced with fragmentation and hadronization Monte Carlos to allow full simulation of event samples at LEP2.

Features:

- `WOPPER` is a Monte Carlo event generator with *un*weighted events, suitable for full simulation of event samples.
- All possible four-fermion final states are generated.
- All cuts can be applied to the final states.
- Initial state QED radiation is implemented in leading logarithmic approximation. The leading logarithms $\propto (\alpha/\pi)(\ln(s/m_e^2) - 1)$ from collinear and soft emission are summed to all orders in a parton shower algorithm using the first order non-singlet splitting functions. A finite p_T for photons and the hard scattering center of mass system is generated according to the $1/pk$ pole.
- Final-state QED radiation is not implemented.
- Decays of final states are left to external packages. Standard interfaces are implemented.
- Coulomb corrections are implemented with finite width according to ref. [25].
- Anomalous couplings are not implemented.
- Finite fermion masses are implemented in the kinematics, but the matrix elements are calculated in the massless limit.
- Fragmentation and hadronization are left to dedicated QCD Monte Carlos. The standard W^+W^-–QCD event generator interface is implemented.
- Currently, only charged current diagrams are implemented, therefore information on color reconnection is neither needed nor available.

Algorithm:

- `WOPPER`'s initialization phase starts with calculating the coupling constants from the input parameters according to the value of `scheme`. The maximum of the total hard cross section $\sigma(s, k_+^2, k_-^2)$ for off-shell $W^\pm$ pair production is determined to allow the generation of *un*weighted events. NB: $k_\pm^2$ do not really correspond to off-shell $W^\pm$'s for singly resonant contributions.

- For event generation, an off-shell $W^{\pm}$ pair is produced with the invariant mass reduced and the center of mass system boosted from radiative corrections. This pair is subsequently decayed, keeping all angular correlations among the four decay fermions.
- A Monte Carlo estimate of the total cross section based on the events generated so far can be requested at any time. In particular, it is produced in the clean-up phase.

Input parameters:

1. **Tuned comparison:**
   - `scheme`: 1, i.e. use G_F, M_W and $\alpha_{QED}(2M_W)$ as input and calculate $\sin^2\theta_W = \pi\alpha_{QED}(2M_W)/(\sqrt{2}G_F M_W^2)$ as well as $\Gamma_W = G_F M_W^3(3 + 2\alpha_{QCD}(2M_W)/\pi)/(\sqrt{8}\pi)$.
   - `mass1z`: $M_Z = 91.1888$
   - `gamm1z`: $\Gamma_Z = 2.4974$
   - `mass1w`: $M_W = 80.23$
   - `gfermi`: $G_F = 1.16639 \cdot 10^{-5}\,\mathrm{GeV}^{-2}$
   - `ahpla`: $1/\alpha_{QED}(2M_W) = 128.07$
   - `alphas`: $\alpha_{QCD} = 0$
   - `ckmvus`: $V_{us} = 0$
   - `ckmvcb`: $V_{cb} = 0$
   - `ckmvub`: $V_{ub} = 0$
   - `coulom`: `false`, i.e. no Coulomb correction
2. **Preferred input:** the input used in the *"Best You Can Do"* event samples is identical to the one used in the tuned comparison, except for
   - `alphas`: $\alpha_{QCD}(M_Z) = 0.123$
   - `ckmvus`: $V_{us} = 0.2196$
   - `ckmvcb`: $V_{cb} = 0.0400$
   - `ckmvub`: $V_{ub} = 0.0032$
   - `coulom`: `true`, i.e. apply Coulomb correction

In addition to the above G_F-scheme, the following schemes are available:

- `scheme` $= -1$: like `scheme` $= 1$, but for Γ_W, which is taken from the input parameter `gamm1w`
- `scheme` $= 2$: use `sin2w` ($\sin^2\theta_W$) as input and calculate $G_F = \pi\alpha_{QED}/(\sqrt{2}\sin^2\theta_W M_W^2)$

- `scheme` $= -2$: like `scheme` $= 2$, but for Γ_W, which is taken from the input parameter `gamm1w`
- `scheme` $= 3$: use `sin2w` ($\sin^2\theta_W$) and `gfermi` (G_F) as independent input parameters and force $\alpha_{QED}(s) = \alpha_{QED}(0)$
- `scheme` $= -3$: like `scheme` $= 3$, but for Γ_W, which is taken from the input parameter `gamm1w`

Output:
After startup and initialization, `WOPPER` prints a version number and a description of the selected input parameter scheme to standard output. Additional `print` commands can be used to print some or all internal flags and parameters. Generated events are stored in the standard `/HEPEVT/` common block and a user routine (by default "`call hepawk('scan')`") is called. At the end of the run, the total cross section and an error estimate is available in the last `/HEPEVT/` record.

Availability:
The `WOPPER` distribution can be obtained directly from the authors or from the internet

- WWW: `http://crunch.ikp.physik.th-darmstadt.de/monte-carlos.html#wopper`
- Anonymous FTP from `crunch.ikp.physik.th-darmstadt.de`, in the directory `pub/ohl/wopper`

Ready-to-run versions are available in the experimental LEP2 collaborations.

2.12 WPHACT

W W and Higgs Physics with **PHACT**

Authors:

E. Accomando accomando@to.infn.it
A. Ballestrero ballestrero@to.infn.it

General description

`WPHACT` is a program created to study four-fermion, WW and Higgs physics at present and future e^+e^- colliders. In its present form, it can compute all SM processes with four fermions in the final state. For NC processes involving b quarks, and no electrons in the final state, finite b masses can be fully taken into account.

Full tree-level matrix elements for all CC and NC processes are computed by means of subroutines which make use of the helicity formalism of ref. [58]. Their code has been written

semi-automatically through the set of routines PHACT [59] (**P**rogram for **H**elicity **A**mplitudes **C**alculations with **T**au matrices) which implements the method in a fast and efficient way.

In the above formalism, eigenstates of the fermion propagators are used to simplify matrix expressions. These eigenstates are chosen to be generalizations of the spinors used in ref.[60]. Essentially, the numerator of fermion propagators are diagonalized in the massless lines and have very simple expressions in the massive ones. The computation of fermion lines reduces to evaluating the matrices corresponding to insertions of vector or scalar lines and combining them together. This is performed most efficiently with the so-called *tau matrices* [58]. The program PHACT writes automatically the optimized fortran code necessary for every insertion and every combination, given the names of the vectors, couplings, etc. From various comparisons made, we have been convinced that in fact the codes for the amplitudes written in this way run very fast, and this is the case also for `WPHACT`.

Different phase spaces, with different random number mappings, are employed in order to take into account the peak structure of the resonating diagrams for the different processes. The adaptive routine `VEGAS`[9] is used for integrating over the phase space.

For additional information, see also the section on event generators for Higgs physics.

Features of the program

`WPHACT` is a Monte Carlo program. For all phase spaces used, all momenta are explicitly computed in terms of the integration variables. This implies that any cut can be implemented, and it can be easily used also as an event generator. The events obtained in this way are of course weighted. `VEGAS` is an adaptive routine, which normally runs a few iterations (good efficiency is normally obtained with about three iterations), seeking for a better grid of the integration space. If one doesn't want to generate too many events, it is better to use the events of the last iteration. Distributions for any variable can also be implemented. Even if various distributions have already been produced, and examples are available, no automatic implementation of distributions has yet been introduced.

All SM final states with four fermions can be calculated. No W's or Z's or Higgs are allowed in the final state. They are always appropriately considered as virtual particles.

Any cut can be performed. Initial state QED radiation is included through Structure Functions $\mathcal{O}(\alpha^2)$. FSR is not implemented. The Coulomb term is implemented with the approach of ref. [25]. Anomalous couplings are available. No interface to hadronization is available.

So far the only fermion masses which can be different from zero are those of quarks in NC processes relevant for Higgs production, like e.g. $e^+e^- \to b\bar{b}b\bar{b}$, $e^+e^- \to \nu_e\bar{\nu}_e b\bar{b}$, etc. The nonzero masses are fully taken into account both in the matrix element and in the phase space. Just because of the helicity formalism adopted, the massive case does not cost much more than the massless one in cpu time.

It is easy to obtain the contributions from different set of diagrams, as every diagram is

evaluated individually for all helicity configurations and then summed to the others before squaring and summing over helicity configurations. Actually, in the case of mixed CC and NC processes the two contributions are evaluated and integrated separately.

As far as speed is concerned, we give some indicative values about the running time on ALPHA AXP 2100/4 OVMS:

CPU time per call for *CC03* without ISR: 5.6×10^{-5} sec.

CPU time per call for *CC11* with ISR: 1.2×10^{-4} sec.

At Lep2 energies, 30 M calls (about one hour) are used to obtain *CC11* with ISR cross section with a typical estimated error of about 1×10^{-4}. The same process can be evaluated in about 2 minutes with 1 M calls at permille level. For *CC03* without ISR 20 M calls (20 minutes) give an estimated error of about 1×10^{-4} and 1 M calls (1 minute) are necessary for permille precision. The same programs are about 5 times slower on a VAXstation 4000/90.

Program layout

The variables by which the phase spaces are described are the W masses for CC contributions, the Z masses for NC contributions, together with the angle of the two virtual particles with respect to the beam, the decay angles in their rest frames, and x_1, x_2, the fractions of momenta carried by the electrons. Appropriate change of variables to take care of peaks in x_1, x_2, M_W or M_Z lead to the real integration variables. For every point chosen by the integration routine, the full set of four-momenta is reconstructed and passed to the subroutine which evaluates the differential cross section with the helicity amplitude formalism. For every point in the integration variables, i.e. for every set of four momenta chosen, `VEGAS` gives a weight which must be used together with the value of the cross section for producing distributions.

Four phase spaces are available and have been used for the different matrix elements contributions, depending on the number of possible resonances. Every single phase space integrates better that particular contribution it has been constructed for. After various tests we however found that the phase space suitable for double resonant contributions is quite precise also in evaluating all contributions together. It turns out to be faster than splitting the contributions and integrating them separately with automatic determination of the relative precision. At present all contributions are normally evaluated together with one single kind of phase space. When mixed CC and NC are present, it is better to run the two contributions separately (adding the interference to the biggest one), as the change of variables necessary to take care of the resonances depends on their masses.

Input parameters, flags, etc.

Normal input parameters are M_W, M_Z, α, α_S. In the tuned comparisons $sin^2\theta_W$ has also been given as an input, while it is usually derived from the relation $sin^2\theta_W = 1 - M_W^2/M_Z^2$.

The main flag of the program is `ich`, which chooses among different final states. Other flags allow to compute with (when their value = 1) or without (when their value = 0) ISR,

Coulomb corrections and α_S corrections. They are respectively : `isr, icoul, iqcd`. The last option refers at present only to CC10 processes. A flag (`iterm`) allows using (`iterm` = 1) or not (`iterm` = 0) some iterations (normally one is enough) for thermalizing. The number of iterations (`itmx`) and of points for iteration (`ncalls`) for the thermalizing phase as well as for the normal one and the accuracy required (`acc`) are read from the input.

Output

The output is just the standard `VEGAS` output, from which one can read the final result and estimated statistical error, as well as the result and error for every iteration. Results with big oscillations among different iterations and corresponding big reported χ^2 simply mean that the number of evaluations per iteration was not sufficient for the integrand, and have to be discarded.

Concluding remarks

As already stated, `WPHACT` makes use of matrix elements which run fast. Speed is in our opinion a relevant issue, not only because it allows to perform complicated calculations, but also for rather short ones. In Monte Carlos, speed corresponds to the possibility of generating in the same time many more events, achieving a much better precision in integration.

The program , which does not make use of any library, has proved to be reliable over a vast range of statistical errors from the percent up to 10^{-5}. Thus it can be used both to obtain very precise results with high statistics runs and to get fast answers.

Availability:
The program is available from the authors or by anonymous ftp from
ftp.to.infn.it/pub/ballestrero.

2.13 WTO

Author:

Giampiero Passarino giampiero@to.infn.it

`WTO` is a *quasi-analytical, deterministic* code for computing observables related to the process $e^+e^- \to \bar{f}_1 f_2 \bar{f}_3 f_4$. The full matrix elements are used and in the present version the following final states are accessible (see [5] for a general classification):

1. *CC03*, *CC11*, *CC20*, *NC21*, *NC24*, *NC32*, *mix43*
2. *NC23* (= *NC21* + Higgs signal), *NC25* (= *NC24* + Higgs signal)

Further extensions will be gradually implemented. To fully specify `WTO`'s setup an option must be chosen for the renormalization scheme (RS). One has the options commonly used for tuned comparisons or the default, i.e.

$$s_W^2 = \frac{\pi\alpha(2M_W)}{\sqrt{2}G_\mu M_W^2}, \qquad g^2 = \frac{4\pi\alpha(2M_W)}{s_W^2}, \tag{7}$$

$$s_W^2 = 1 - \frac{M_W^2}{M_Z^2}, \qquad g^2 = 4\sqrt{2}G_\mu M_W^2 \tag{8}$$

where $\alpha^{-1}(2M_W) = 128.07$ and G_μ is the Fermi coupling constant. Final state QCD corrections are not taken into account in the present version, except for the Higgs signal (NC21-NC25) where the pole quark masses, $m_q(m_q^2)$, are in input. The code will compute the correct running, up to terms $\mathcal{O}(\alpha_s^2)$, i.e. $m_{b,c}(m_H^2)$ and will include 'effectively' a final state QCD correction.

The matrix elements are obtained with the helicity method described in ref.[61]. The whole answer is written in terms of invariants, *i.e.*

$$e^+(p_+)e^-(p_-) \rightarrow f(q_1)\bar{f}(q_2)f'(q_3)\bar{f}'(q_4), \tag{9}$$

$$x_{ij}s = -\left(q_{i-2}+q_{j-2}\right)^2, \quad x_{1i}s = -\left(p_+ + q_{i-2}\right)^2, \tag{10}$$

$$x_{2i}s = -\left(p_- + q_{i-2}\right)^2, \quad s_1 s^2 = \epsilon\left(p_+, p_-, q_1, q_2\right), \ldots \tag{11}$$

and the integration variables are chosen to be $m_-^2 = x_{24}$, $m_+^2 = x_{56}$, $M_0^2 = x_{45}$, $m_0^2 = x_{36}$, $m^2 = x_{35}$, $t_1 = x_{13}$, $t_W = x_{13}+x_{14}$. The convention for the final states in `WTO` is: $e^+e^- \rightarrow 1+2+3+4$. For CC processes $1 = d, 2 = \bar{u}, 3 = u', 4 = \bar{d}'$, with $u = \nu, u, c$ and $d = l, d, s, b$. For NC processes the adopted convention is $1 = f, 2 = \bar{f}, 3 = f'$ and $4 = \bar{f}'$. Initial state QED radiation is included through the Structure Function approach up to $O(\alpha^2)$. The code will return results according to three (pre-selected) options, i.e $\beta^2\eta$ (default) [62], β^3 [63] and $\beta\eta^2$ [7] where $\beta = 2\,\frac{\alpha}{\pi}\left(\log\frac{s}{m_e^2} - 1\right)$, $\eta = 2\,\frac{\alpha}{\pi}\log\frac{s}{m_e^2}$. QED corrections also include the Coulomb term correction [25] for the *CC03* part of the cross section. When initial-state QED radiation is included, there are two additional integrations over the fractions of the beam energies lost through radiation, $x_\pm$. This description of the phase space gives full cuts-availability through an analytical control of the boundaries of the phase space. Upon specification of the input flags it is therefore possible to cut on all final state invariant masses, all (LAB) final state energies $E_i, i = 1, 4$, all (LAB) scattering angles, $\theta_i, i = 1, 4$ all (LAB) final state angles, $\psi_{ij}, i, j = 1, 4$.

Both the matrix elements and the phase space are given for massless fermions. There is no interface with hadronization. The integration is performed with the help of the NAG [64] routine D01GCF. This routine uses the Korobov-Conroy number theoretic approach with a MC error estimate arising from converting the number theoretic formula for the n-cube $[0, 1]^n$ into a stochastic integration rule. This allows a 'standard error' to be estimated. Prior to a call to D01GCF the peak structure of the integrand is treated with the appropriate mappings.

Whenever the program is called it will start the actual calculation of one of the following observables: cross section or a pre-selected sample of moments of distributions, for instance $< x_\gamma^n >$. Since `WTO` does not generate hard and non-collinear photons, E_γ is just the total radiated photon energy. There is no adaptive strategy at work since the routine D01GCF,

being a deterministic one, will use a fixed grid. The evaluation of the specified observable will be repeated NRAND times to give the final answer, however there is no possibility to examine the partial results but only the average and the resulting standard error will be printed. The error in evaluating , say, a cross section, satisfies $E < CK\, p^{-\alpha} \log^{\alpha\beta} p$, where p =NPTS, α and C are real numbers depending on the convergence rate of the Fourier series, β is a constant depending on the dimensionality n of the integral and K is a constant depending on α and n.

Numerical input parameters such as $\alpha(0), G_\mu, M_{_Z}, M_{_W}, \ldots$ are stored in a BLOCK DATA. There are various flags to be initialized to run `WTO`. Here follows a short description of the most relevant ones:

NPTS - INTEGER, NPTS=1,10 chooses the actual number of points for applying the Korobov-Conroy number theoretic formulas. The built-in choices correspond to to a number of actual points ranging from 2129 up to 5,931,551.

NRAND - INTEGER, NRAND specifies the number of random samples to be generated in the error estimation (usually $5-6$).

OXCM - CHARACTER*1, the main decision branch for the process: [C(N)] for CC, (NC).

OTYPEM - CHARACTER*4,Specifies the process, i.e. *CC03*, *CC11*, *CC20* for CC processes and *NC19, NC24, NC21, NC25, NC32* for NC processes.

ITCM - INTEGER, the type of observable requested (0 for cross section). For *CC11* ($e^+e^- \to \mu^-\bar{\nu}_\mu u\bar{d}$) a number of distributions are available (for instance $< x_\gamma^n >$). If the n-th moment of a distribution is requested then

ITCNM - INTEGER, must be set to n.

OCOUL - CHARACTER*1, controls the inclusion of the Coulomb correction factor [Y/N].

IOS - INTEGER, two options $[1, 2]$ (1 =default for tuned comparisons) for the renormalization scheme.

IOSF - INTEGER, three options $[1-3]$ for the $\eta - \beta$ choice in the structure functions.

CHDM... - REAL, Electric charges, third component of isospin for the final states.

`WTO` is a robust one call - one result code, thus in the output one gets a list of all relevant input parameters plus the result of the requested observable with an estimate of the numerical error. A very rough estimate of the theoretical error (very subjective to say the least) can be obtained by repeating runs with different IOS, IOSF options. A rough estimate of the requested CPU time (on a VAXstation $4000 \cdot 90$) vs precision can be inferred from the following table which refers to $\sigma(e^+e^- \to \mu^-\bar{\nu}_\mu u\bar{d})$ at $\sqrt{s} = 161\,\mathrm{GeV}$

GENTLE			0.1269543
σ (nb)	0.1266300 $\pm$ 0.822D-03	0.1268430 $\pm$ 0.171D-03	0.1269526 $\pm$ 0.381D-05
W/G(%)	0.26	0.09	$1.\times 10^{-3}$
CPU	00:03:17.78	00:19:25.00	18:56:25.99

After initialization for the background process $e^+e^- \to \bar{\nu}_\mu \nu_\mu \bar{b}b$ with $M_z - 25\,\mathrm{GeV} < M_{\nu\nu} < M_z + 25$ GeV, $M_{\bar{b}b} > 30$ GeV and with the b angle with respect to the beams $> 20^o$, the typical output will look as follows:

```
This run is with:

NPTS         =  7
NRAND        =  6

E_cm (GeV) =          0.17500E+03
beta       =          0.11376E+00 sin^2     =          0.23103E+00
M_W  (GeV) =          0.80230E+02 M_Z (GeV) =          0.91189E+02
G_W  (GeV) =          0.20337E+01 G_Z (GeV) =          0.24974E+01

No QED Radiation
There are cuts on fs invariant masses, no cuts on fs energies,
cuts on scattering angles, no cut on fs angles

\emph{NC24}-diagrams : charges    -0.3333    0.0000
                isospin    -0.5000    0.5000

On exit IFAIL = 0 - Cross-Section

CPU time  41 min  28 sec, sec per call    =     0.415E-02
# of calls      =     599946

sigma       =       0.1489801E-02   +-          0.1930508E-05

Rel. error of      0.130 %
```

2.14 WWF 2.2

Author:

Geert Jan van Oldenborgh gj@rulkol.LeidenUniv.nl

Description

This Monte Carlo is the beginning of a full one-loop Monte Carlo [65]-[66]. At the moment it includes a tree level part (`WWFT`, which participated in the tuned comparisons), hard and soft bremsstrahlung (`WWFTSH`, exact matrix element, resummed in the forward and backward

region), and the factorizable virtual graphs (`WWFTSHV`, on request only). We are working on the missing parts, the non-factorizable loop graphs. t-channel graphs for electrons in the final state, and a shower algorithm for the forward/backward photons.

Features of the program

There are two forms of the program: an event generator (`wwfax`) and 'integrator' (`wwfmc`), the latter has a parallel option (`wwfpvmmc`, `wwfpvmslave`). Interfaces to `BASES/SPRING` are also provided.

The program can generate all final states which are reachable through two W bosons. The user can specify whether the final states should be leptonic, semileptonic and/or hadronic, and which leptons should be included in leptonic decays, for instance 'all semi-leptonic and leptonic channels with electrons and muons'. All cuts can be implemented after the event is generated. To optimize event generation one can specify the minimum photon energy, the minimum and maximum angle of photons to the beam, minimum angle to charged particles, and the maximum virtuality of the W's.

Two methods have been implemented to compute ISR: structure functions (Leiden 2-loop and YFS 3-loop leading logarithmic, with the possibility of giving the photon bunch a one-photon spectrum p_T), and the explicit 1-photon matrix element (for *CC03* and *CC11* processes), minus the leading log part of this matrix element, plus the resummed leading log structure functions mentioned above. In the latter case an estimate of the missing virtual corrections is included, which makes it unsuitable for total cross section predictions. For FSR we use the exact one-photon matrix element; there is an option to reduce the leading logarithmic part of this by an arbitrary factor to compensate for the excess near jets (which are described by on-shell quarks). The default event generation routine calls `JETSET` to do all the hadronization and τ decays. No polarization information is passed as yet, although all particles come from W bosons and the helicities are therefore fixed. There is a `JETSET` interface, which will soon be adapted to the proposed standard. There is no possibility to get information about subsets of diagrams yet, but this will be included in this interface.

We have the possibility to shift the Coulomb term from the virtual corrections to the the tree level terms (and therefore include it in the hard and soft radiation as well). For this we take the one-loop expression given in ref. [25]. Anomalous couplings are implemented only at the tree level, we follow the conventions of Jegerlehner [67]. In the hard radiation matrix element there is the option to include the full effect of finite fermion masses; the default is to include the leading effects only. The tree level ME can also include some mass effects. The phase space is always taken massive.

Program layout

The 'integrator' program `wwfmc` is a stand alone program, which reads its data from a file `wwf.dat`, which defines the input parameters, and `vegas.dat`, which gives the parameters for the integration by `VEGAS` (adaptive weighted integration) or `NVEGAS` (integrates many quantities, like the tuned comparison data).

tuned	best	description
80.23	80.26	W mass in GeV, LEP1 definition (running width)
-1	-1	W width, if < 0 it is computed
-1	-1	Z mass, if < 0 it is taken to be 91.188 GeV
-1	-1	Z width, if < 0 it is taken to be 2.4974 GeV
100	300	Higgs mass (only used in virtual corrections)
176	165	top quark mass (only used in virtual corrections)
2	0/2	0: constant width (use for hard & virtual corrections)
		2: s-dependent width (preferred for tree level only)
4	2	renormalization scheme: 1: α, 2: G_μ with α for soft radiation, 3: G_μ
		4: the tuned comparison scheme
2	2	1: narrow-width approximation, 2: full off-shell calculation
		(not defined with virtual), 3: pole scheme calculation
1	1	1: fast massless matrix element, 2: slower massive matrix element
0	0	0: include all diagrams
0	0	0: include corrections both to production and decay
0/1	0/1	0: only resonant tree level diagrams (*CC03*)
		1: same plus universal non-resonant diagrams (*CC11*)
0/1	0/1	same for radiative graphs
0	.123	α_s
2	0–7	decay channel, sum of 1: leptonic, 2: semileptonic, 4: hadronic
0	0–7	W^+ decay channels, sum of 1: $e^+\nu_e$, 2: $\mu^+\nu_\mu$, 4: $\tau^+\nu_\tau$, 8: $u\bar{d}$
2	0–7	W^- decay channels, sum of 1: $e^-\bar{\nu}_e$, 2: $\mu^-\bar{\nu}_\mu$, 4: $\tau^-\bar{\nu}_\tau$, 8: $\bar{u}d$
0	0.01	$E_\gamma^{\min}$ needed for hard/soft cut-off
0	0	$\theta_{\gamma,f}^{\min}$ used to optimize event generation
0	0	$\theta_{\gamma,e}^{\min}$ used to optimize event generation
180	180	$\theta_{\gamma,e}^{\max}$ used to optimize event generation
0	0	if $c > 0$ generate $\lvert\sqrt{s_\pm} - M_W\rvert < c$ GeV
0/1	0/1	0: no cuts, 1: canonical cuts, 2: require one observable photon
3	3	0: no extra initial-state radiation,
		1: use Leiden 2-loop structure functions,
		2: use YFS 3-loop structure functions.
180	180/10	cone around beam pipe where radiation is exponentiated
		(use 5–10 degrees when including explicit hard radiation)
1	1	1: use crude p_T algorithms for ISR photons
0	0	1: exclude leading logarithmic initial-state radiation
0	0/20	cone around final state particles where FSR is reduced
0	0/0.4	fraction of leading log final-state radiation off quarks to leave out
0	0/1	1: include explicit hard photon radiation matrix element
0	0/1	1: include explicit soft photon matrix element
0	0	1: include loop graphs (not yet complete)
1	1	1: include tree level matrix element
0	1	1: include the Coulomb term in tree

Table 3: Input file format of `WWF 2.2`

The event generator is a set of three routines:
– `axinit`: preparation, this also establishes the maximum of the function,
– `axeven`: generates one event
– `axexit`: finalization, prints statistics, gives cross section and weight per event.
The use of these routines is demonstrated in the program `wwfax`. The event generation does not use any adaptive strategies. The event is presented in a subroutine `wwfeve`, the default version of which calls `JETSET` and lists the event on standard output.

Input
The input parameters are expected to be in a file `wwf.dat` with the information described in table 3

Output

The program `wwfax` (or the equivalent routines) will give call the routine `wwfeve` for each event generated; the default is to list the event on standard output. Some informative messages will also appear on standard output:
– while initializing: the current maximum, a measure of the progress towards this maximum and the largest negative event found so far,
– at the end of initialization: the maximum used and a summary of the negative events,
– while generating: error messages (mainly inaccuracies and negative weights) and the numbers of events generated at powers of two,
– at exit: the cross section, weight per event, efficiency, CPU time used and a summary of the impact of the negative weight events. The program `wwfmc` integrates the cross section and the tuned comparison quantities, and will dump these in this format. One can make plots by editing wwfill and the file `h.dat`.

Availability
The programs can be obtained from
`ftp://rulgm4.LeidenUniv.nl/pub/gj`,
`http://rulgm4.LeidenUniv.nl`
either as a compressed archive `wwf.tar.gz` or separate files. The package includes a makefile and is known to compile without problems on HP, DEC, Linux, NeXT and Sun workstations.

2.15 WWGENPV/HIGGSPV

Authors:

Guido Montagna	montagna@pv.infn.it
Oreste Nicrosini	nicrosini@vxcern.cern.ch, nicrosini@pv.infn.it
Fulvio Piccinini	piccinini@pv.infn.it

Description:
`WWGENPV` and `HIGGSPV` are four-fermion Monte Carlo codes, originally conceived for W-boson

and Higgs-boson physics, respectively. The present version of `WWGENPV` is an upgrade of the published version. A detailed description of the formalism adopted and the physical ideas behind it can be found in the original literature, namely ref. [63] and references therein. A detailed description of `HIGGSPV` can be found in the report of the "Event Generators for Discovery Physics" Working Group, these proceedings.

The programs are based on the exact tree-level calculation of several four-fermion final states. Any cut on the final state configuration can be implemented. Initial- and final-state QED corrections are taken into account at the leading logarithmic level by proper structure functions, including p_T/p_L effects. An hadronization interface is at present available for *CC03* processes, and is under development [68]. All the relevant presently known non-QED corrections are also taken into account.

Features of the programs:
The codes consist of three Monte Carlo branches, in which the importance-sampling technique is employed to take care of the peaking behavior of the integrand:

- Unweighted event generation. The codes provide a sample of unweighted events, defined as the components of the four final-state fermions momenta, plus the components of the initial- and final-state photons, plus $\sqrt{s}$, stored into proper n-tuples. The programs must be linked to CERNLIB for graphical interfaces.
- Weighted event integration. It is intended for computation only. In particular, the codes return the values of several observables together with a Monte Carlo estimate of the errors. The programs must be linked to CERNLIB for the evaluation of few special functions.
- Adaptive integration. It is intended for computation only, but offering high precision performances. On top of importance sampling, an adaptive Monte Carlo integration algorithm is used. The program must be linked to NAG library for the Monte Carlo adaptive routines. Full consistency between non-adaptive and adaptive integrations has been explicitly proven. Neither final-state radiation nor p_T splitting are taken into account in this branch.

The non-adaptive branches rely upon the random number generator RANLUX.

As far as the physical features are concerned, the most important items are:

- Several Charged Current (`WWGENPV`) and Neutral Current (`HIGGSPV`) processes are available, namely *CC11*, *CC20*, *NC21* (*NC23* = *NC21* + Higgs signals), *NC24* (*NC25* = *NC24* + Higgs signals), *NC32*, *NC48* (*NC50* = *NC48* + Higgs signals) and all their subsets. The extension to other classes is under development.
- Any kind of cuts can be imposed.

- Initial- and final-state photon radiation is implemented at the leading logarithmic level in the structure function formalism. The structure function used is explicitly written in [63]. Moreover, p_T/p_L effects are taken into account.
- The Coulomb correction is taken into account (see [63] and references therein), together with flavor mixing and the presently known QCD corrections.
- An interface to hadronization packages is available for *CC03* processes and the extension to other classes is under development [68].
- There is the possibility of getting information on the contribution of subsets of the diagrams by setting proper flags.

At present, neither final state decays nor anomalous couplings are implemented. Moreover, finite fermion mass effects are partially taken into account only at the phase space boundary.

Program layout
After the initialization of the Standard Model parameters and of the electromagnetic quantities, the independent variables are generated, according to proper importance samplings, within the allowed range for an extrapolated set-up. The analytical control of the phase-space boundaries allows to reach an efficiency which, for an extrapolated set-up, is unitary, and remains very high for a wide range of (reasonable) cuts. By means of the solution of the exact kinematics, the four-momenta of the outgoing fermions are reconstructed in the laboratory frame, together with the four-momenta of all the generated photons. If the event satisfies the cuts imposed by the user in SUBROUTINE CUTUSER, the matrix element is called, otherwise it is set to zero.

In the generation branch, an additional random number is generated in order to implement the hit-or-miss algorithm and if the event is accepted it is recorded into an n-tuple.

In the non-adaptive integration branch, the integration of several (see below) observables is performed in a single run, by cumulating in parallel all the contributions to the integrands.

In the adaptive integration branch (ref.: NAG routine D01GBF), on top of importance sampling the integration routine automatically subdivides the integration region into subregions and iterates the procedure where the integrand is found more variant. The program stops when a required relative precision is satisfied.

INPUT parameters and flags (`WWGENPV`):
A sample of the input flags that can be used is the following:

`OGEN = I` choice between integration [I] and generation [G] branch

`RS =` c.m. energy (GeV)

`OFAST = N` choice between adaptive [Y] or non adaptive [N] branch

`NHITWMAX =` number of weighted events

`IQED = 1` choice for Born [0] or QED corrected [1] predictions

`ODIS = T` choice for a total cross section [T] or an invariant mass distribution [W]

`OWIDTH = Y` W-boson width computed within the SM according to LEP2 standard input [Y] or input the preferred value [N]

`NSCH = 2` Renormalization Scheme choice (three possible choices)

`ALPHM1 = 128.07D0` $1/\alpha$ value (LEP2 standard input)

`OCOUL = N` option for Coulombic correction [Y] or not [N]

`SRES = Y` option for *CC11* [Y] or *CC03* [N] diagrams

A detailed account of the other relevant possibilities offered by the code (namely, command files for generation and adaptive integration branches) will be given elsewhere [68].

Description of the OUTPUT:
For all three branches the output contains the values of the Standard Model parameters and of the couplings appearing in the Feynman rules.

In the generation branch, besides the output file containing the value of the cross sections for unweighted events, together with a Monte Carlo estimate of the error, also an n-tuple containing the generated events is written.

In the adaptive branch, the values of the cross section with its numerical error plus (when ISR is included) the energy and invariant mass losses with their errors are then printed.

In the non-adaptive branch, together with the cross sections, the estimates of the moments used in the tuned comparisons and of the histograms are also printed, together with the Monte Carlo errors.

Availability:
The codes are available upon request to one of the authors.

2.16 Summary

We will now briefly summarize the features of the programs presented in the previous subsections. Table 4 gives an overview over the features of the programs participating in the comparisons. It is just intended as a brief digest and the short writeups in the previous section should be consulted for reference. Here is a description of the columns of table 4:

Type:
one of the four types of programs: *EG*: (unweighted) event generator, *MC*: (weighted) Monte Carlo integration program, *Int.*: deterministic integration program, and *SA*: semi-analytical integration program.

Diagrams:
the subset(s) of Feynman diagrams implemented in the hard matrix element: *CC03*: the three basic $e^+e^- \to W^+W^-$ charged current diagrams from figure 1, *CC11*: the eleven charged current diagrams from figure 2, see table 1; *NC24* and *NC21* subsets of neutral current diagrams, see table 2; *NNC=NC32/NC21/NC48/NC4×16*; *NCC=CC11/CC20/NC32/NC21/mix43/NC48/NC4×16*; *all*: all diagrams.We emphasize, that we have listed only those processes in this column for which participating codes have contributed at least one number, see also the tables in [69]. This entry may therefore differ from that presented in the program descriptions.

ISR:
the type of initial-state radiation implementation: *SF*: structure functions; *FF*: flux functions; *REMT*: REMT routines, see subsection 2.8. *PS*: parton showers; *YFS*: Yennie-Frautschi-Suura exponentiation; and *ME*: matrix element (exact lowest order bremsstrahlung matrix element and infrared divergent virtual contributions); *BME*: the one photon bremsstrahlung matrix element is available; no virtual contributions.

FSR:
the type of final-state radiation implemented, see also section 3.1.15; *PH*: FSR is implemented by making use of `PHOTOS` package; the other symbols are the same as in the ISR column.

NQCD:
naive, inclusive QCD correction to $W^\pm$ decays. A '+' does not imply that hard QCD radiation is implemented in the program (see page 67 for more details).

Coul.:
Coulomb correction (see page 66 for more details).

AC:
availability of anomalous couplings in the three gauge boson vertices. Since we have not compared predictions with anomalous couplings in this study, the entries in this column are identical to what is advertized in the program descriptions.

m_f:
treatment of fermion masses: +: all fermion masses taken into account, ±: massless matrix elements with massive kinematics (mostly Källén λ-functions), and finally −: all fermions massless. It must be remarked here that 'all' does not necessarily mean that nonzero masses have been included in all processes presented in the comparisons.

Hadr.:
availability of an interface to hadronization libraries. With the exception of `PYTHIA`, no program includes hadronization code. All rely on `HERWIG` or `JETSET` to perform this task. The interface with hadronization packages and its interplay with final-state QCD radiation deserves a longer comment. For some codes a minus in this column is a direct consequence of the adopted strategy, e.g. semianalytical codes were never meant for this interface.

Program	Type	Diagrams	ISR	FSR	NQCD	Coul.	AC	m_f	Hadr.
ALPHA	MC	all	BME	−	−	−	−	+	−
CompHEP	EG	all	SF	−	−	−	−	+	−
ERATO	MC	CC11/CC20	SF	−	+	−	+	−	+
EXCALIBUR	MC	all	SF	−	+	+	+	−	−
GENTLE	SA	CC11/NC32	SF/FF	−	+	+	−	±	−
grc4f	EG	all	SF/PS	PS	+	+	+	+	+
HIGGSPV	EG	NNC	SF(p_T)	−	+		−	±	−
KORALW	EG	CC11	YFS	PH	+	+	+	±	+
LEPWW	EG	CC03	REMT	PH	+	−	+	−	+
LPWW02	EG	CC03	SF	PH	+	+	−	±	+
PYTHIA	EG	CC03	SF+PS	PS	+	+	−	±	+
WOPPER	EG	CC03	PS	−	+	+	−	±	+
WPHACT	MC	all	SF	−	+	+	+	+	−
WTO	Int.	NCC	SF	−	+	+	−	−	−
WWF	EG	CC11	SF+ME	ME	+	+	+	+	+
WWGENPV	EG	CC11/CC20	SF(p_T)	SF(p_T)	+	+	−	±	+

Table 4: Overview of the participating programs.

3 Comparisons of CC Processes

We now come to a detailed comparison of the Monte Carlo Event Generators and semianalytical programs available for the study of four-fermion processes at LEP2. The next subsection contains our most comprehensive study of *CC10* processes. Much shorter studies of *CC11* and *NC* processes are presented in the following subsection and the next section. Finally, the cross sections for *all* four-fermion processes are presented.

3.1 *CC10* processes

In a set of *tuned comparisons* of *CC* processes we have tested the implementation of the *CC10* family for a prescribed set of approximations. Because the *CC03* set (cf. fig. 1) is available in *all* programs, one of the *tuned comparison* has been restricted to this subset of all contributing diagrams.

It was then extended to the process $e^+e^- \to \mu^-\bar{\nu}_\mu u\bar{d}$, where from the *CC11* set of diagrams only 10 contribute, because the photon does not couple to the neutrino (cf. fig. 2).

In a second set of *unleashed comparisons* all the contributors have presented their preferred scenario for the process ($e^+e^- \to \mu^-\bar{\nu}_\mu u\bar{d}$) or, in short, they have produced the *best prediction they can give* at present. The latter comparison can show which part of the spread in predictions is due to the different approximations used.

3.1.1 Observables

In comparing of predictions for exclusive observables, we have concentrated on the prototypical "semileptonic" *CC10* process

$$e^+e^- \to \mu^-\bar{\nu}_\mu u\bar{d}\,, \tag{12}$$

which belongs to the *CC11* family. This choice is also partially motivated by the fact that the same process can be computed by restricting the calculation to the *CC03* class, thus allowing more codes to participate. Moreover, it is known that at LEP 2 energies the ratio of *CC03/CC10* cross sections is very near to one, although the difference is seen in some of the distributions. It should be mentioned that for the other semi-leptonic process $e^+e^- \to e^-\bar{\nu}_e u\bar{d}$ even the total cross section can not be well approximated by the *CC03* limit.

The following simple observables have received particular attention, because they are of prime importance for the measurement of the properties of the charged intermediate $W^\pm$ bosons at LEP2.

- The total cross section σ, with and without canonical cuts (see section 3.1.6 for a precise definition).
- The moments of the production angle θ_W of the W^+ with respect to the e^+-beam:

  $$\langle \cos\theta_W \rangle_{1,2} = \frac{1}{\sigma}\int T_{1,2}(\cos\theta_W)\, d\sigma \tag{13}$$

  where the $T_n(\cos\theta) = \cos(n\theta)$ are the Chebyshev polynomials $T_1(x) = x$ and $T_2(x) = 2x^2 - 1$. The distribution of the production angle will be used in some studies of the non-abelian $W^\pm$ couplings. A precise description of the standard model prediction for this observable is therefore mandatory for this fundamental test of the non-abelian gauge structure of the standard model.
- From the invariant masses $s_\pm$ of the hadronic (W^+) and leptonic (W^-) decay products we have constructed the following moments:

  $$\langle x_m \rangle_{1,2} = \frac{1}{\sigma}\int \left(\frac{\sqrt{s_+} + \sqrt{s_-} - 2M_W}{2E_B} \right)^{1,2} d\sigma \tag{14}$$

  These quantities will of course be of prime importance for the $W^\pm$-mass measurement.

- The moments of the sum E_γ of the energies of all radiated photons

$$\langle x_\gamma \rangle_1 = \frac{1}{\sigma} \int \left(\frac{E_\gamma}{E_B} \right)^1 d\sigma \tag{15}$$

  For constraint fits of the $W^\pm$-mass, a precise knowledge of the energy lost by initial-state radiation is mandatory. This quantity has to be described by all programs with high accuracy.

- Also, moments of the lost and visible photon energies $E_\gamma^{\text{lost/vis.}}$. The latter are accessible only in programs which generate non-vanishing p_T for ISR photons.

We have also looked at the following leptonic variables.

- The moments of the production angle θ_μ of the μ^- with respect to the e^--beam:

$$\langle \cos\theta_\mu \rangle_{1,2} = \frac{1}{\sigma} \int T_{1,2}(\cos\theta_\mu) d\sigma \tag{16}$$

- The moments of the decay angle θ_μ^* of the μ^- with respect to the direction of the decaying W^-, measured in the latter's rest frame:

$$\langle \cos\theta_\mu^* \rangle_{1,2} = \frac{1}{\sigma} \int T_{1,2}(\cos\theta_\mu^*) d\sigma \tag{17}$$

  This is another quantity that can gainfully be used in the determination of the non-abelian $W^\pm$-couplings.

- The moments of the energy E_μ of the μ^-:

$$\langle x_\mu \rangle_{1,2} = \frac{1}{\sigma} \int \left(\frac{E_\mu}{E_B} \right)^{1,2} d\sigma \tag{18}$$

However, the numerical results will be given only for the first moments of leptonic variables.

During early stages of the comparison effort, we have additionally considered the third and fourth order moments of these observables. It turned out, however, that these moments typically receive very large statistical errors. They have therefore been dropped. Together with the moments, we have produced histograms for the observables. Presenting these histograms for all programs is next to impossible, however. It has turned out that the moments that have been just described are much more powerful tools for the sake of comparison. The histograms have therefore been dropped, together with the higher order moments. Towards the end of the comparison effort, some codes have also performed a study of various distributions, e.g. $d\sigma/dE_\gamma, d\sigma/ds_+(s_-)$ etc, where the relevant range of the variables has been divided in a large number of bins (typically $\approx 50 - 100$). Also for distributions we have registered a very good agreement, showing among other things that moments can be reconstructed to high precision from the distributions.

3.1.2 Tuned Comparisons

Our first task was to verify that all programs implement their advertised features correctly within the given statistical and numerical uncertainty, at least for *CC03,CC10*. Obviously, this is only straightforward, if all programs implement the same features. This is not the case, of course. Therefore we have performed a set of so-called *tuned comparisons* in which only a common subset of features has been enabled and identical inputs have been used, as far as possible. Actually a semi-tuned comparison has also been attempted by several codes for *all processes* and the results will be described in subsection 5.

Ideally, all programs would have options to emulate *all* other programs. Then all programs should give the same results (up to Monte Carlo errors), if running in the same mode and using the same input. This approach has been adopted in a study [70] of electroweak radiative corrections at the Z-resonance.

In the case at hand, this approach presents a more severe problem because electromagnetic radiative corrections are implemented in a variety of styles: some programs are using structure functions or flux functions, while other programs employ parton shower algorithms, see [71] for details. There are even hybrids of structure functions and matrix elements available. Since these algorithms are central to the respective programs, it is not possible to exchange them without destroying the identity of the programs. In any case one should be aware that there are different implementations of the QED corrections and that this issue is deeply related to a quest for a fully gauge-invariant description of QED radiation in 4f-processes; this goal has *not* been achieved so far.

3.1.3 Input parameters

The choice of input parameters is related to the choice of the electroweak renormalization scheme (RS). Actually, we have at our disposal the usual set of precisely measured parameters

$$\alpha(0), G_{_F}, M_{_Z}, \tag{19}$$

and we want to include $M_{_W}$, [71]. Given the fact that the $\mathcal{O}(\alpha)$ electroweak corrections are not available for the *off-shell* case,we end up with an additional freedom in fixing the weak-mixing angle and the $SU(2)_L$ coupling constant. There are at least two *natural* choices, one of which had been adopted for the tuned comparisons, although it does not respect the proper Ward identities (more a question of principle than of numerical relevance). In this scheme, the effective weak mixing angle is determined as

$$\sin^2\theta_W = \frac{\pi\alpha(2M_W)}{\sqrt{2}G_F M_W^2}\,. \tag{20}$$

In order to achieve agreement in a tuned comparison, all programs have to agree on the

Quantity	Value
M_Z	$91.1888\,\mathrm{GeV}$
Γ_Z	$2.4974\,\mathrm{GeV}$
M_W	$80.23\,\mathrm{GeV}$
Γ_W	$3G_F M_W^3/(\sqrt{8}\pi)$
$\alpha(0)$	$1/137.0359895$
$\alpha(2M_W)$	$1/128.07$
G_F	$1.16639 \cdot 10^{-5}\,\mathrm{GeV}^{-2}$
α_{QCD}	0
V_{CKM}	**1**

Table 5: Input parameters used in the *tuned comparisons*

effective coupling constants entering the hard matrix element; this has been controlled by printing out these constants, for which all the codes have registered an agreement up to computer precision: $g_V = -0.0141$, $g_A = -0.18579$, $g = 0.23041$, $g_{ZWW} = .057148$, $g_{\gamma WW} = 0.31324$.

The photonic corrections employed in the tuned comparisons are only those corresponding to a leading-logarithmic approximation of initial-state radiation, final-state radiation being implemented in only a few programs so far (for more details we refer to the section on FSR). The non-logarithmic QED radiative corrections have been fixed by demanding that structure functions and parton showers should use $\beta = \ln(s/m^2) - 1$ instead of $\eta = \ln(s/m^2)$. Other universal corrections should be left out, see page 68 for a brief discussion of flux functions. Such pragmatic renormalization schemes are not easily reconciled with the schemes used in $\mathcal{O}(\alpha)$ calculations. A complete calculation of this kind is, however, not available and it is important to resum the dominant contributions (cf. [71]), therefore this pragmatic approach has been taken.

3.1.4 Presentation

The comparisons are presented graphically in the style familiar from the comparisons of experimental LEP1 results. The predictions are aligned vertically with horizontal error bars. The scale at the bottom of each plot gives the absolute value of the observables.

We provide also two tools to simplify the interpretation of the results: at the top of each plot, a scale with the relative deviation from some (insignificant) central value is drawn. This can be used to gauge the numerical accuracy of the results, which is of particular importance for the tuned comparisons. It should be noted, however, that such a scale can be misleading for quantities that vanish in a first approximation. This 'fine tuning' occurs for $\langle x_m \rangle$: further comments are given below.

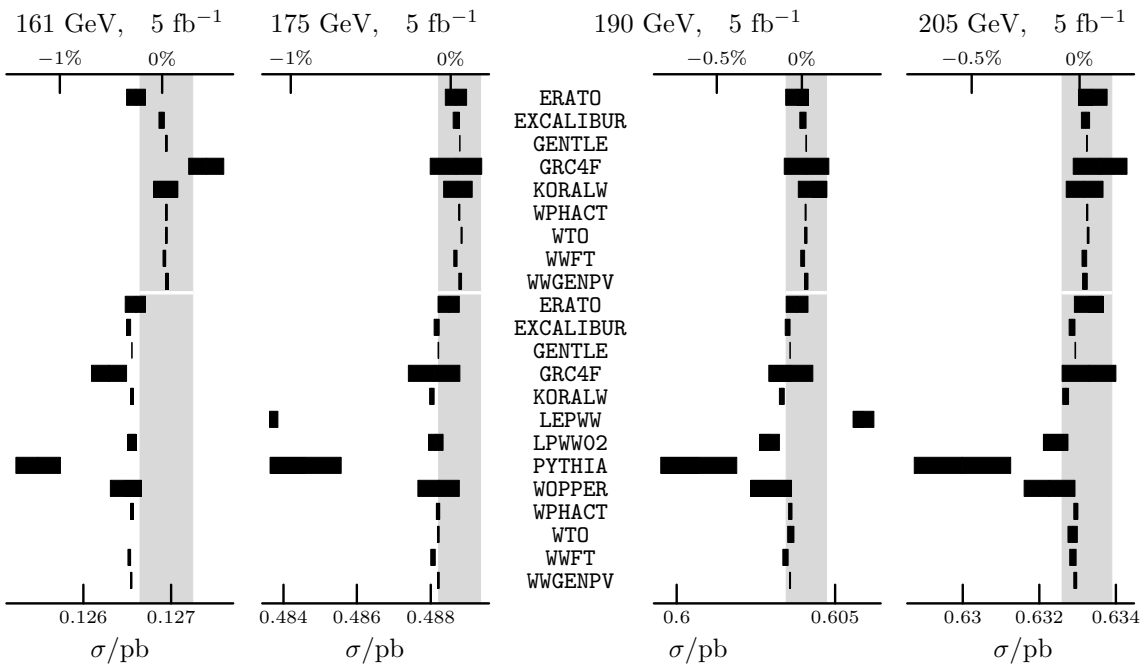


Figure 5: Tuned predictions for the total cross section for $e^+e^- \to \mu^-\bar{\nu}_\mu u\bar{d}$ without cuts.

In addition there is a gray band drawn around the central value, corresponding to a rough estimate of the experimental errors for a suitable integrated luminosity. This band is of particular importance for the *unleashed comparisons*, since it can be used by experimentalists to gauge the theorists' predictive power in relation to the experimental accuracy available at LEP2.

The results for both sets of Feynman diagrams are combined into one plot for the *tuned comparisons*. The upper half corresponds to the *CC10* set, while the *CC03* values are shown in the lower half, separated by a thin white line. This style of presentation clearly shows the effect of the *incompleteness error* caused by leaving out a class of diagrams. For the interpretation of the *incompleteness error* shown in the plots, two competing effects must be taken into account: the $e^+e^- \to \mu^-\bar{\nu}_\mu u\bar{d}$ final state under consideration is known to be less sensitive to "background" diagrams than final states with electrons. On the other hand, we have *not* applied any invariant mass cuts, which would reduce the contribution of "background" diagrams in an experimental analysis.

3.1.5 Experimental Errors

The statistical errors at an integrated luminosity of $500\,\mathrm{pb}^{-1}$ have been estimated by rescaling the errors from a high statistics ($\mathcal{O}(10^7)$ events) simulation using `WOPPER`[7]. For the error on the

[7]A change of even a few percent in this error estimate would have no impact on our conclusions. The choice of event generator is therefore completely irrelevant for our purposes and has been accidental.

total cross section, we use the naive statistical error

$$\frac{\Delta\sigma}{\sigma} \approx \frac{1}{\sqrt{N}} \tag{21}$$

from the event count $N = \sigma \cdot 500\,\mathrm{pb}^{-1}$ for *all* final states at $500\,\mathrm{pb}^{-1}$. This will *under*estimate the error on the cross section for the $\mu^-\bar{\nu}_\mu u\bar{d}$ final state by a factor of ≈ 5. At the same time it is a more realistic number for a cross section measurement in which events from a substantial fraction of all final states will be counted. The error on the moments is derived by rescaling the statistical errors of the high statistics `WOPPER` run by

$$\sqrt{\frac{N_{\mathrm{generated}}}{N(500\,\mathrm{pb}^{-1})}} = \sqrt{\frac{\mathcal{L}_{\mathrm{generated}}}{500\,\mathrm{pb}^{-1}}}\,. \tag{22}$$

Again, the event count for *all* final states is used, but also here the actual measurements will involve events of a variety of final states. The resulting relative errors are collected in table 6. It must be kept in mind that these errors are meant as order-of-magnitude estimates for gauging the accuracy of the theoretical predictions only. The actual measurement will be able to reduce these errors by intelligent use of constraints. At the same time, systematic errors will increase the experimental errors.

Some errors in table 6 appear suspiciously large, but their origin can be understood easily. The quantity $\langle x_m\rangle = \langle\sqrt{s_+}+\sqrt{s_-}-2M_W\rangle/(2E_B)$ vanishes in the narrow width approximation. Therefore it is a *fine tuned* quantity for which the relative error can be of order one. The absolute error on $\langle\sqrt{s_+}+\sqrt{s_-}\rangle$ is about 70 MeV (200 MeV at 161 GeV). Experimentalists expect that the error on the W mass will be smaller by virtue of constraint fits. The errors on the photonic observables at 161 GeV are simply caused by the small radiated energy and the small number of hard, observable photons close to threshold.

In the plots below, the errors are presented for an integrated luminosity of $\mathcal{L}_0 = 500\,\mathrm{pb}^{-1}$. If the corresponding error is larger than the spread of the predictions, $\mathcal{L}_0$ is multiplied by an appropriate power of ten. According to the target set in [71], our predictions should have an error of less than one third of the expected experimental error. The spread of values in the plots below must therefore be inside a gray band corresponding to $5\,\mathrm{fb}^{-1}$.

At this point we should emphasize for the first time, that possible discrepancies in the *tuned comparisons* must *not* be mistaken for *theoretical* errors. They rather point to *incorrect* implementations and/or to still undiscovered bugs.

$\sqrt{s}$	161 GeV	175 GeV	190 GeV	205 GeV
σ	2.4%	1.2%	1.1%	1.1%
$\langle T_1(\cos\theta_W)\rangle$	6.8%	2.1%	1.4%	1.1%
$\langle T_2(\cos\theta_W)\rangle$	5.3%	3.7%	5.9%	15.3%
$\langle (x_m)^1\rangle$	3.2%	6.4%	38.1%	19.6%
$\langle (x_m)^2\rangle$	7.4%	5.8%	4.5%	4.0%
$\langle (x_\gamma)^1\rangle$	8.9%	2.9%	2.5%	2.4%
$\langle (x_\gamma)^2\rangle$	26.4%	6.3%	4.1%	3.7%
$\left\langle (x_\gamma^{\rm lost})^1\right\rangle$	11.0%	3.7%	3.2%	3.0%
$\left\langle (x_\gamma^{\rm lost})^2\right\rangle$	32.7%	7.9%	5.2%	4.8%
$\left\langle (x_\gamma^{\rm vis.})^1\right\rangle$	14.9%	5.0%	4.2%	4.1%
$\left\langle (x_\gamma^{\rm vis.})^2\right\rangle$	45.2%	10.6%	7.0%	6.3%
$\langle T_1(\cos\theta_\mu)\rangle$	4.1%	1.8%	1.3%	1.1%
$\langle T_2(\cos\theta_\mu)\rangle$	3.5%	2.1%	2.4%	3.1%
$\left\langle T_1(\cos\theta_\mu^*)\right\rangle$	16.6%	5.0%	3.2%	2.6%
$\left\langle T_2(\cos\theta_\mu^*)\right\rangle$	4.4%	2.4%	2.2%	2.3%
$\langle (x_\mu)^1\rangle$	0.4%	0.3%	0.3%	0.3%
$\langle (x_\mu)^2\rangle$	0.8%	0.5%	0.5%	0.6%

Table 6: Estimated statistical errors at $\mathcal{L}_0 = 500\,\mathrm{pb}^{-1}$.

3.1.6 Canonical Cuts

Canonical cuts (a.k.a. `ADLO/TH`) have been defined in collaboration with ALEPH, DELPHI, L3 and OPAL. The following *acceptance cuts* define an optimistic union of the phase spaces that the four collaborations expect to cover:

- the energy of light charged leptons (e, μ) must be greater than 1 GeV;
- light charged leptons (e, μ) will be seen down to 10 degrees from either beam;
- the energy of a jet must be greater than 3 GeV. For the purpose of our study, jets will be identified with quarks;
- jets can be detected in the entire 4π of solid angle;
- photons must have an energy of at least 100 MeV to be identified;
- photons will be seen down to 1 degree from either beam.

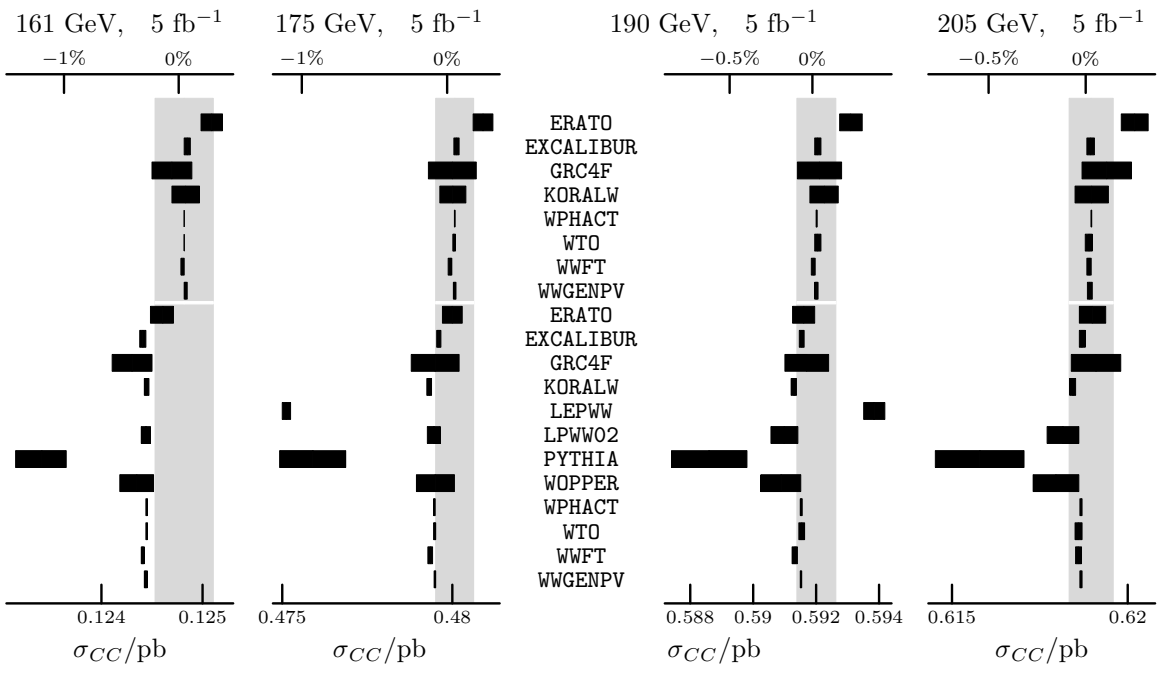


Figure 6: Tuned predictions for the total cross section for $e^+e^- \to \mu^-\bar{\nu}_\mu u\bar{d}$ after canonical (`ADLO/TH`) cuts.

These cuts do not address the issue of τ-identification. For the purpose of theoretical studies, τ's can be treated like the light charged leptons e and μ. It is understood that the programs considered here will have to be interfaced to external τ-decay packages. These *acceptance cuts* are supplemented by the following set of *separation cuts*:

- light charged leptons (e, μ) must be separated by at least 5 degrees from jets. Jets will again be identified with quarks.
- the invariant mass of two jets that are resolved as two separate jets must be greater than 5 GeV
- photons must be separated by at least 5 degrees from light charged leptons (e, μ) and jets

τ's will again be treated like the light charged leptons e and μ. If any of the charged particles of our final state fails any of these cuts, the event will be discarded.

Programs using the strict collinear limit for photons will count all photons as lost and assign them to initial-state radiation. If a program generates photons with a finite p_T, a more detailed treatment is necessary. Photons failing the separation cuts from charged final-state particles will not simply be discarded. Instead, their four momentum is added to the closest charged particle. Photons missing the acceptance cut around the beam pipe will be counted as lost

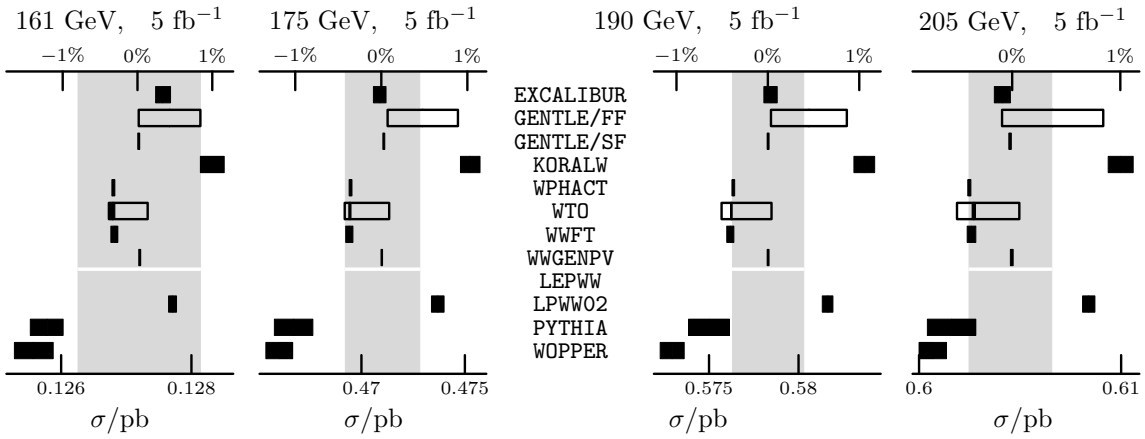


Figure 7: Unleashed predictions for the total cross section for $e^+e^- \to \mu^-\bar{\nu}_\mu u\bar{d}$ without cuts. The transparent, framed error bars are theoretical errors (cf. page 70).

and will be assigned to initial-state radiation. The question if this procedure is appropriate for dealing with final-state radiation will be discussed below in section 3.1.15. There the size of the separation cut will be discussed in more detail.

These cuts serve two purposes. Firstly they are important for testing programs under more realistic conditions. Secondly, they are required to give well-defined predictions without the need for internal technical cuts cutting out singular regions in phase space. However, for final states involving photons and for programs using massless fermions, some care must be taken in interpreting the results. Indeed, the canonical cuts when applied to a final-state l^+l^- allow for a minimum invariant l^+l^-- mass of 87.2 MeV which is below $2\,m_\mu$.

Comparing figures 5 and 6, we observe that the effect of the canonical cuts are rather small. This shows that the effect of the internal technical cuts are very similar for all programs under consideration.

3.1.7 "Unleashed" Comparisons

Some numerically important corrections to the total cross section have been left out in the *tuned comparisons*. They have been studied in separate set of comparisons. In these *unleashed comparisons*, all program authors have been asked to provide the *"Best Prediction They Can Make"*. It is of course clear that this is a moving target and the data presented in this report must be viewed as a snapshot of the situation at the end of 1995. This is different from the *tuned comparisons*, which implement a fixed set of approximations and input parameters. These predictions should not change in time, unless bugs are found in some codes.

The *Coulomb correction* (see [71] for a detailed formula) is well established and can be implemented easily as a factor multiplying the part of the cross section emanating from the

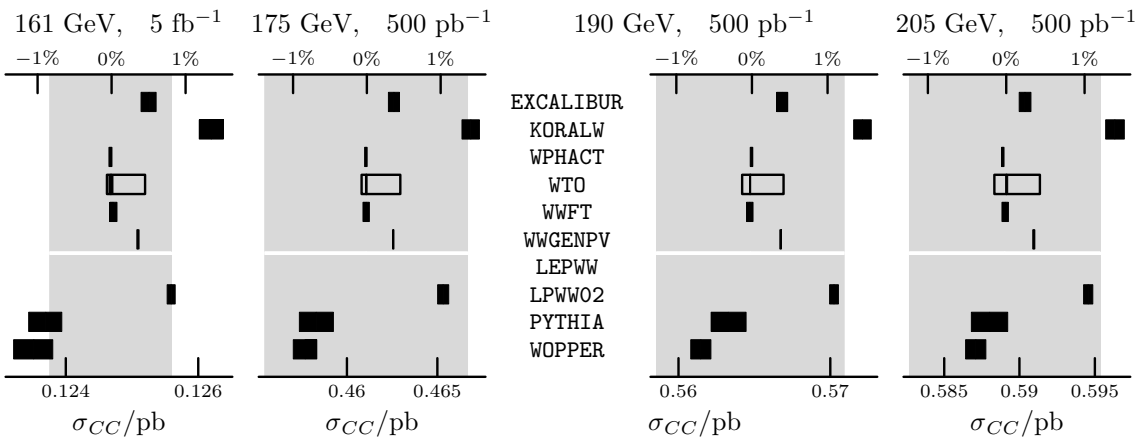


Figure 8: Unleashed predictions for the total cross section for $e^+e^- \to \mu^-\bar{\nu}_\mu u\bar{d}$ after canonical (`ADLO/TH`) cuts. The transparent, framed error bars are theoretical errors (cf. page 70).

CC03 subset of diagrams. Using a narrow-width approximation exaggerates the effect of the Coulomb correction.

The *QCD corrections* to the hadronic $W^\pm$ width, $\Gamma_W^{\text{hadr.}}$, must be properly included in processes with $q\bar{q}$ pair(s). We have adopted a *naive QCD* factor (NQCD):

$$\Gamma^0_{W\to\text{hadr.}} \to \sum_{\bar{q}q}\left(\Gamma^0_{W\to\bar{q}q}+\Gamma^1_{W\to\bar{q}q}\right)+\sum_{\bar{q}qg}\Gamma^1_{W\to\bar{q}qg}=\sum_{\bar{q}q}\Gamma^0_{W\to\text{hadr.}}\cdot\left(1+\frac{\alpha_{QCD}}{\pi}\right) \qquad (23)$$

It is certainly correct for inclusive quantities like the total cross section without cuts if only the *CC03* diagrams are taken into account.

At the same time it is questionable for exclusive quantities and for diagrams that can not be factorized in the production and decay of a W^+W^- pair. Without a complete $\mathcal{O}(\alpha_{QCD})$ calculation including gluons in the final state, we can not prove that the correction is really of this magnitude in the presence of cuts. Similarly, we can not be sure about the *CC11* diagrams without a calculation of the QCD box diagram corrections. Here, we are faced with the very familiar problem of whether we can shrink EW interactions to a point in the presence of gluon emission.

On the other hand, for our set of canonical (`ADLO/TH`) cuts with complete (4π) coverage of jets, the *"naive correction"* could be very close to the truth for the *CC03* diagrams. Furthermore, even if the size of the correction to the *CC11* diagrams has not been calculated, we know that it is a $\mathcal{O}(\alpha_{QCD})$ correction to a $\mathcal{O}(\Gamma_W/M_W)$ correction and it makes pragmatical sense to include the overall NQCD correction anyway. The factor (23) has therefore been included by all programs in the numbers below.

In connection with implementation of NQCD we emphasize that the effect of NQCD on some moments, typically $\langle x_m\rangle_n$, is quite large, i.e. of the order of few percent. For instance

both WPHACT and WTO have analyzed $\langle x_m \rangle_1$ with and without the inclusion of NQCD. The latter has a net effect of changing $\langle x_m \rangle_1$ of 1.5% at $\sqrt{s} = 161\,\mathrm{GeV}$ and of 2.6% at $\sqrt{s} = 175\,\mathrm{GeV}$. This is a considerable correction factor which, in general, calls for a better understanding of the QCD corrections to have full reliability of the order of magnitude of the effect.

Finally, the whole problem of the implementation of NQCD must be seen in the light of describing the relationship between the QCD matrix elements and the interface with hadronization. Ideally, we would have at our disposal a chain of cross checking programs starting from an exact semianalytical program, continuing with less precise but more flexible integration programs and ending with Monte Carlo event generators that can implement any cut and can be be interfaced with hadronization. In the last step *double-counting* should be carefully avoided. It must be kept in mind, however, that many hadronization codes will affect differential distributions only, without correcting the total cross section. Therefore such corrections have to be put in by hand. At the same time, hadronization may suffer from its own problems, connected with the identification of the proper *color-singlet* structure which is far from clear in the presence of complicated diagrams.

The *QED corrections*: Using the *current-splitting trick* [22], it is possible to identify a set of non-logarithmic universal QED radiative corrections and to implement them in so-called *flux functions*. In order to assess the effect from these contributions, GENTLE has contributed two numbers to the *unleashed comparisons*: one (GENTLE/SF) using structure functions, like most other programs and a second (GENTLE/FF) using flux functions. This also allows us to understand the apparent deviation of the KORALW number from the others: there, the so-called YFS form factor has been included, which is essentially equivalent with going from the SF to the FF description: indeed, the GENTLE result with FF is in good agreement with the KORALW one.

The *EW corrections* are the theoretically most demanding problem. There is a theoretical uncertainty from having to choose a particular resummation scheme. In the *tuned comparisons*, this uncertainty has artificially been removed by demanding a particular choice of input parameters. In the *unleashed comparisons*, the spread of predictions *can* point to a theoretical uncertainty. This is, however, not due to EW uncertainties because a sizeable fraction of the programs have used a scheme very similar to the *tuned comparisons*.

The *CKM quark mixing correction* is a trivial correction arising from non-trivial quark mixing:

$$\Gamma_W^{q\bar{q}} \propto |V_{q\bar{q}}|^2 \,. \tag{24}$$

Due to the unitarity of the CKM-matrix, the effects on the widths are negligible. If light quark flavors are summed over, as is required by experimental procedures anyway, the effect on exclusive final states will be small, except for the occasional b-quark. Since the range for $|V_{ud}|^2$ is larger than the uncertainties from other factors, the plots in figures 7 and 8 have been normalized to $|V_{ud}|^2 = 0.9518$.

The *fermionic masses* could, in principle, be included everywhere in the various calculations, but we point out that there are essentially three places where they become relevant. First of

all, the electron mass in *CC20*, whenever the $e^-(e^+)$ scattering angle is considered without cuts (gauge invariance is also involved here). Secondly, whenever a charged fermion-antifermion pair occurs in the final state, particular care should be devoted to study the threshold region in $\gamma^* \to f\bar{f}$. In the third place, the b-quark should be taken massive for a fully consistent study of Higgs boson production and of its background. For the last case, and for quarks in general, one should worry about which value to use, i.e. the pole mass or the running mass and, if the latter is chosen, at which scale. It is not at all an academic problem in view of the large difference between, say, $m_b(m_b)$ and $m_b(M_W)$ or $m_b(m_H)$.

Programs that implement the complete *CC10* set of diagrams have contributed to the *unleashed comparisons* as well as programs restricted to the doubly resonant *CC03* subset. In the context of a *"Best Prediction They Can Make"* the comparison of programs from both sets are justified. In order to help the reader, the *CC10* programs have been collected at the top of each plot, while the *CC03* programs are shown at the bottom, separated by a thin white line.

3.1.8 Theoretical uncertainties

At the level of our present knowledge, it is impossible to expect a common treatment of the *theoretical error*, something which is by definition highly subjective. However our preliminary investigations (mostly `GENTLE` and `WTO`) have shown that even the most crude and naive estimate of the theoretical error gives quite a wide spread of answers.

Ideally, a theoretical error should be inferred by estimating the differences originating from different treatments of leading higher order effects as well as from non-leading ones, whose size is notoriously much more difficult to guess. Obviously, a theoretical error is bound to disappear whenever real progress is achieved under the form of new and *complete* calculations. Most of the time, the potentialities claimed in the summary table only refer to some *naive* treatment of a particular effect. There is no particular harm in that, as long as *naive* estimates are kept well separated from the *precise* calculations. From this point of view the extension from *CC03* to *CC10* (or even better to *CC20*) is a well-established piece of work while the inclusion of final state QCD corrections is, at this stage, a *naive* although *educated* guess.

By referring to a *theoretical error* we can only admit a very partial attempt to understand the missing components of our calculations. Specifically, we can get a feeling of what is missing by allowing different implementations of the SF approach (η-scheme versus β-scheme or even the mixed one) and by judging in a very crude (and most probably underestimated) way the effect of terms of order $\alpha \times$ *constant*. The same can be attempted by comparing the SF and the FF approaches. In the end the codes implementing SF have adopted the β-scheme for tuned comparisons (although it violates gauge invariance), since there are plausibility arguments showing that whenever the full answer is known in other processes then the β-scheme gives the best numerical approximation.

Very simple analyses of theoretical errors have been performed by `GENTLE` and `WTO`. They used different sets of *working options*.

GENTLE ran over 6 options: 5 IZERO×IQEDHS (see subsection 2.5) options using FF plus the standard SF treatment of ISR. In this way, the error due to different treatment of ISR was simulated. GENTLE results for σ , $\langle E_\gamma \rangle$ and $\langle 10x_m \rangle_1$ are presented in table 7.

E_{cm} /IZERO-IQEQHS	0-0	0-1	0-2	0-3	1-3	SF
σ, pb						
161	0.13420	0.13366	0.13380	0.13379	0.13460	0.13364
175	0.49598	0.49522	0.49562	0.49561	0.49862	0.49493
190	0.60787	0.60801	0.60841	0.60838	0.61212	0.60758
205	0.63483	0.63558	0.63592	0.63590	0.63984	0.63512
$\langle (m,E)_\gamma \rangle$, GeV						
161	0.4671	0.4754	0.4746	0.4746	0.4749	0.4759
175	1.1055	1.1267	1.1248	1.1249	1.1254	1.1271
190	2.1052	2.1518	2.1473	2.1473	2.1488	2.1565
205	3.1388	3.2084	3.2010	3.2010	3.2041	3.2223
$\langle 10x_m \rangle_1$						
161	-.38320	-.38410	-.38401	-.38401	-.38403	-.38400
175	-.066431	-.066714	-.066684	-.066684	-.066695	-.066701
190	-.012318	-.012516	-.012492	-.012492	-.012502	-.012508
205	.015638	.015478	.015501	.015501	.015489	.015450

Table 7: GENTLE theoretical errors

Two comments are in order here. First, since for IQEDHS=0 only $\mathcal{O}(\alpha)$ exponentiated FF ISR corrections are used, while for IQEDHS=1,2,3 different realizations of $\mathcal{O}(\alpha^2)$ are applied, one should consider the difference between IQEDHS=0 and IQEDHS$\geq$1 as an illustration of the importance of $\mathcal{O}(\alpha^2)$ corrections rather than as an estimate of theoretical errors. Second, in the FF method, one may access only $\langle m_\gamma \rangle$, whose difference from $\langle E_\gamma \rangle$ grows rapidly with energy, see [72]. So, in this case one should not consider the difference between FF and SF calculations as a theoretical uncertainty. The GENTLE theoretical errors are exhibited in figures 7 and 16 by a transparent, framed error bar.

WTO ran over $6 = 2 \times 3$ IOS×IOSF options. Two options, IOS, for the renormalization of the weak sector, see eqs. 7-8, and three options, IOSF for initial-state radiation structure functions implementations, adopted respectively in [7, 62, 63]. WTO results for σ and $\langle E_\gamma \rangle$ are given in table 8.

The largest uncertainty for $\langle E_\gamma \rangle$ is of $1.9, 3.2, 9.9, 20.5\,\mathrm{MeV}$ for $E_{cm} = 161, 175, 190, 205\,\mathrm{GeV}$ respectively.

In figures 7, 8 and 20 these uncertainties are exhibited by a transparent, framed error bar drawn around the black statistical error bar.

Inspecting figures 7 and 8, we see that the theoretical error derived this way nicely reproduces

E_{cm} /IOS-IOSF	1-1	1-2	1-3	2-1	2-2	2-3
σ, pb						
161	0.13206	0.13204	0.13250	0.13201	0.13198	0.13244
175	0.49207	0.49186	0.49358	0.49177	0.49156	0.49329
190	0.60240	0.60192	0.60404	0.60188	0.60139	0.60352
205	0.62828	0.62754	0.62977	0.62764	0.62691	0.62913
$\langle E_\gamma \rangle$, GeV						
161	0.4688	0.4673	0.4674	0.4685	0.4669	0.4670
175	1.1250	1.1219	1.1221	1.1251	1.1220	1.1222
190	2.1579	2.1484	2.1489	2.1583	2.1488	2.1493
205	3.2317	3.2119	3.2129	3.2324	3.2126	3.2135

Table 8: WTO theoretical errors

the range in predictions defined by WPHACT and WWF at the low end and EXCALIBUR, GENTLE (structure function) and WWGENPV at the high end. On the other hand we must not rush to the judgment that the theoretical error will always be given by the spread in predictions from different programs. A detailed analysis like the one performed by WTO is more reliable. In figure 20 below, we will see an example in which the theoretical error estimated from scanning the options is slightly larger than the spread in predictions.

3.1.9 Total Cross Sections

As can be seen in figures 5 and 6, the agreement among the programs is generally good for the total cross sections. As expected, the effect of the *CC11* diagrams is most notable at 161 GeV. Even though it will be hard to reach this level of experimental accuracy, the programs that are still restricted to the *CC03* subset should aim at implementing a more complete subset.

For most energies, the predictions of LEPWW have not been included in the plots because they are too far off from the other programs. This is caused by an insufficient implementation of initial state radiation in this program, which is of mostly historical interest.

The agreement of the predictions of PYTHIA with the rest of the programs is unsatisfactory.

It should come as no surprise that the spread of predictions is larger in the *unleashed comparisons*. It remains however at or below the expected experimental accuracy of LEP2.

The qualitative pictures with and without cuts are very similar. For this reason, we will show (with one exception) only results without cuts for the tuned comparisons and only results with cuts for the unleashed comparisons of exclusive observables below.

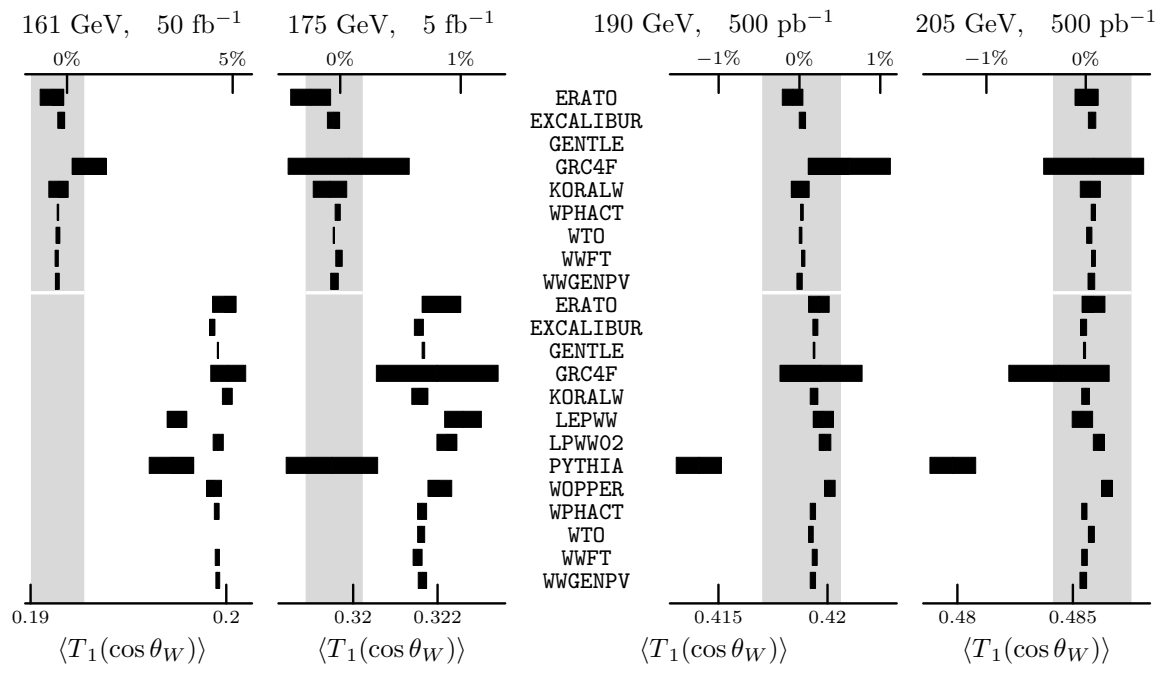


Figure 9: Tuned predictions for the first Chebyshev polynomial of the W production angle in $e^+e^- \to \mu^-\bar{\nu}_\mu u\bar{d}$ without cuts.

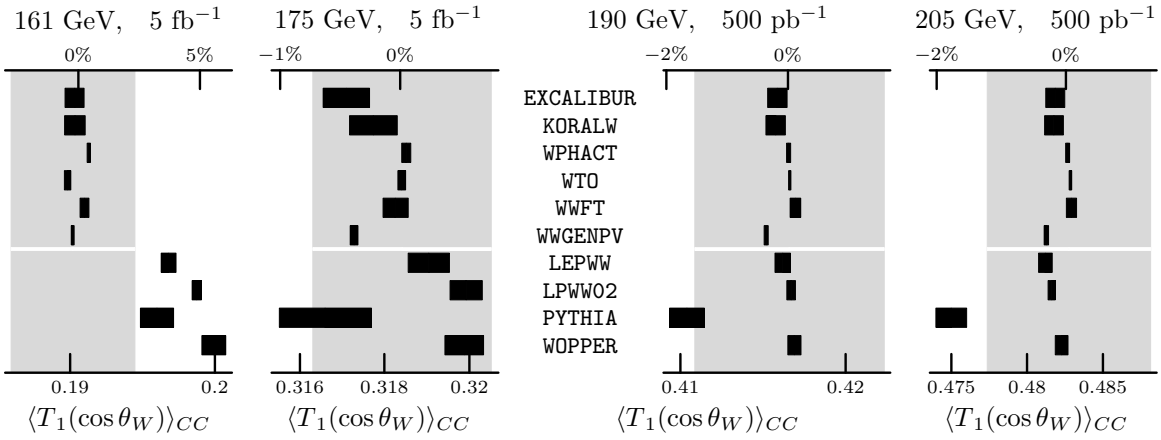


Figure 10: Unleashed predictions for the first Chebyshev polynomial of the W production angle in $e^+e^- \to \mu^-\bar{\nu}_\mu u\bar{d}$ with canonical (`ADLO/TH`) cuts.

3.1.10 W Production Angle

The trend observed in the total cross section continues in the moments of the W production angle. The deviations of `PYTHIA`'s results are again not acceptable for precision measurements.

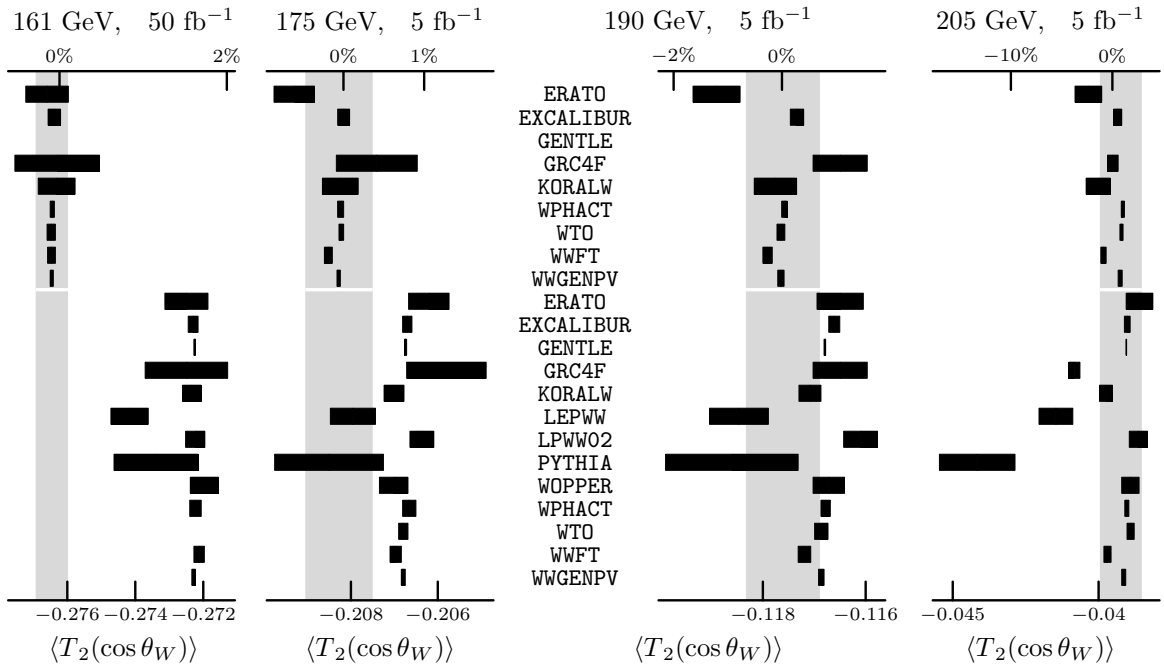


Figure 11: Tuned predictions for the second Chebyshev polynomial of the W production angle in $e^+e^- \to \mu^-\bar{\nu}_\mu u\bar{d}$ without cuts.

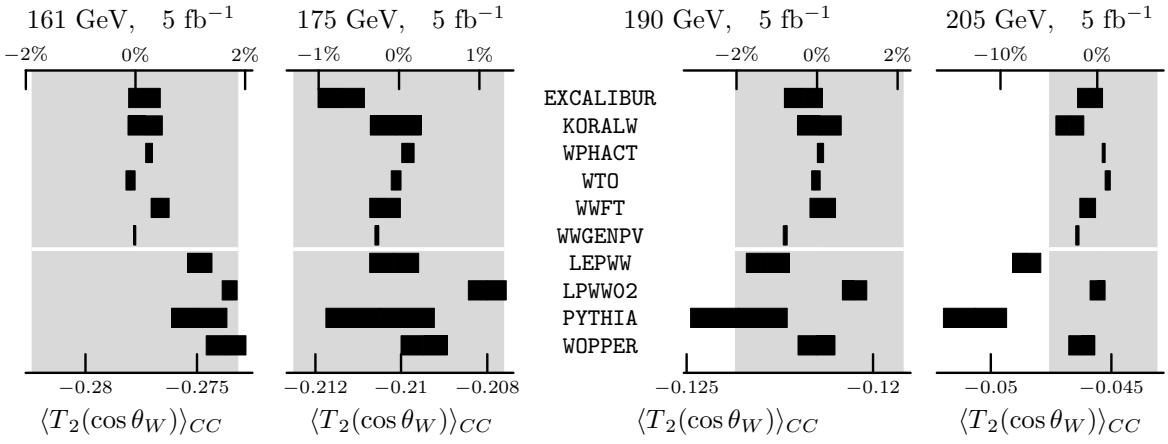


Figure 12: Unleashed predictions for the second Chebyshev polynomial of the W production angle in $e^+e^- \to \mu^-\bar{\nu}_\mu u\bar{d}$ with canonical (ADLO/TH) cuts.

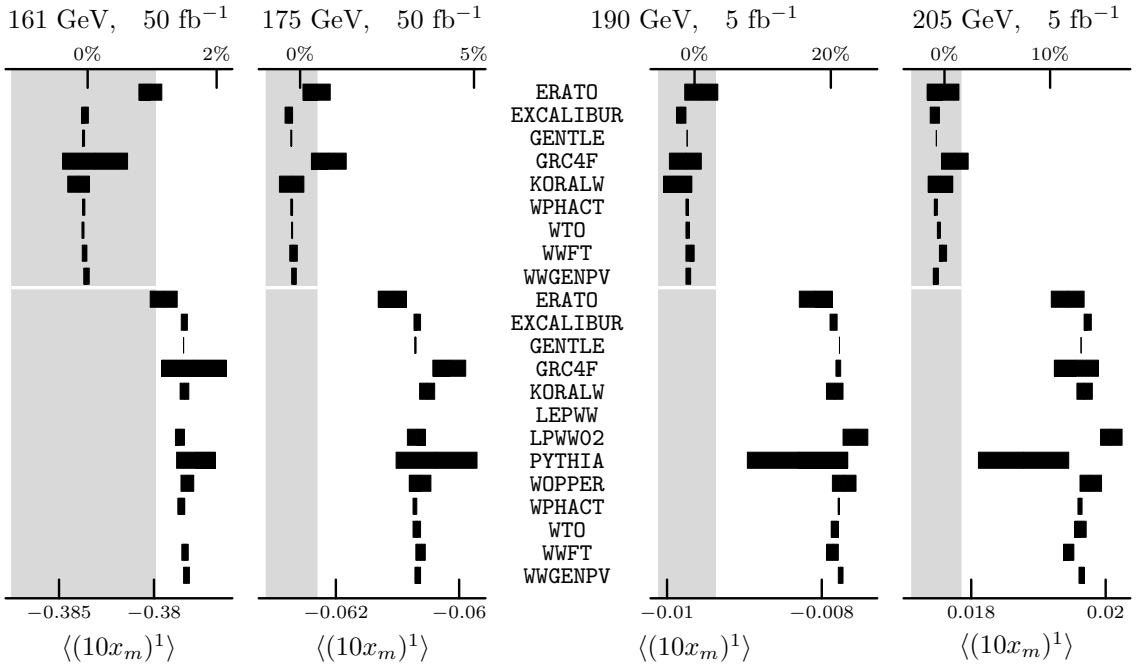


Figure 13: Tuned predictions for the deviation of the sum of invariant W-masses from $2M_W$ in $e^+e^- \to \mu^-\bar{\nu}_\mu u\bar{d}$ without cuts.

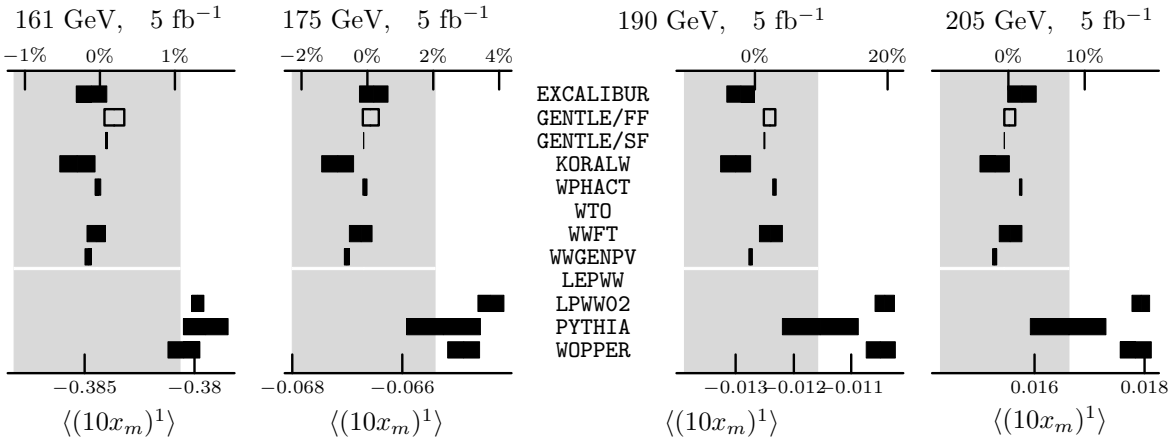


Figure 14: Unleashed predictions for the deviation of the sum of invariant W-masses from $2M_W$ in $e^+e^- \to \mu^-\bar{\nu}_\mu u\bar{d}$ without cuts. The transparent, framed error bars are theoretical errors (cf. page 70).

3.1.11 Invariant Masses

The effect of the *incompleteness error* of leaving out the *CC10* diagrams is of course most drastic in this observable. While the effect will be reduced somewhat by the necessary invariant mass

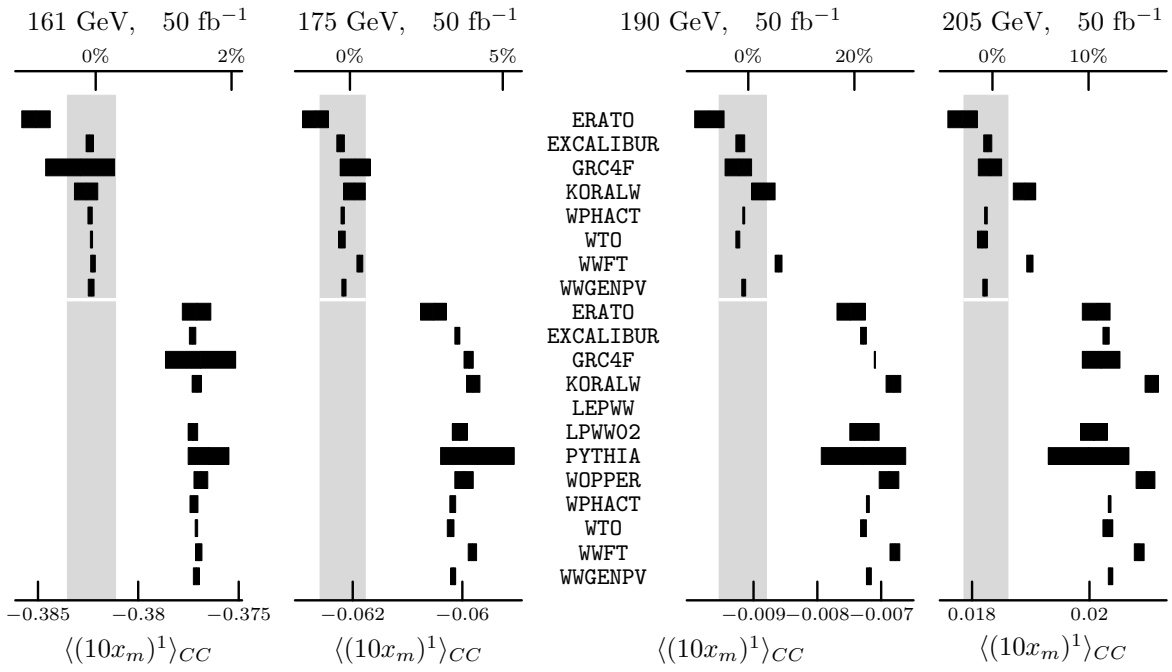


Figure 15: Tuned predictions for the deviation of the sum of invariant W-masses from $2M_W$ in $e^+e^- \to \mu^-\bar{\nu}_\mu u\bar{d}$ after canonical (ADLO/TH) cuts.

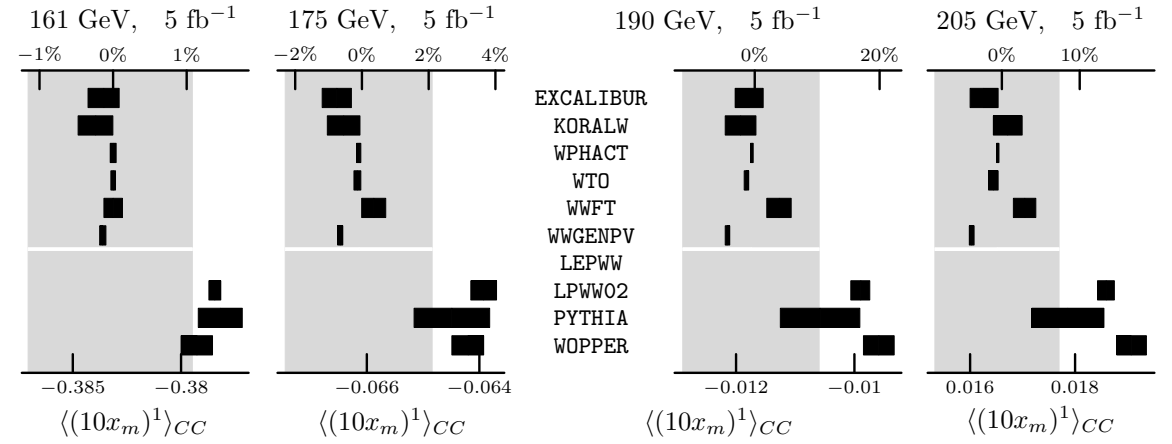


Figure 16: Unleashed predictions for the the deviation of the sum of invariant W-masses from $2M_W$ in $e^+e^- \to \mu^-\bar{\nu}_\mu u\bar{d}$ after canonical (ADLO/TH) cuts.

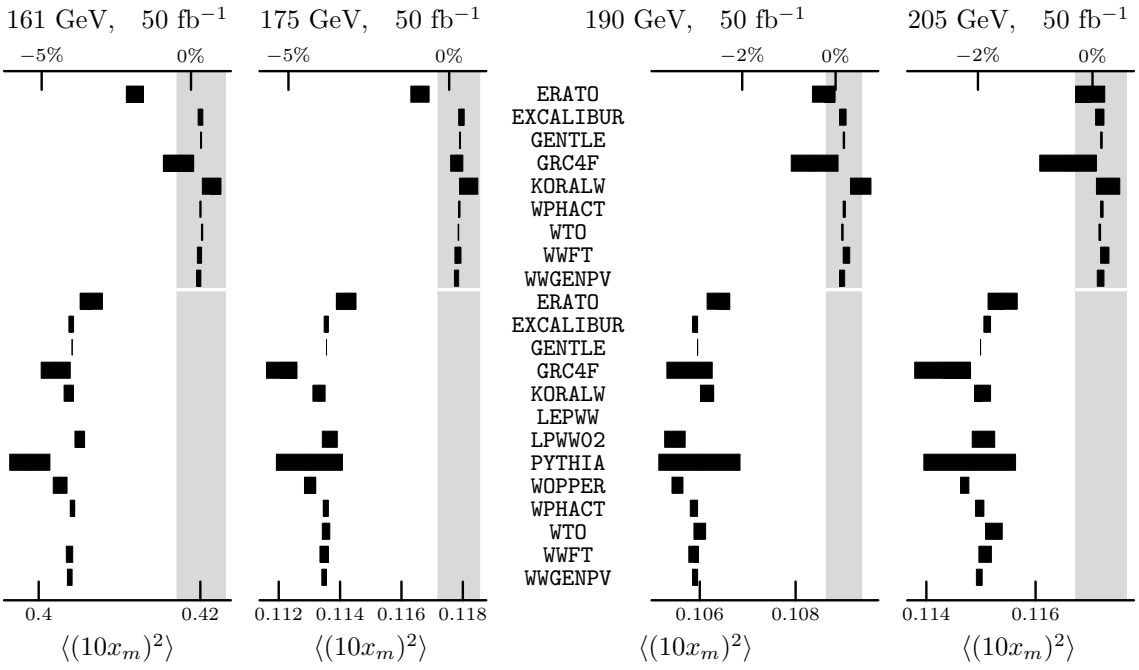


Figure 17: Tuned predictions for the square of the deviation of the sum of invariant W-masses from $2M_W$ in $e^+e^- \to \mu^-\bar{\nu}_\mu u\bar{d}$ without cuts.

cuts for reducing the non-$W^\pm$ background, all programs which are still restricted to the *CC03* set ought to attempt to lift this restriction.

As has been discussed before, this observable vanishes in the zero width approximation and we have to expect *relative* errors which are substantially larger than those for the other observables.

Comparing figures 13 and 15, we observe a nontrivial effect of using a finite p_T for photons. At the higher energies, where a substantial number of hard photons is radiated, the first moment of the invariant masses is slightly higher for the programs with finite photonic p_T (`KORALW`, `WOPPER` and `WWF`), when the `ADLO/TH` cuts are applied. `WWGENPV` gives also finite p_T to the photons, but the numbers quoted in the figures have been produced with an intermediate version of the code, in which the p_T is not transferred to the beam particles. Hence, this small effect is absent in this particular case.

3.1.12 γ Energy

The trend continues for the total energy radiated by photons. Here, it should be noted that the *incompleteness error* caused by leaving out the *CC10* diagrams is most notable in the *second* moment, while it is hardly noticeable in the first moment.

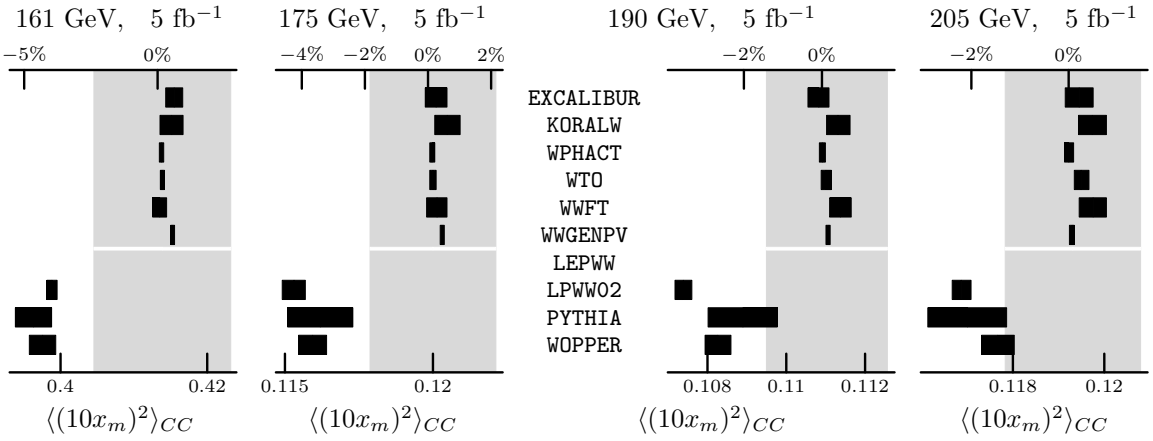


Figure 18: Unleashed predictions for the square of the deviation of the sum of invariant W-masses from $2M_W$ in $e^+e^- \to \mu^-\bar{\nu}_\mu u\bar{d}$ after canonical (ADLO/TH) cuts.

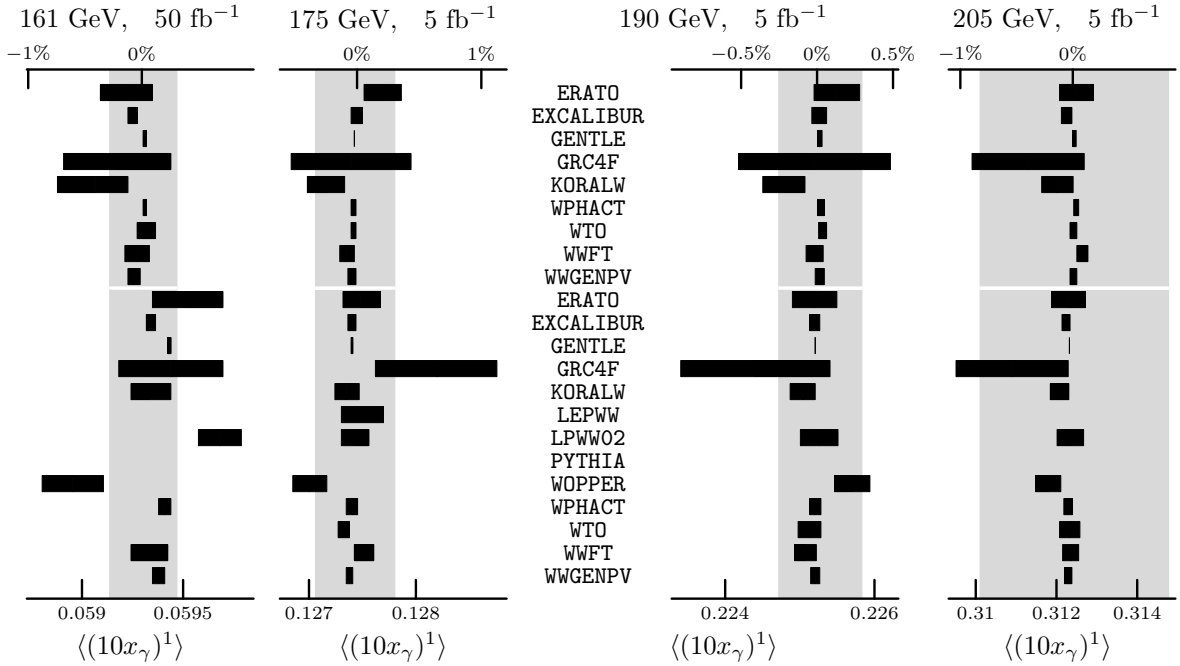


Figure 19: Tuned predictions for the total radiated γ energy in $e^+e^- \to \mu^-\bar{\nu}_\mu u\bar{d}$ without cuts.

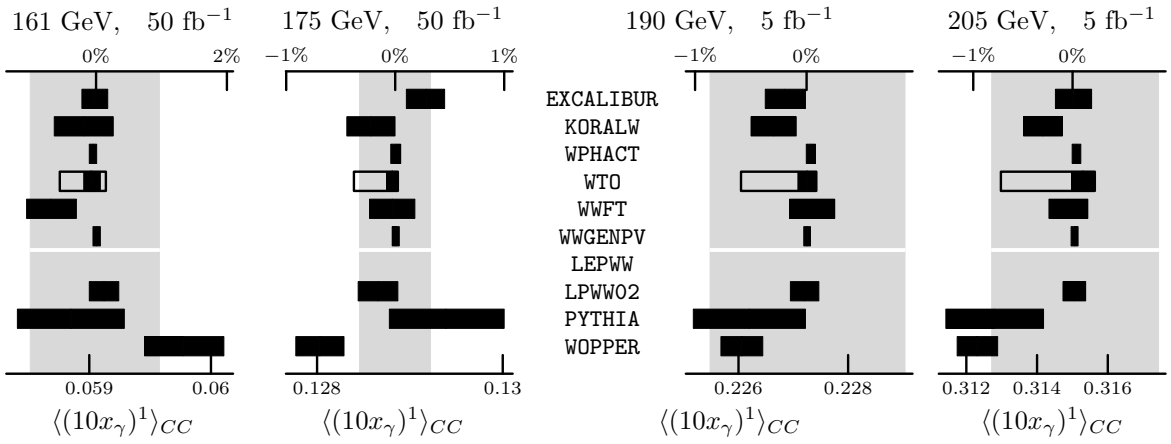


Figure 20: Unleashed predictions for the total radiated γ energy in $e^+e^- \to \mu^-\bar{\nu}_\mu u\bar{d}$ after canonical (`ADLO/TH`) cuts. The transparent, framed error bars are theoretical errors (cf. page 70).

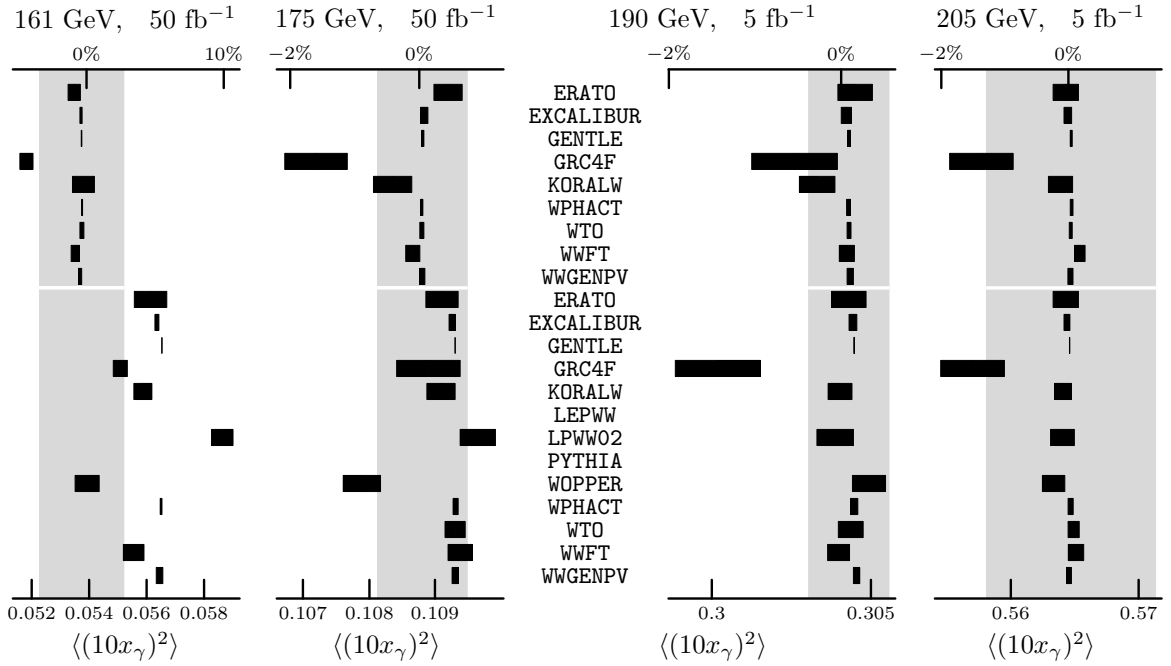


Figure 21: Tuned predictions for the square of the total radiated γ energy in $e^+e^- \to \mu^-\bar{\nu}_\mu u\bar{d}$ without cuts.

We must keep in mind that this quantity is somewhat artificial and has been used only for comparing the implementation of initial-state radiation among programs which have finite p_T and those who have not. Without the inclusion of final-state radiation, this quantity is not measurable.

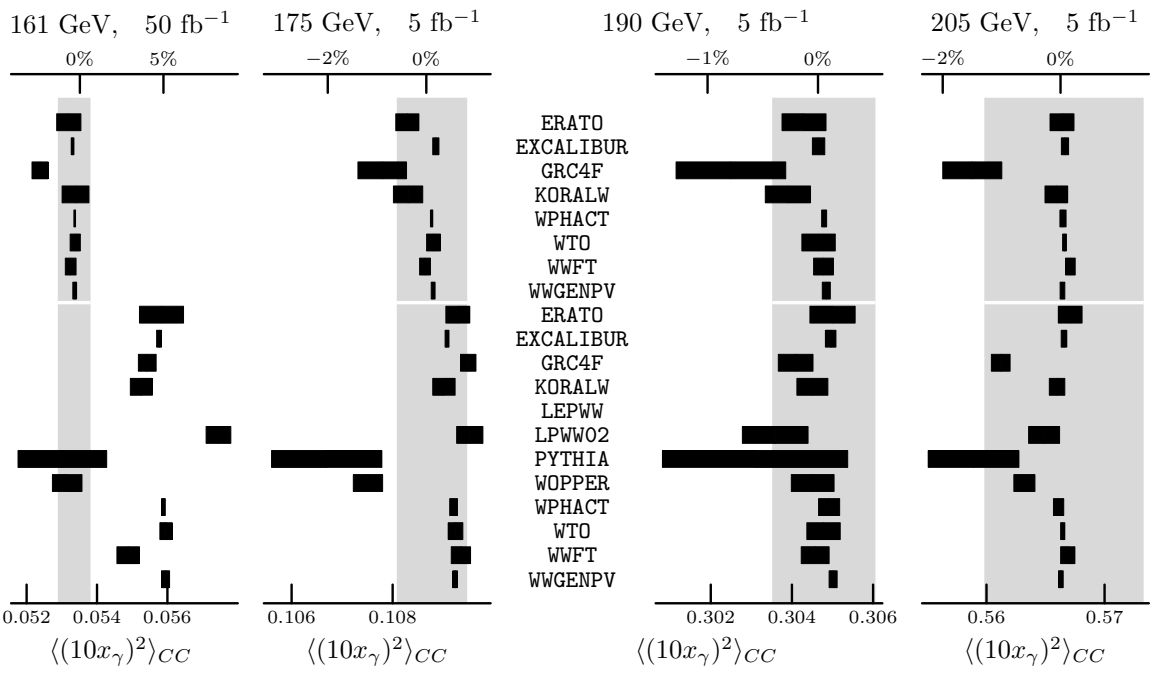


Figure 22: Tuned predictions for the square of the total radiated γ energy in $e^+e^- \to \mu^-\bar{\nu}_\mu u\bar{d}$ after canonical (`ADLO/TH`) cuts.

3.1.13 Leptonic Observables

The lepton angles and lepton energies are very well under control. For the lepton energies, the effect of the *incompleteness error* from leaving out the *CC11* diagrams is not even noticeable.

The *incompleteness error* for the lepton angles is noticeable, but hardly measurable. `PYTHIA`'s predictions are significantly different from the other programs.

3.1.14 Visible γ Energy

The situation for exclusive photonic observables is much less satisfactory than the situation for the other observables studied. This should not be surprising, however. The leading-logarithmic approximation is theoretically justified using the renormalization group and an operator product expansion for observables which are totally inclusive in the photons. A majority of programs implements this result with structure functions and treats photons inclusively, treating *all* photons as emitted collinearly.

It is nevertheless possible to investigate the structure of the Feynman diagrams contributing to the renormalization group evolution of the structure functions. This investigation shows that

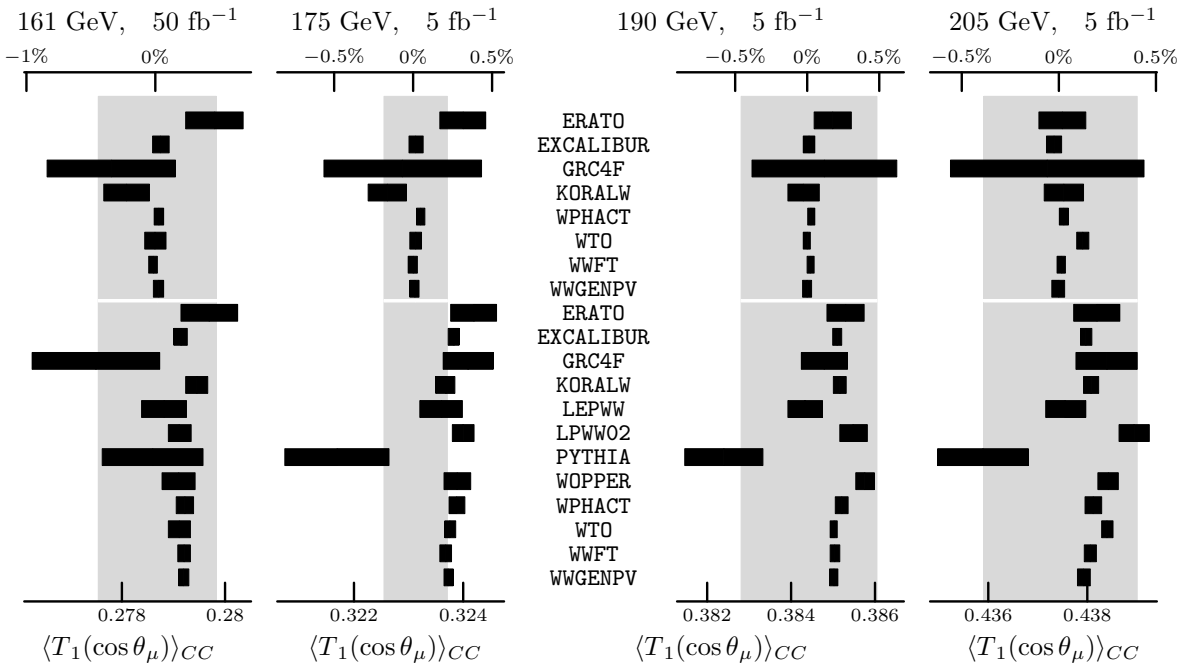


Figure 23: Tuned predictions for the first Chebyshev polynomial of the μ production angle in the laboratory frame in $e^+e^- \to \mu^-\bar{\nu}_\mu u\bar{d}$ after canonical (ADLO/TH) cuts.

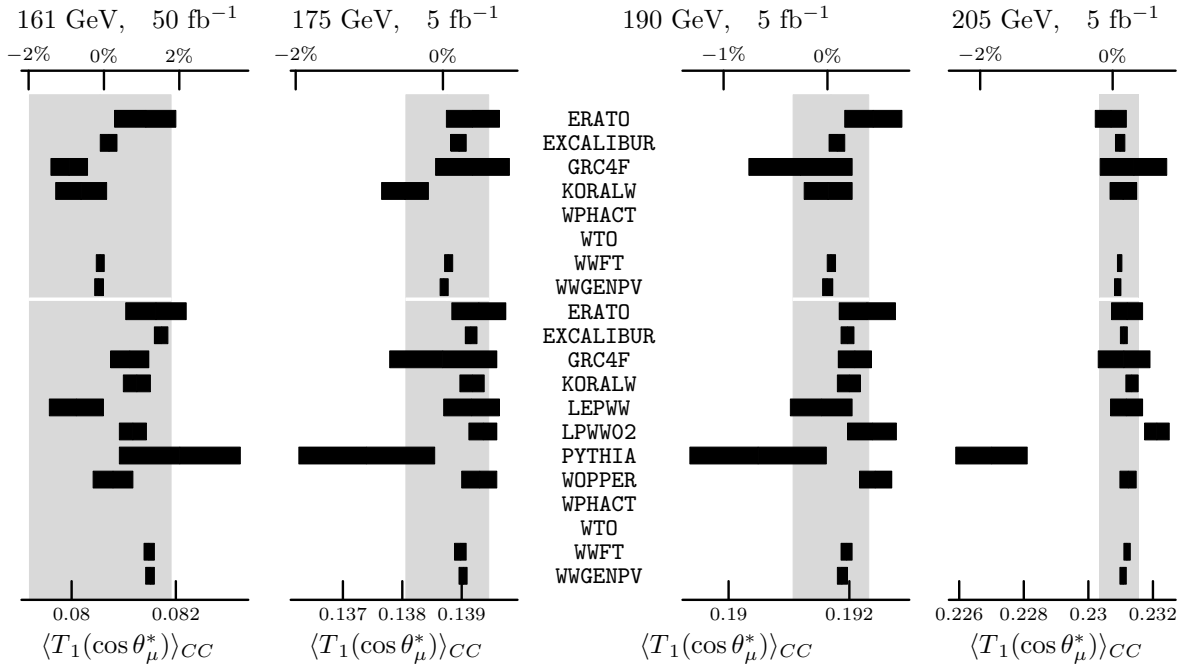


Figure 24: Tuned predictions for the first Chebyshev polynomial of the μ decay angle in the rest frame of the W^- in $e^+e^- \to \mu^-\bar{\nu}_\mu u\bar{d}$ after canonical (ADLO/TH) cuts.

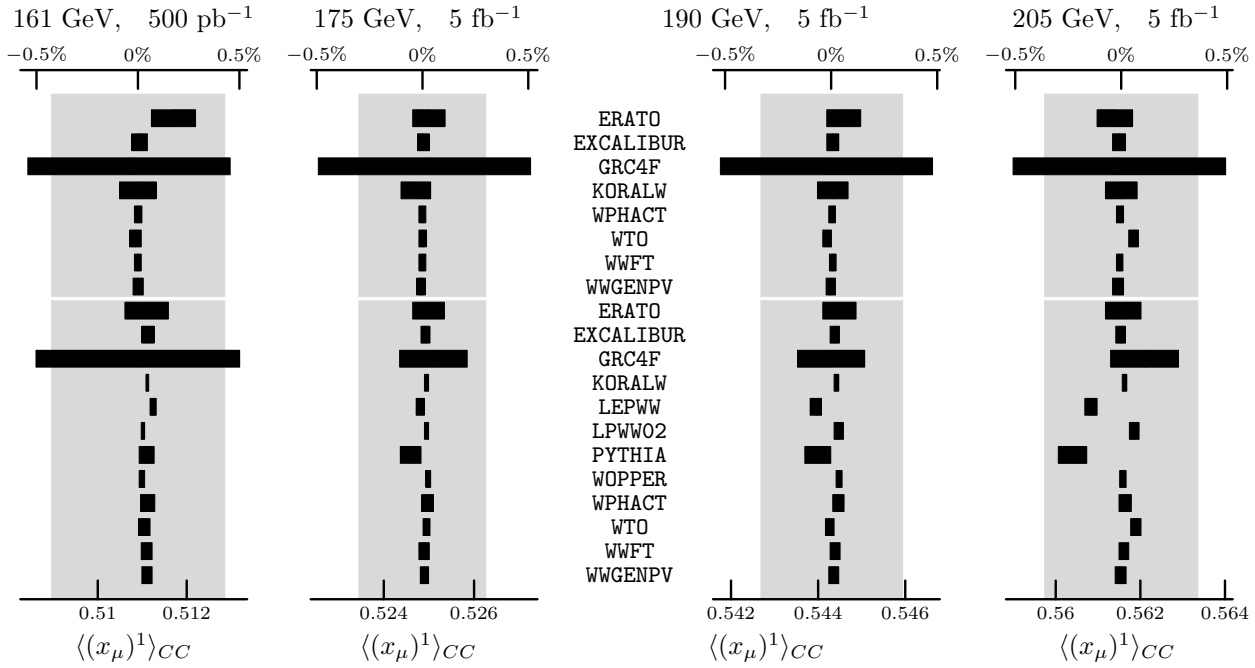


Figure 25: Tuned predictions for the μ energy in $e^+e^- \to \mu^-\bar{\nu}_\mu u\bar{d}$ after canonical (ADLO/TH) cuts.

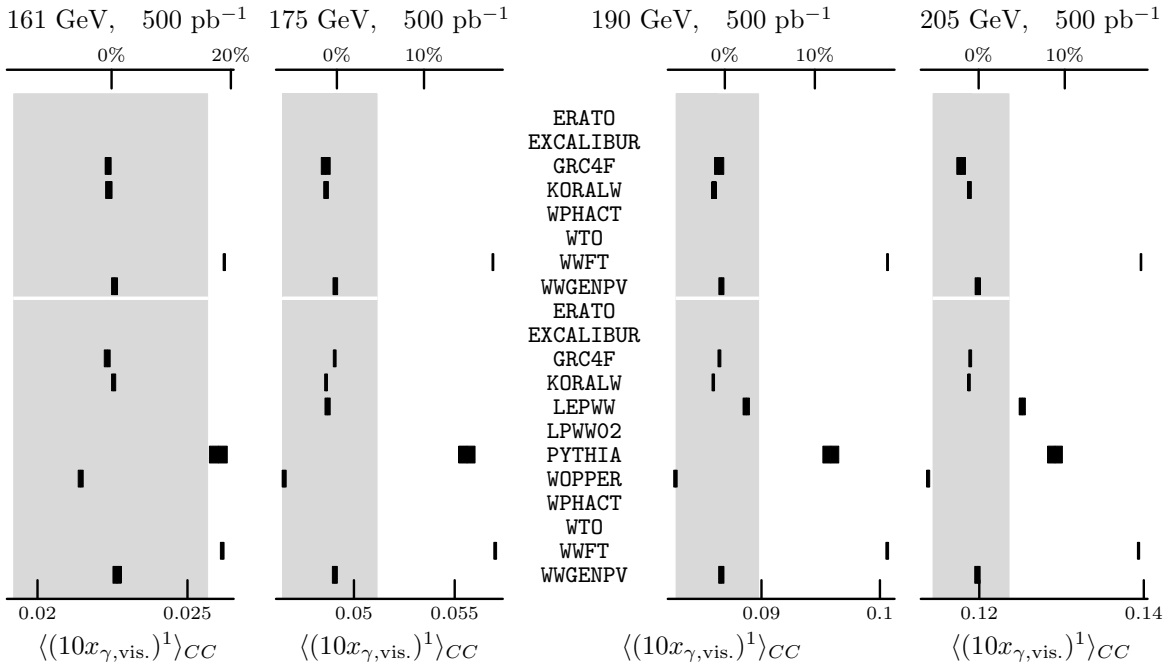


Figure 26: Tuned predictions for the visible γ energy in $e^+e^- \to \mu^-\bar{\nu}_\mu u\bar{d}$ after canonical (ADLO/TH) cuts.

the leading logarithms originate from a propagator pole

$$\ln\left(\frac{s}{m_e^2}\right) = \int_{m_e^2}^{s} \frac{d(pk)}{pk} \tag{25}$$

caused by the emission of almost collinear photons. This observation can be used to implement various parton shower algorithms for such photons. Another approach is to use p_T-dependent structure functions that recover the p_T-dependence of the first-order matrix element.

In contrast to the structure function method which is unambiguously defined by the renormalization group, these explicit resummations of Feynman diagrams are not uniquely defined and can lead to differing results. These differences are reflected in our results.

3.1.15 Final State Radiation

The canonical (`ADLO/TH`) cuts are of calorimetric nature, i.e. photons are combined with nearby charged particles. Therefore we should expect the effect of final-state radiation to be very small and furthermore the leading-logarithmic approximation to be sufficient. Since some programs have implemented final-state radiation, this assertion has to be checked.

We must, of course, again stress the fact that a theoretically meaningful (i.e. gauge invariant) separation of initial and final-state radiation is *not* possible in $e^+e^- \to 4f + \gamma$. The leading logarithmic corrections, however, can be traced back to the mass singularities in initial-state radiation, and do form a gauge invariant subset. From a pragmatical point of view, it is also possible to calculate the bremsstrahlung from the charged final-state particles. The radiation from off-shell intermediate states will likely contribute less than the radiation from on-shell final states, because the latter contains infrared and mass singularities. Therefore one can argue that the dominant radiative corrections will come from these diagrams.

This procedure has some pragmatical merit, but it should be kept in mind that it could be justified only *a posteriori*, after a full calculation of the non-logarithmic terms is available.

At the time of the final meeting, a rather substantial effect for exclusive observables was reported from a preliminary study using the `ADLO/TH` cuts. The separation cut of 5 degrees for photons from charged particles is rather tight, however. For a realistic assessment of the effect, a looser separation cut should be used. A study [56] from 1994 (comparing version 1.1 of `WOPPER` and version 1.0 of `WWF`) had shown that about 20 degrees are required for cutting the effect of final-state radiation at LEP2 energies.

Therefore, another study with modified canonical cuts has been performed. These cuts are identical to `ADLO/TH`, except for the photonic separation cuts. In the results shown below, a photon is counted as initial-state radiation if it is closer to a beam than to any charged particle. All other photons are counted as final-state radiation and are combined with the closest charged particle.

In order to finish the study before the deadline, it was agreed to perform only tuned comparisons, for the *CC03* subset of diagrams.

The plots feature eight data sets:

- `KORALW/FSR` and `KORALW`: results from `KORALW`, with and without final-state radiation, using the *CC03* diagrams. The final-state radiation is generated using the `PHOTOS` package [36]. `PHOTOS` has been modified to generate final-state radiation for quarks as well.
- `LPWW02/FSR` and `LPWW02`: results from `LPWW02`, with and without final-state radiation, using the *CC03* diagrams. The final-state radiation is generated using again the modified `PHOTOS` version. `LPWW02` does not include a finite p_T for the initial-state radiation. This will reduce the effect from final-state radiation considerably.
- `WWF/FSR` and `WWF`: results from `WWF`, with and without final-state radiation, using the *CC03* diagrams. `WWF/FSR` is the only data set in this study which uses a complete $\mathcal{O}(\alpha)$ matrix element for hard radiation. The virtual corrections are not complete but the most important contributions have been included consistently by demanding the cancellation of infrared and mass divergences, leaving a theoretical uncertainty of $\mathcal{O}(\alpha)$.
- `WWGENPV/FSR` and `WWGENPV`: results from `WWGENPV`, with and without final-state radiation, using the *CC03* diagrams. The final-state radiation is generated in leading-logarithmic approximation, using fragmentation functions (the final state equivalent of structure functions).

For some programs, another set of cuts has also been studied: `ADLO/TH` with a separation cut of 20 degrees. These results will not be shown, because they do not reveal anything unexpected. They are inbetween the results from fully inclusive and those from the `ADLO/TH` cuts, but closer to the former.

For completely inclusive observables like the total cross section, we should not expect any effect from final state parton showers, as implemented in `PHOTOS` or in `WWGENPV`. The sum of the probabilities for radiating zero or N photons has to add up to one. This expectation is confirmed in figure 27. Since we are applying acceptance cuts, a small residual effect will remain from charged particles, that are "kicked" out of, or into, the acceptance cuts.

This is different for calculations including the complete $\mathcal{O}(\alpha)$ matrix element for hard radiation, where non-trivial effects are possible. The result from `WWF` in figure 27 shows that there is an uncertainty, because the non -(infrared or mass)-divergent virtual contributions are not taken into account and the total cross section is expected to have a theoretical error almost as big as the apparent deviation.

The phenomenologically most important issue is certainly the effect of final-state radiation on the measured $W^{\pm}$ masses. If a final-state particle radiates a sufficiently hard photon that is not included in the corresponding "jet", a smaller invariant mass will be measured. We have

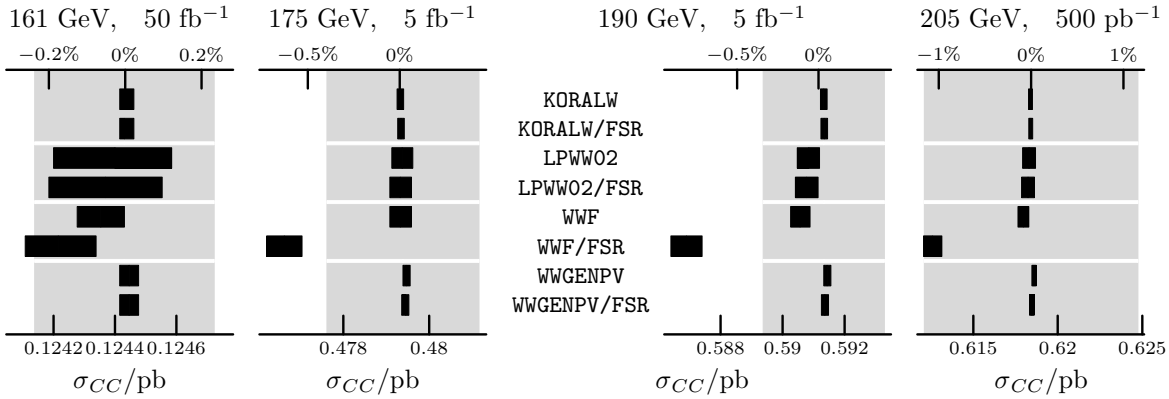


Figure 27: The total cross sections with cuts are not affected by the inclusion of leading logarithmic final-state radiation. See page 83 for comments.

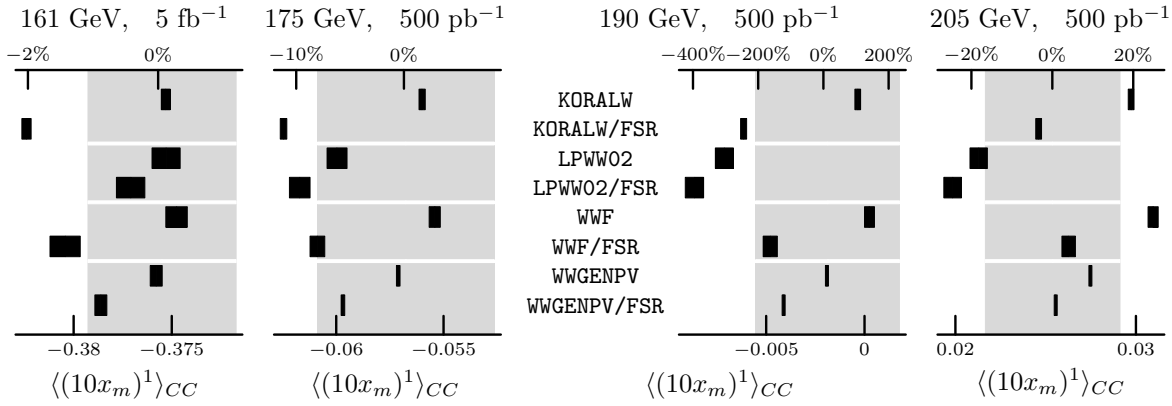


Figure 28: The seemingly large shifts in $\langle x_m \rangle$ correspond to rather moderate shifts in the absolute values of the sum of invariant masses. For the case of `WWF` we have shifts of $\approx 90\,\mathrm{MeV}$. See page 84 for comments.

to answer the question of whether this shift is numerically important, and whether it is under control.

From figure 28, we see that both `KORALW` and `WWF` predict a shift in the sum of invariant masses in the 80–90 MeV range. Toggling options in `WWF`, it can be verified that this shift is dominated by the leading logarithms and that non-factorizable contributions are negligible.

On the other hand, `WWGENPV` and `LPWW02` predict smaller shifts of 40 MeV and 30 MeV, respectively. For `LPWW02`, the difference can, presumably, be traced back to the missing p_T in the initial-state radiation. As for `WWGENPV`, the difference is probably due to differences in the formulations.

As already observed in figures 13 and 15, a finite p_T of the hard scattering system has

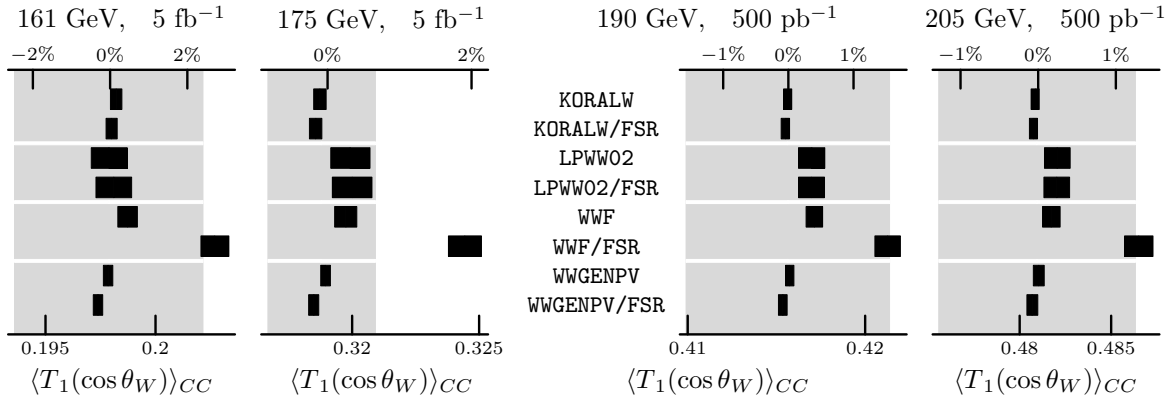


Figure 29: The programs based on leading logarithms show no measurable effect in the $W^{\pm}$ production angle.

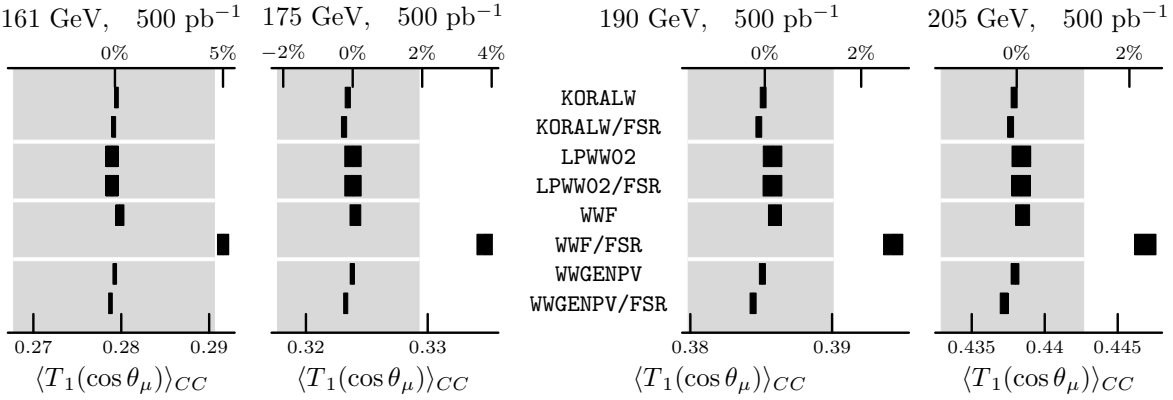


Figure 30: The programs based on leading logarithms show no measurable effect in the μ production angle.

a noticeable effect on the invariant masses if `ADLO/TH` cuts are applied. It must be noted, however, that these results are still very fresh, and the work on this issue must be considered as still in progress. Still, it can be said that all the p_T codes give (apart from small differences in particularly sensitive observables) consistent results on the FSR issue.

Extrapolating the shift predicted by `KORALW` and `WWF` naively to a single $W^{\pm}$, we have an effect of about 40 MeV. Measuring exclusive photons and making use of constraints, the experiments should be able to control this shift if event generators include final-state radiation in leading logarithmic approximation and initial-state radiation with finite p_T. At the end of the day, the uncertainty from final-state radiation will drop well below the anticipated experimental resolution.

There is a hardly measurable effect of the hard-radiation matrix element in `WWF` on the $W^{\pm}$ production angle, as shown in figure 29. This effect is of the order of $1\% \approx 4\alpha/\pi$ and

corresponds to non-logarithmic contributions, which can not be reproduced in the structure function and parton shower calculations.

There is a similar effect of the hard-radiation matrix element on the μ production angle, as shown in figure 30, where the μ's are pulled towards the forward direction.

For the decay angle of the μ in the $W^{\pm}$'s decay frame as well as for its energy in the laboratory frame, there is a tiny effect from final-state radiation, which is neither measurable nor different for the LL programs from `WWF`. It is completely absent in `LPWW02`.

About one of the important quantities, the 'lost' photon energy, we want to remark the following. All four programs that enter this comparison have studied the total energy lost to 'initial-state' radiation. This, however, being not an unambiguously defined quantity, we have settled on a definition as described above, where a photon is deemed to be ISR if its angle with respect to one of the beams is smaller than that with respect to any other charged particle. We have studied the average value of both the *total* energy of emitted bremsstrahlung and that of the *lost* amount of energy. The total energy results from the four programs are in a rather good agreement, with about twice as much energy lost under ISR + FSR than under ISR alone. If, however, we impose the cuts intended to define the more meaningful 'lost' bremsstrahlung energy, the agreement is not so good at this moment. We ascribe this to yet remaining differences in the cuts' implementation, and we refrain from presenting a plot here, since we feel that it does not adequately reflect the situation, which has to be clarified in the near future.

Summing up, we see that the effects of final-state radiation are at the level of the experimental resolution or below. They have to be studied in particular for a reliable determination of the $W^{\pm}$ mass. Therefore an inclusion of final-state radiation in the event generators is desirable from a pragmatical point of view, even before a theoretically satisfactory $\mathcal{O}(\alpha)$ matrix element calculation is available.

It has, however, to be noted that the effect of final-state radiation beyond the collinear approximation is crucially dependent on the details of the cuts, and that the quantitative determination of it has to rely on the use of those codes which implement such an effect.

The differences between the leading logarithms and the $\mathcal{O}(\alpha)$ matrix element for hard radiation in the total cross section and some angular distributions will have to be reevaluated when the virtual contributions in the latter calculation will be complete.

3.1.16 Conclusions

Most Monte Carlo event generators, integration programs and semi-analytic programs are ready for physics at LEP2, at least for the early, low-luminosity stages. However, once enough integrated luminosity has been collected, only the high precision programs should be used:

- Programs with *incompleteness errors*, i.e. omission of Feynman diagrams will have to be

upgraded or retired. This effort is known to be under way in some cases and users are encouraged to ask the authors for updated versions once in a while.

- We have concentrated on a typical *CC10* process, which is dominated by the *CC03* diagrams. For processes with electrons in the final state, and also for processes like $u\bar{u}d\bar{d}$, the *incompleteness errors* could be much larger. For these processes, the high-precision complete programs are relevant, unless fairly stringent invariant mass cuts are applied. Of course, to *prove* that such cuts indeed allow for the use of an incomplete program, one has again to rely on a complete program after all.

- For several observables, the effect of finite p_T on both initial and final-state radiation is important. For these observables the programs implementing the effect of finite p_T on photonic radiation are relevant, unless particular experimental cuts are applied.

- Authors of programs with bugs are encouraged to fix them. *At the very least, the results of this comparative study should be mentioned in the respective user manuals.* Let us again repeat that deviations in the *tuned comparisons* are *not* theoretical errors but symptoms of bugs.

- From the considerations of the effect of changes in the theoretical approach (SF versus FF, or the use of η versus that of β in the ISR), it is clear that the theoretical error is *not* much smaller than the expected experimental one, at least for several important quantities. Therefore we conclude that the calculation of the complete one-loop electroweak radiative correction is of much more than purely academic interest.

In any case, it is safe to say that the perfect, all-round Ultimate Monte Carlo event generator for $W^{\pm}$-physics at LEP2 does *not* exist. In all likelihood it will *never* exist because different implementation strategies lead to different strengths and weaknesses. Usually this reflects more of the preferences and interests of the respective authors than their ability to provide complete and bug-free codes.

One important issue that has not been studied in detail by our group is the implementation of *anomalous couplings* [73]. While a precise experimental determination of such couplings will in all likelihood not be possible at LEP2, a similarly detailed analysis would be valuable and might be performed in the future.

3.2 *CC11* processes

E_{cm}	GE/4fan	WPHACT	WTO	WWGENPV
Born				
95	.52886(0)	.52890(10)	—	.52895(8)
100	.63217(0)	.63220(10)	—	.63218(6)
130	9.0560(0)	9.0559(5)	—	9.0560(7)
	9.0517(1)	*9.0522(4)*	*9.0530(25)*	*9.0515(4)*
160	.38447(0)	.38447(1)	—	.38446(1)
161	.53580(0)	.53581(2)	—	.53580(2)
175	1.77062(0)	1.77061(6)	—	1.77061(6)
176	1.80481(0)	1.80483(7)	—	1.80483(7)
	1.80445(2)	*1.80450(5)*	*1.80446(4)*	*1.80447(7)*
190	2.04049(0)	2.04053(8)	2.0403(1)	2.04048(10)
205	2.05733(0)	2.05738(8)	—	2.05743(10)
	2.05631(2)	*2.05640(6)*	*2.05637(8)*	*2.05641(10)*
300	1.49733(0)	1.49742(8)	—	1.49735(7)
500	.81482(0)	.81483(7)	—	.81480(6)
1000	.32607(0)	.32607(5)	—	.32602(6)
2000	.16684(0)	.16683(5)	—	.16682(7)
	.10734(0)	*.10737(7)*	*.10782(6)*	*.10727(5)*
With ISR				
95	.55170(1)	.55170(10)	.55190(70)	.55140(55)
100	.57908(1)	.57910(10)	.57930(50)	.57937(34)
130	7.5225(1)	7.5221(7)	7.5219(13)	7.5214(15)
	7.5187(1)	*7.5195(5)*	*7.5215(15)*	*7.5186(17)*
160	.27563(1)	.27563(2)	—	.27563(3)
161	.38090(2)	.38090(2)	.38092(4)	.38092(4)
175	1.46646(1)	1.46649(6)	—	1.46643(6)
176	1.50459(2)	1.50457(9)	1.50464(10)	1.50453(7)
	1.50430(2)	*1.50433(6)*	*1.50423(12)*	*1.50426(6)*
190	1.81236(2)	1.81235(7)	1.81229(11)	1.81235(7)
205	1.89984(2)	1.89986(12)	1.89995(8)	1.89996(10)
	1.89897(2)	*1.89900(7)*	*1.89896(34)*	*1.89899(10)*
300	1.51351(2)	1.51353(10)	1.51353(20)	1.51349(11)
500	.86950(1)	.86956(9)	.86960(25)	.86956(14)
1000	.36514(1)	.36515(5)	.36554(49)	.36530(35)
2000	.18247(1)	.18250(4)	—	.18247(13)
	.12800(0)	*.12797(12)*	*.12858(48)*	*.12806(13)*

Table 9: *CC11* process. Cross sections are in *fb* for $E_{cm} = 95, 100, 130$ GeV, in *pb* for higher energies. Numbers in *italics* correspond to constant Z width.

E_{cm}	175	190	205
Born			
ALPHA	0.8152 ± 0.0004	9.505±0.005	12.505±0.006
CompHEP	0.8160 ± 0.0013	9.514±0.011	12.506±0.014
EXCALIBUR	0.8162 ± 0.0011	9.514±0.008	12.499±0.010
GENTLE/4fan	0.8157 ± .00001	9.511±.0001	12.500±.0001
HIGGSPV	0.8159 ± 0.0004	9.506±0.005	12.505±0.008
WPHACT	0.8150 ± 0.0008	9.509±0.006	12.501±0.007
WTO	0.8168 ± 0.0003	9.517±0.002	12.509±0.013
with ISR			
EXCALIBUR	0.6478 ± 0.0004	7.371±0.003	10.789±0.004
GENTLE/4fan	0.6481 ± 0.0001	7.370±0.001	10.791±0.001
HIGGSPV	0.6481 ± 0.0003	7.371±0.003	10.789±0.006
WPHACT	0.6482 ± 0.0006	7.367±0.007	10.784±0.008
WTO	0.6477 ± 0.0010	7.373±0.003	10.792±0.005
Born			
ALPHA	0.7724 ± 0.0004	9.036±0.005	11.804±0.006
CompHEP	0.7732 ± 0.0014	9.058±0.012	11.834±0.016
EXCALIBUR	0.7728 ± 0.0004	9.036±0.003	11.809±0.003
HIGGSPV	0.7728 ± 0.0003	9.034±0.006	11.814±0.006
WPHACT	0.7723 ± 0.0006	9.034±0.006	11.810±0.007
WTO	0.7739 ± 0.0002	9.042±0.002	11.818±0.001
with ISR			
EXCALIBUR	0.6119 ± 0.0004	7.004±0.003	10.199±0.004
HIGGSPV	0.6128 ± 0.0003	7.002±0.004	10.199±0.005
WPHACT	0.6129 ± 0.0006	7.000±0.007	10.193±0.008
WTO	0.6128 ± 0.0010	7.007±0.002	10.203±0.006

Table 10: Cross sections for the process $e^+e^- \to \mu^+\mu^- b\bar{b}$, with invariant mass cuts: $M_Z - 15 < m_{\mu\mu} < M_Z + 15$ GeV, $m_{bb} > 30$ GeV, $m_b = 0$. The two lower parts have additional cuts: lepton momenta > 10 GeV, lepton polar angles with beams $> 15^0$.

A few codes have performed a very precise ($\simeq 10^{-4}$) *tuned comparison* of the total cross section of a *CC11* process, $e^+e^- \to u\bar{d}s\bar{c}$, in a broad CM energy range, $130 \div 2000$ GeV, using the input parameters of tuned comparison, as in table 5 both with *running* and *constant* Z widths. The results are given in table 9.

An interesting conclusion can be drawn from comparing these two cases. There is practically no difference between running at constant Z widths result at LEP2 energies, whereas at $E_{cm} =$ 2000 GeV the running Z width results starts to blow up. This is an illustration of gauge-invariance violation, see [71].

This comparison was attempted at an early phase of our work. The extreme accuracy served

E_{cm}	175	190	205
Born			
ALPHA	1.5863 ± 0.0009	18.375±0.009	24.138±0.012
CompHEP	1.5785 ± 0.0030	18.352±0.030	24.180±0.039
EXCALIBUR	1.5916 ± 0.0020	18.398±0.020	24.141±0.015
GENTLE/4fan	1.5878 ±0.00002	18.381±.0002	24.150±.0002
HIGGSPV	1.5876 ± 0.0011	18.376±0.014	24.150±0.021
WPHACT	1.5868 ± 0.0013	18.383±0.011	24.151±0.013
WTO	1.5864 ± 0.0024	18.378±0.002	24.159±0.008
with ISR			
EXCALIBUR	1.2770 ± 0.0008	14.243±0.008	20.840±0.010
GENTLE/4fan	1.2782 ± 0.0001	14.243±0.001	20.838±0.002
HIGGSPV	1.2781 ± 0.0008	14.248±0.009	20.846±0.014
WPHACT	1.2773 ± 0.0010	14.235±0.014	20.827±0.017
WTO	1.2799 ± 0.0027	14.246±0.004	20.833±0.005
Born			
ALPHA	1.4204 ± 0.0008	16.767±0.008	21.784±0.010
CompHEP	1.4141 ± 0.0032	16.748±0.032	21.851±0.044
EXCALIBUR	1.4197 ± 0.0009	16.750±0.008	21.782±0.010
HIGGSPV	1.4199 ± 0.0009	16.771±0.012	21.782±0.016
WPHACT	1.4197 ± 0.0014	16.775±0.013	21.785±0.015
WTO	1.4169 ± 0.0021	16.766±0.002	21.776±0.004
with ISR			
EXCALIBUR	1.1423 ± 0.0008	12.995±0.008	18.812±0.010
HIGGSPV	1.1437 ± 0.0007	13.001±0.011	18.799±0.017
WPHACT	1.1430 ± 0.0010	13.001±0.009	18.813±0.018
WTO	1.1449 ± 0.0021	13.003±0.003	18.814±0.007

Table 11: Cross sections for the process $e^+e^- \to \nu_\mu \bar{\nu}_\mu b\bar{b}$ with invariant mass cuts: $M_Z - 25 < m_{\mu\mu} < M_Z + 25$ GeV, $m_{bb} > 30$ GeV, $m_b = 0$. The lower parts have an addition cut of 20 degrees on the angle of the b's with respect to both beams.

as a very efficient tool for hunting down many tiny bugs. Furthermore, it demonstrates that a level of precision of the order 10^{-4} is now within the reach of not only semi-analytical but also adaptive Monte Carlo integrators.

4 Comparisons of NC processes

Here we present the results of the *tuned* comparison for three *NC* processes *NC24, NC10, NC21*. We computed only cross sections at three c.m.s energies: 175, 190 and 205 GeV with

E_{cm}	175	190	205
Born			
ALPHA	1.3940 ± 0.0007	18.299±0.009	26.361±0.013
CompHEP	1.3909 ± 0.0029	18.309±0.031	26.470±0.051
HIGGSPV	1.3946 ± 0.0005	18.294±0.011	26.348±0.011
WPHACT	1.3955 ± 0.0010	18.314±0.012	26.384±0.017
WTO	1.3937 ± 0.0029	18.304±0.004	26.386±0.008
with ISR			
HIGGSPV	1.1444 ± 0.0004	14.053±0.009	22.490±0.012
WPHACT	1.1440 ± 0.0010	14.064±0.010	22.505±0.020
WTO	1.1483 ± 0.0028	14.068±0.003	22.508±0.009
Born			
ALPHA	1.2466 ± 0.0007	16.732±0.008	23.843±0.012
CompHEP	1.2430 ± 0.0031	16.761±0.034	23.965±0.054
EXCALIBUR	1.2458 ± 0.0008	16.727±0.008	23.862±0.015
HIGGSPV	1.2463 ± 0.0005	16.715±0.009	23.822±0.013
WPHACT	1.2473 ± 0.0010	16.749±0.013	23.855±0.018
WTO	1.2457 ± 0.0023	16.735±0.004	23.855±0.006
with ISR			
EXCALIBUR	1.0227 ± 0.0007	12.865±0.008	20.381±0.015
HIGGSPV	1.0239 ± 0.0004	12.853±0.008	20.306±0.042
WPHACT	1.0229 ± 0.0010	12.865±0.010	20.378±0.015
WTO	1.0263 ± 0.0022	12.864±0.003	20.377±0.008

Table 12: Cross sections for the process $e^+e^- \to \nu_e\bar{\nu}_e b\bar{b}$ under the same cuts as table 11.

simple cuts. Seven codes participated in this comparison.

We have concentrated on processes where a $b\bar{b}$ pair is produced together with two leptons, since these can form an important background for the production and decay of a light Higgs boson. All cross sections are given in fb: since they are quite small, we have not pursued detailed comparisons of other quantities as we have done for the CC processes.

From the tables it is apparent that the agreement among the various codes is very good, both at the Born level and after inclusion of ISR. The cuts have been chosen so as to be more or less realistic in an experimental Higgs search.

5 All four-fermion processes

In the following two subsections we present the cross sections for many four fermion processes at only one center-of-mass energy, $\sqrt{s} = 190$ GeV, in the massless approximation $m_f = 0$, with the Standard LEP2 Input, see table 5. In the first subsection, *all* 32 four-fermion processes are presented. They are calculated with the standard Canonical Cuts. The four-fermion processes are ordered in accordance with the classification of tables 1-2. For historical reasons, the Born cross sections are presented in the Report of the Working Group on Standard Model Processes, [69]. The tables of the next subsection contain numbers computed *with* the ISR radiation (SF) and *with* gluon exchange diagrams for non-leptonic processes.

Since this is a tuned comparison all codes have used a fixed strong coupling constant, $\alpha_s = 0.12$. Obviously, any further study of the non-leptonic processes must include some educated guess on the scale of α_s, e.g. $\alpha_s(s_\pm)$ (running) or $\alpha_s(2M_W)$ (fixed).

The precision of the computation is quite high, normally better than .1%. These numbers are supposed to provide benchmarks for future calculations of four-fermion processes.

5.1 AYC, Canonical Cuts

final state	CompHEP	EXCALIBUR	grc4f	WPHACT	WTO	WWGENPV
$\mu^-\bar{\nu}_\mu\nu_\tau\tau^+$	.1947(5)	.1941(1)	.1941(2)	.1942(2)	.1941(0)	.1941(1)
$\mu^-\bar{\nu}_\mu u\bar{d}$	.5917(11)	.5916(3)	.5919(5)	.5921(5)	.5919(0)	.5920(6)
$u\bar{d}s\bar{c}$	1.791(5)	1.788(1)	1.791(2)	1.789(1)	1.788(0)	1.789(1)

Table 13: *CC11, CC10, CC09* family. Cross sections in pb.

final state	CompHEP	ERATO	EXCALIB	grc4f	WPHACT	WTO	WWGENPV
$e^-\bar{\nu}_e\nu_\mu\mu^+$	.2012(6)	—	.2014(1)	.2014(3)	.2015(1)	.2014(2)	.2013(4)
$e^-\bar{\nu}_e u\bar{d}$	.6131(12)	.6139(6)	.6140(4)	.6135(4)	.6135(6)	.6137(6)	.6134(12)

Table 14: *CC20, CC18* family. Cross sections in pb.

final state	CompHEP	EXCALIBUR	grc4f	WPHACT	WTO
$\mu^+\mu^-\nu_\mu\bar{\nu}_\mu$	.2018(8)	.2049(1)	.2029(4)	.2050(0)	.2032(3)
$u\bar{u}d\bar{d}$	1.967(8)	1.992(2)	1.985(4)	1.992(0)	1.980(6)

Table 15: mix43 family. Cross sections in pb.

final state	CompHEP	EXCALIBUR	grc4f	WPHACT
$e^-e^+\nu_e\bar{\nu}_e$	.2244(12)	.2294(2)	.2289(7)	.2292(2)

Table 16: mix56 process. Cross sections in pb.

final state	CompHEP	EXCALIB	grc4f	HIGGSPV	WPHACT	WTO
$\mu^+\mu^-\tau^+\tau^-$	13.19(9)	13.38(3)	13.28(4)	13.32(1)	13.33(2)	13.26(14)
$\nu_\tau\bar{\nu}_\tau\mu^+\mu^-$	10.75(4)	10.71(2)	10.71(1)	10.720(4)	10.72(1)	10.76(13)
$\nu_\mu\bar{\nu}_\mu\nu_\tau\bar{\nu}_\tau$	6.366(8)	6.377(3)	6.373(4)	6.377(5)	6.376(1)	6.375(0)
$\mu^+\mu^-u\bar{u}$	27.09(9)	27.29(5)	27.20(2)	27.22(2)	27.24(3)	27.16(24)
$\mu^+\mu^-d\bar{d}$	25.39(17)	25.49(5)	25.44(2)	25.48(1)	25.49(2)	25.37(13)
$\nu_\mu\bar{\nu}_\mu u\bar{u}$	18.17(6)	18.22(1)	18.20(3)	18.22(1)	18.21(1)	18.22(5)
$\nu_\mu\bar{\nu}_\mu d\bar{d}$	15.80(5)	15.84(1)	15.85(2)	15.83(1)	15.83(1)	15.83(1)
$u\bar{u}c\bar{c}$	210.7(15)	206.8(7)	208.3(4)	207.8(2)	208.0(2)	208.9(5)
$u\bar{u}s\bar{s}$	203.6(13)	203.5(8)	203.7(6)	203.0(2)	203.2(2)	204.4(5)
$d\bar{d}s\bar{s}$	183.8(19)	182.2(10)	181.0(4)	181.2(2)	181.3(2)	182.6(5)

Table 17: *NC32, NC24, NC10, NC06* family. Cross sections in fb.

final state	CompHEP	EXCALIB	grc4f	HIGGSPV	WPHACT	WTO
$\nu_e\bar{\nu}_e\mu^+\mu^-$	18.07(8)	18.03(5)	17.98(5)	18.07(1)	18.05(2)	17.83(13)
$\nu_e\bar{\nu}_e\nu_\mu\bar{\nu}_\mu$	6.408(9)	6.417(3)	6.408(5)	6.364(91)	6.416(1)	6.439(5)
$\nu_e\bar{\nu}_e u\bar{u}$	20.78(5)	20.74(1)	20.74(4)	20.78(16)	20.72(3)	20.95(9)
$\nu_e\bar{\nu}_e d\bar{d}$	16.12(4)	16.48(1)	16.48(2)	16.37(17)	16.46(2)	16.67(15)

Table 18: *NC21, NC12* family. Cross sections in fb.

final state	CompHEP	EXCALIBUR	grc4f	HIGGSPV	WPHACT
$e^+e^-\mu^+\mu^-$	.1231(15)	.1251(2)	.1247(5)	.1192(21)	.1253(2)
$e^+e^-\nu_\mu\bar{\nu}_\mu$	.01421(8)	.01426(2)	.01421(2)	.01445(18)	.01429(2)
$e^+e^-u\bar{u}$	.09070(76)	.09234(11)	.09226(12)	.09003(89)	.09244(14)
$e^+e^-d\bar{d}$	.04259(45)	.04427(6)	.04425(4)	.04491(46)	.04429(8)

Table 19: *NC48* family. Cross sections in pb.

final state	CompHEP	EXCALIBUR	grc4f	HIGGSPV	WPHACT
$\mu^+\mu^-\mu^+\mu^-$	—	.006650(17)	.006643(30)	.006671(85)	.006622(13)
$\nu_\mu\bar{\nu}_\mu\nu_\mu\bar{\nu}_\mu$	.003176(7)	.003142(1)	.003141(4)	.003142(7)	.003142(1)
$u\bar{u}u\bar{u}$	—	.1017(3)	.1020(5)	—	.1014(1)
$d\bar{d}d\bar{d}$	—	.08765(38)	.08767(17)	—	.08788(22)

Table 20: *NC4x16, NC4x12* family. Cross sections in pb.

final state	CompHEP	EXCALIBUR	grc4f	WPHACT
$e^+e^-e^+e^-$	—	.1169(2)	.1156(11)	.1169(2)
$\nu_e\bar{\nu}_e\nu_e\bar{\nu}_e$	.003194(18)	.003123(1)	.003128(3)	.003125(1)

Table 21: *NC4x36* and *NC4x9* processes. Cross sections in pb.

5.2 AYC, Simple Cuts

final state	ALPHA	EXCALIB	GE/4fan	grc4f	WPHACT	WTO	WWGENPV
Born							
$\mu^-\bar{\nu}_\mu\nu_\tau\tau^+$	.2264(2)	.2267(1)	.2267(0)	.2267(1)	.2267(0)	.2267(0)	.2267(0)
$\mu^-\bar{\nu}_\mu u\bar{d}$	.6804(4)	.6801(4)	.6801(0)	.6799(2)	.6801(1)	.6801(0)	.6801(0)
$u\bar{d}s\bar{c}$	2.040(1)	2.040(1)	2.040(0)	2.040(1)	2.041(0)	2.040(0)	2.040(0)
With ISR							
$\mu^-\bar{\nu}_\mu\nu_\tau\tau^+$	—	.2013(1)	.2014(0)	.2014(1)	.2014(0)	—	.2014(0)
$\mu^-\bar{\nu}_\mu u\bar{d}$	—	.6036(4)	.6041(0)	.6041(3)	.6041(0)	.6041(0)	.6041(1)
$u\bar{d}s\bar{c}$	—	1.811(1)	1.812(0)	1.812(1)	1.812(0)	1.812(0)	1.812(0)

Table 22: *CC11, CC10, CC09* family. Cross sections in pb.

final state	ALPHA	EXCALIB	grc4f	HIGGSPV	WPHACT
Born					
$\nu_e\bar{\nu}_e\mu^+\mu^-$	12.40(1)	12.38(1)	12.37(1)	12.37(1)	12.38(1)
$\nu_e\bar{\nu}_e\nu_\mu\bar{\nu}_\mu$	8.335(4)	8.336(3)	8.335(6)	8.342(5)	8.339(1)
$\nu_e\bar{\nu}_e u\bar{u}$	24.95(2)	24.92(1)	24.92(2)	25.01(3)	24.91(1)
$\nu_e\bar{\nu}_e d\bar{d}$	20.91(2)	20.92(1)	20.91(1)	20.90(3)	20.92(1)
With ISR					
$\nu_e\bar{\nu}_e\mu^+\mu^-$	—	11.59(1)	11.59(1)	11.59(1)	11.60(0)
$\nu_e\bar{\nu}_e\nu_\mu\bar{\nu}_\mu$	—	6.412(3)	6.408(5)	6.411(7)	6.416(1)
$\nu_e\bar{\nu}_e u\bar{u}$	—	21.87(1)	21.88(2)	21.94(2)	21.86(1)
$\nu_e\bar{\nu}_e d\bar{d}$	—	16.75(1)	16.76(1)	16.74(2)	16.75(1)

Table 23: *NC21, NC12* family. Cross sections in pb.

In this subsection, only those processes are given that were treated within the semi-analytic approach with Simple Cuts on the invariant mass of any charged fermion-antifermion pair. The latter cut value is chosen to be 5 GeV. Every table contains two sets of numbers which are computed:
1. in the Born approximation and without gluon exchange diagrams for non-leptonic processes;
2. with the ISR radiation (SF) and with gluon exchange diagrams for non-leptonic processes.

5.3 Conclusions

We want to stress that many of the codes contributing to the "all you can" comparison have been developed during this workshop. The level of agreement documented in these tables

final state	ALPHA	EXCALIB	GE/4fan	grc4f	HIGGSPV	WPHACT	WTO
Born, without gluon exchange diagrams							
$\mu^+\mu^-\tau^+\tau^-$	10.06(9)	10.08(0)	10.07(0)	10.07(0)	10.07(0)	10.07(0)	10.14(7)
$\nu_\tau\bar{\nu}_\tau\mu^+\mu^-$	9.894(10)	9.872(3)	9.871(0)	9.875(4)	9.872(3)	9.873(3)	9.884(10)
$\nu_\mu\bar{\nu}_\mu\nu_\tau\bar{\nu}_\tau$	8.245(4)	8.242(3)	8.241(0)	8.240(4)	8.237(6)	8.241(1)	8.241(1)
$\mu^+\mu^-u\bar{u}$	23.99(2)	24.04(1)	24.03(0)	24.04(2)	24.03(1)	24.04(1)	—
$\mu^+\mu^-d\bar{d}$	23.46(2)	23.45(1)	23.45(0)	23.46(2)	23.45(1)	23.46(1)	—
$\nu_\mu\bar{\nu}_\mu u\bar{u}$	21.59(2)	21.59(1)	21.59(0)	21.58(1)	21.58(1)	21.59(1)	21.63(3)
$\nu_\mu\bar{\nu}_\mu d\bar{d}$	20.00(2)	19.99(1)	19.99(0)	20.00(1)	20.00(1)	19.99(1)	20.00(1)
$u\bar{u}c\bar{c}$	54.80(5)	54.75(2)	54.74(0)	54.73(4)	54.69(4)	54.74(2)	—
$u\bar{u}s\bar{s}$	51.83(5)	51.86(1)	51.86(0)	51.85(2)	51.85(5)	51.87(2)	—
$d\bar{d}s\bar{s}$	48.30(5)	48.33(2)	48.33(0)	48.34(1)	48.27(6)	48.34(1)	—
With ISR, with gluon exchange diagrams							
$\mu^+\mu^-\tau^+\tau^-$	—	10.29(0)	10.30(0)	10.29(1)	10.30(0)	10.30(0)	—
$\nu_\tau\bar{\nu}_\tau\mu^+\mu^-$	—	9.279(3)	9.284(1)	9.278(7)	9.283(3)	9.284(4)	—
$\nu_\mu\bar{\nu}_\mu\nu_\tau\bar{\nu}_\tau$	—	6.379(3)	6.376(1)	6.373(4)	6.377(5)	6.377(1)	6.379(2)
$\mu^+\mu^-u\bar{u}$	—	23.74(1)	23.76(0)	23.77(2)	23.75(1)	23.75(1)	—
$\mu^+\mu^-d\bar{d}$	—	22.31(1)	22.34(0)	22.33(1)	22.33(1)	22.34(1)	—
$\nu_\mu\bar{\nu}_\mu u\bar{u}$	—	18.83(1)	18.84(0)	18.84(1)	18.85(1)	18.84(1)	—
$\nu_\mu\bar{\nu}_\mu d\bar{d}$	—	16.00(1)	15.99(0)	15.99(1)	16.00(1)	15.99(0)	—
$u\bar{u}c\bar{c}$	—	272.6(9)	272.3(0)	271.4(9)	272.1(1)	272.2(1)	—
$u\bar{u}s\bar{s}$	—	267.0(10)	266.8(0)	266.5(6)	266.8(1)	266.8(1)	—
$d\bar{d}s\bar{s}$	—	240.7(11)	240.8(0)	240.5(6)	240.6(4)	240.8(1)	—

Table 24: *NC32, NC24, NC10, NC06* family. Cross sections in fb.

demonstrates a substantial progress in our understanding of the general $e^+e^- \to 4f$ cross section.

However, this comparison revealed also some problems, e.g.: some numbers still disagree within declared errors; during the collection of these tables, some codes exhibited fluctuations much larger than the statistical errors; we didn't attempt a comparison of CPU times, needed by different codes to reach a given accuracy. All these items deserve a more thorough study in the future.

Acknowledgments

We have to thank Francesca Cavallari, Jules Gascon, Martin Grünewald, Niels Kjaer, and Jerome Schwindling for helping us to define realistic ADLO/TH cuts, which have been used extensively in the comparisons of our programs.

References

[1] T. Muta, R. Najima and S. Wakaizumi, *Mod. Phys. Letters* **A1** (1986) 203.

[2] D. Bardin and T. Riemann, preprint DESY 95–167 (1995), to appear in *Nucl. Phys.* **B**, [hep-ph/9509341].

[3] E.N. Argyres et al., *Phys. Lett.* **B358** (1995) 339;
C.G. Papadopoulos, *Phys. Lett.* **B352** (1995) 144;
U. Baur and D. Zeppenfeld, *Phys. Rev. Lett.* **75** (1995) 1002.

[4] E. Boos et al., `CompHEP`: computer system for calculation of particle collision characteristics at high energies, version 2.3 (1991), Moscow State Univ. preprint MGU-89-63/140 (1989); preprint KEK 92-47 (1992).

[5] D. Bardin, M. Bilenky, D. Lehner, A. Olchevski and T. Riemann, in: T. Riemann and J. Blümlein (eds.), Proc. of the Zeuthen Workshop on Elementary Particle Theory – Physics at LEP200 and Beyond, Teupitz, Germany, April 10–15, 1994, *Nucl. Phys.* (Proc. Suppl.) **37B** (1994) p. 148.

[6] D. Bardin, A. Leike and T. Riemann, *Phys. Lett.* **B353** (1995) 513.

[7] F.A. Berends, R. Kleiss and R. Pittau, *Nucl. Phys.* **B424** (1994) 308; *Nucl. Phys.* **B426** (1994) 344; *Nucl. Phys.* (Proc. Suppl.) **37B** (1994) 163-168;
R. Pittau, *Phys. Lett.* **B335** (1994) 490-493.

[8] F. Caravaglios and M. Moretti, *Phys. Lett.* **B358** (1995) 332;

[9] G.P. Lepage, *J. Comp. Phys.* **27** (1978) 192.

[10] E. Boos, M. Dubinin, V. Edneral, V. Ilyin, A. Kryukov, A. Pukhov, S. Shichanin, in: "New Computing Techniques in Physics Research II", ed.by D. Perret-Gallix, World Scientific, Singapore, 1992, p. 665
in: Proc. of the XXVI Recontre de Moriond, ed. by Tranh Than Van, Editions Frontieres, 1991, p. 501

E.Boos, M.Dubinin, V.Ilyin, A.Pukhov, V.Savrin, preprint INP MSU 94-36/358, 1994 (hep-ph/9503280)

[11] S. Kawabata, *Comp. Phys. Comm.* **41** (1986) 127.

[12] V.Ilyin, D.Kovalenko, A.Pukhov, preprint INP MSU 95-2/366, 1995

[13] E.Kuraev, V.Fadin, *Yad. Phys.* **41** (1985) 733

[14] E.N. Argyres and C.G. Papadopoulos, *Phys. Lett.* **B263** (1991) 298.

[15] C.G. Papadopoulos, writeup in preparation.

[16] T. Stelzer (Durham U.) and W.F. Long (Wisconsin U., Madison), *Comp. Phys. Comm.* **81** (1994) 357-371.

[17] G. Marchesini *et al. Comp. Phys. Comm.* **67** (1992) 465-508.

[18] R. Kleiss and R. Pittau, *Comp. Phys. Comm.* **83** (1994) 141.

[19] F.A. Berends and A.I. van Sighem, Leiden preprint INLO-PUB-7/95.

[20] D. Bardin, A. Leike, T. Riemann and M. Sachwitz, *Phys. Letters* **206B** (1988) 539.

[21] D. Bardin, A. Leike, T. Riemann, report of the *Searches Event Generators Working Group*, these proceedings.

[22] D. Bardin, M. Bilenky, A. Olchevski and T. Riemann, *Phys. Lett.* **B308** (1993) 403; E: [hep-ph/9507277].

[23] D. Bardin, D. Lehner and T. Riemann, preprint DESY 94–216 (1994), to appear in the proceedings of the IX^{th} *International Workshop "High Energy Physics and Quantum Field Theory", Zvenigorod, Moscow Region, Russia, September 1994* [hep-ph/9411321];
D. Lehner, Ph.D. thesis, Humboldt-Universität zu Berlin (1995), unpublished, available from `http://www.ifh.de/~lehner`.

[24] D. Bardin, A. Leike and T. Riemann, *Phys. Lett.* **B344** (1995) 383.

[25] D. Bardin, W. Beenakker, A. Denner, *Phys. Lett.* **B317** (1991) 213.

[26] Minami-Tateya collaboration, "`GRACE` manual ver 1.0", KEK Report **92-19**, 1993,
Minami-Tateya collaboration, Brief Manual of `GRACE` system ver 2.0/β, 1995.

[27] Y.Kurihara, J.Fujimoto, T.Munehisa, Y.Shimizu, KEK CP-035, KEK 95-126, 1995.

[28] T. Sjöstrand, *Comp. Phys. Comm.* **39** (1986) 347;
T. Sjöstrand and M. Bengtsson, *Comp. Phys. Comm.* **43** (1987) 367.
T. Sjöstrand and H.-U. Bengtsson, *Comp. Phys. Comm.* **46** (1987) 43.

[29] S. Kawabata, *Comp. Phys. Comm.* **88** (1995) 309.

[30] CERN CN Division, KUIP, CERN Program Library Long Writeup I102, 1993.

[31] CERN CN Division, PAW++, CERN Program Library Long Writeup Q121, 1993.

[32] CERN CN Division, HBOOK, CERN Program Library Long Writeup Y250, 1995.

[33] M. Skrzypek, S. Jadach, W. Płaczek, and Z. Wąs, Monte Carlo program `KORALW 1.02` for W-pair production at LEP2/NLC energies with Yennie-Frautschi-Suura exponentiation, CERN preprint CERN-TH/95-205 to appear in *Comp. Phys. Comm.*

[34] M. Skrzypek *et al.*, Initial state QED Corrections to W-pair Production at LEP2/NLC – Monte Carlo Versus Semianalytical Approach, CERN preprint CERN-TH/95-246 (unpublished).

[35] R. Decker, S. Jadach, J.H. Kühn, Z. Wąs, CERN-TH 6793/93, *Comp. Phys. Comm.* **76** (1993) 361.

[36] E. Barberio, B. van Eijk, Z. Wąs, *Comp. Phys. Comm.* **79** (1994) 291.

[37] V. Fadin, V. Khoze, A. Martin, and W. Stirling, Higher-order Coulomb Corrections to the Threshold $e^+e^- \to W^+W^-$ Cross Section (unpublished), preprint DTP/95/64.

[38] M. Aguilar-Benitez *et al.*, *Phys. Rev.* **D50** (1994) 1173.

[39] R. Kleiss, Private Communication.

[40] F.A. Berends and R. Kleiss, "Radiative Effects in Higgs Production at LEP", Leiden Preprint, see also *Nucl. Phys.* **178** (1981) 141.

[41] K. Hagiwara, R. D. Peccei, D. Zeppenfeld and K. Hikasa, *Nucl. Phys.* **B282** (1987) 253.

[42] R. Kleiss, program `LEPWW`, unpublished.

[43] R. Miquel, M. Schmitt, CERN-PPE/95-109 (*Z. Phys.* **C**, in press).

[44] E. .A. Kuraev, V. S. Fadin, *Sov. J. Nucl. Phys.* **41** (1985) 466.

[45] O. Nicrosini, L. Trentadue, *Phys. Lett.* **B196** (1987) 551.

[46] V. S. Fadin, V. A. Khoze, A. D. Martin and A. Chapovskii, *Phys. Rev.* **D52** (1995) 1377.

[47] T. Sjöstrand, *Comp. Phys. Comm.* **82** (1994) 74.

[48] T. Sjöstrand, Lund University report LU TP 95–20 (1995).

[49] R. Kleiss et al., in Z Physics at LEP 1, eds. G. Altarelli, R. Kleiss and C. Verzegnassi, CERN 89–08 (Geneva, 1989), Vol. 3, p. 1.

[50] T. Sjöstrand, *Phys. Lett.* **157B** (1985) 321.

[51] M. Bengtsson and T. Sjöstrand, *Phys. Lett.* **B185** (1987) 435.

[52] J.F. Gunion and Z. Kunszt, *Phys. Rev.* **D33** (1986) 665.

[53] V.A. Khoze and T. Sjöstrand, DTP/95/68 and LU TP 95–18, to appear in *Z. Phys.* **C**.

[54] V.S. Fadin, V.A. Khoze and A.D. Martin, *Phys. Lett.* **B311** (1993) 311.

[55] H. Anlauf, J. Biebel, H. D. Dahmen, A. Himmler, P. Manakos, T. Mannel, W. Schönau, *Comp. Phys. Comm.* **79** (1994) 487 and references cited therein.

[56] H. Anlauf, H. D. Dahmen, A. Himmler, P. Manakos, T. Mannel, T. Ohl, *Nucl. Phys.* **B** (Proc. Suppl.) **37B** (1994) 81.

[57] H. Anlauf, H. D. Dahmen, A. Himmler, P. Manakos, T. Mannel, T. Ohl, hep-ex/9504006, IKDA 95/14, SI 95-3. (Updated versions of this writeup are part of the `WOPPER` distribution.)

[58] A. Ballestrero, E. Maina, *Phys. Lett.* **B350** (1995) 225.

[59] A. Ballestrero, in preparation.

[60] F.A. Berends, P.H. Daverveldt and R. Kleiss *Nucl. Phys.* **B253** (1985) 441; R. Kleiss and W.J. Stirling, *Nucl. Phys.* **B262** (1985) 235.

[61] G. Passarino, *Nucl. Phys.* **B237** (1984) 249.

[62] G. Montagna, O. Nicrosini, G. Passarino and F. Piccinini, *Phys. Lett.* **B348** (1995) 178.

[63] G. Montagna, O. Nicrosini and F. Piccinini, *Comp. Phys. Comm.* **90** (1995) 141.

[64] NAG Fortran Library manual Mark 15 (Numerical Algorithms Group, Oxford, 1991).

[65] G. J. van Oldenborgh, P. J. Franzini, and A. Borrelli, *Comp. Phys. Comm.* **83**(1994)14. This describes the original, hard-photon only version of `WWF (1.0)`.

[66] *Hard photons in W pair production at LEP 2*, G. J. van Oldenborgh, INLO-PUB-95/04 (revised). Here the extensions to include the soft matrix element, and the combination of hard photon matrix element and structure functions is discussed.

[67] F. Jegerlehner in: T. Riemann and J. Blümlein (eds.), Proc. of the Zeuthen Workshop on Elementary Particle Theory – Physics at LEP200 and Beyond, Teupitz, Germany, April 10–15, 1994, *Nucl. Phys.* (Proc. Suppl.) **37B** (1994) p. 129.

[68] `WWGENPV` - Technical and Physical upgrades, by D. Charlton, G. Montagna, O. Nicrosini and F. Piccinini, in preparation.

[69] *Report of the Working Group on Standard Model Processes* , this report.

[70] *Electroweak Working Group Report* in *Reports of the Working Group on Precision Calculations for the Z-Resonance*, D. Bardin, W. Hollik, G. Passarino (eds.), Yellow Report, CERN 95-03, Geneva, 1995.

[71] *Report of the Working Group on $W^{\pm}$ Physics*, this report.

[72] *Report of the Working Group on W mass*, this report.

[73] *Report of the Working Group on Triple Gauge Boson Couplings*, this report.